CONTINUOUS EVOLUTION IN COLABORATIONS BETWEEN MOLDOVAN AND ITALIAN CHEMISTS

Bilateral collaborations represent an efficient tool for fruitful valorization by scientific communities of their own research potential and proved beneficial in most research areas. This is true indeed, since the most valuable research results lay on the interface of different research areas, and developing collaborations between researches working in complementary fields is most likely to provide valuable solutions.

In the past decades Moldovan researches have been constrained to develop such collaborations with different international partners due to the precarious state of the Modovan research infrastructure. Institute of Chemistry was in the forefront of this strategy, with multiple examples of joint research projects developed first of all with European colleagues. One of such examples is provided by the Laboratory of Terpenoid Chemistry, led by Prof. Nicon Ungur which involves Italian partners from Centro Nazionale della Ricerca (CNR), namely Institute of Biomolecular Chemistry (ICB), Naples. This collaboration has started in 1994, with a kind agreement of Prof. Guido Cimino, at that time director of ICB, to provide hosting to Prof. Nicon Ungur in order to develop a research project devoted to synthesis of marine natural products. This start was extremely successful and the collaboration got a tremendous development. The last year provided additional opportunities in this context, connected to the agreement between ASM and CNR to develop joint bilateral projects. This circumstance has let the Moldovan chemists to host the Italian partners in Chisinau and to organize in premiere for the last 20 years an international seminar devoted to the chemistry of natural products.

The formal reason of this seminar was a bilateral ASM-CNR project aimed to the investigation of terpenes from cannabinoid family. The *Cannabis sativa* plant represents a isolation source for more then 400 chemical compounds, of which more then 100 compounds possess prenylated aromatic structures. These mero-terpenoids have been called phytocannabinoids and are found almost exclusively in this plant. The structural feature of these compounds is given by the presence of two distinct structural parts of differnt biogenetical origine: the aromatic part, specifically a derivative of chromene and the isoprenoidic part. Biosynthetically, the initial steps involve condensation of the aromatic part (olivetol) with geranyl pyrophosphate to provide the first, most simple representative of the family – cannabigerol (scheme 1). Following enzymatic cyclisations lead to different families of phytocannabinoids, including the most known cannabichromene- and cannabidiol-type compounds.

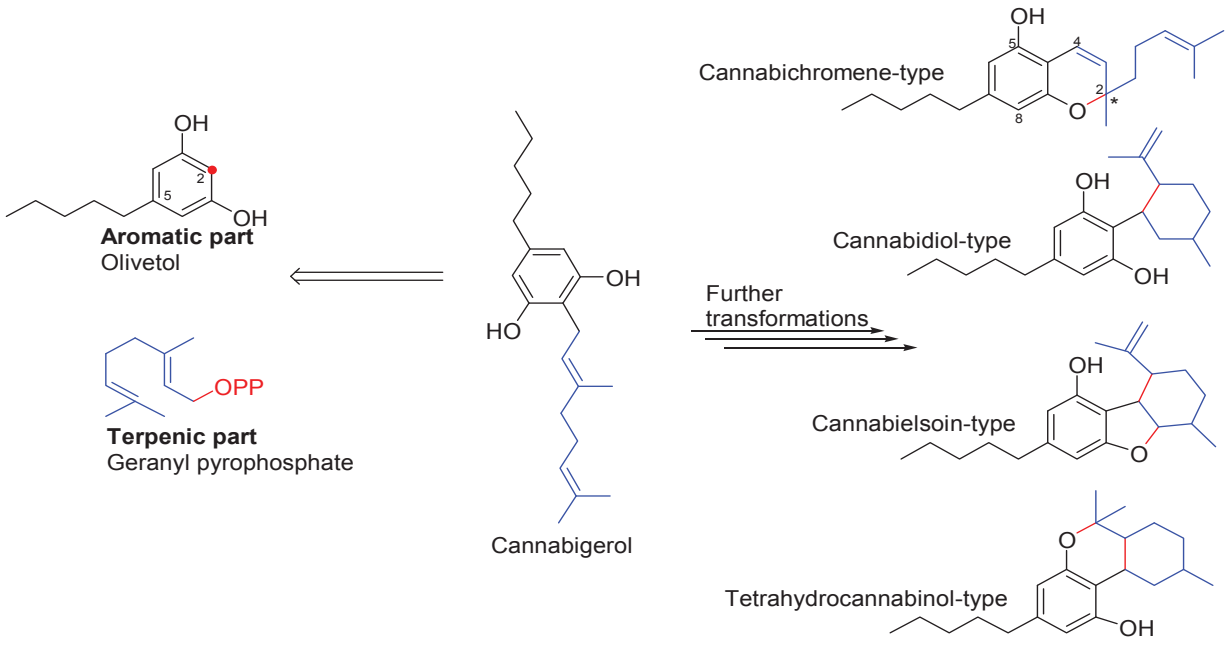

Scheme 1

For evident reasons, the basic attention during the study of this natural product family has been paid to Δ9-tetrahydrocannabinol (Δ9-THC), which is the well known compound with psychotropic activity from cannabis. Nevertheless, recent studies has shown that other non- psychotropic phytocannabinoids possess a broad spectrum of biological activities, most of them being associated with therapeutic applications. Among these, cannabichromene-type compounds have drawn attention due to their antiinflamatory, analgesic, antimicrobial, antiproliferative and bone growing stimulation actions. It made them challenging targets for chemical synthesis.

Our current ASM-CNR project includes elaboration of novel methods for the chemical synthesis, evaluation of absolute stereochemistry and biological activity of cannabichromene-type compounds. The synthetic aproach is considered, provided the fact that the most relevant compounds of this class are still not avilable from natural sources in sufficient ammounts and consequently can not be explored for therapeutical purpose. In the same time, determination of the absolute stereochemistry of most representatives is not a trivial task and can be sucsesfully solved only basing on a complex aproach, including concurent synthesis and degradation studies. Finally, broadening the structural features of prenylated cannabinoids, especially on varying the structure of isoprenic residue can lead to novel substances with new and still unexplored properties.

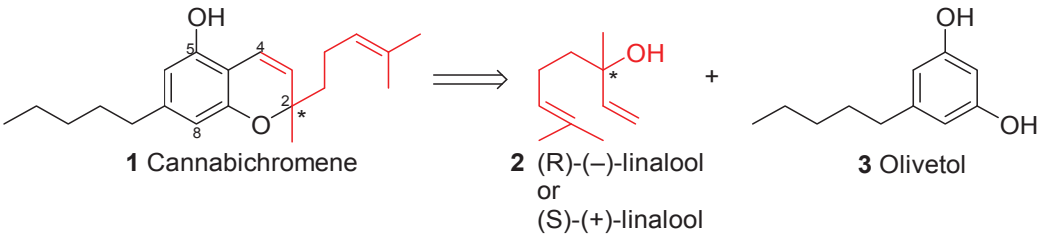

Scheme 2

Basing on available preliminary information, we have focused our project on the synthesis of cannabichromene – one of the basic representatives of prenylated cannabinoids, having as the final goal the elaboration of a general procedure for the synthesis of a whole series of prenylated cannabinoids. We intend to apply a combination of enantioselective and diastereoselective synthesis in order to access desired prenylated chromenes in enantiomericaly pure form (scheme 2). Following degradation studies and stereochemical correlation will allow determination of chromene absolute stereochemistry. In the long run, generation of a library of prenylated chromenes will support Structure-Activity Relationship (SAR) studies for identification of novel compounds with prominent biological activity.

The seminar's motto: *New Frontiers in the Chemistry of Natural Products* has addressed numerous students and researchers acting in the fields of chemistry, biology, pharmacy, genetics, biophysics as well as specialists from the R&D sector of companies with chemico-pharmaceutical profile. The general project overview was provided to the seminar audience.

Following presentations of project participants stressed the attention to the recent research directions of partner institutions. A special emphasize was placed on the use o modern analytical techniques for the structural elucidation of complex natural compounds, including those of marine origin. This issue was of special interest to Moldovan colleagues, due to the fact that modern analytical facilities, including a high-field NMR spectrometer became available in the Institute of Chemistry recently. Italian partners have shared their experience of world leaders in the area of marine chemistry.

Following multiple solicitations coming from seminar audience, made us provide in the current issue of the "Chemistry Journal of Moldova. General, Industrial and Ecological Chemistry" a condensed abstract of the seminar presentations. We do really hope that our joint event will give further impetus to our collaboration and will also motivate other researchers from Moldova to develop partnerships with European colleagues.

Dr. Margherita GAVAGNIN, CNR
Dr. Veaceslav KULCITKI, ASM
ASM-CNR joint project coordinators

APPLICATION OF NMR TECHNIQUE IN THE ELUCIDATION OF MARINE NATURAL COMPOUNDS

Maria Letizia Ciavatta

Istituto di Chimica Biomolecolare, (CNR), Via Campi Flegrei 34 –I-80078 Pozzuoli
e-mail: lciavatta@icb.cnr.it; Phone 0039 0818675243- Fax 0039 0818675340

Abstract: The topic of the seminar held in the Institute of Chemistry, Academy of Sciences of Moldova on 30th September in the frame of the joint Moldo-Italian seminar "New frontiers in natural product chemistry", concerned the use of NMR techniques in the elucidation of natural products. Step by step, two marine compounds (Fulvyne C and Tritoniopsin A) belonging to different chemical classes have been analyzed, by using suitable NMR experiments. This powerful technique allowed the elucidation of compounds as fulvynes, long chain polyacetylenes with the same functional groups but differently located in the chain, as well as tritoniopsins, cyclic diterpenes with a new skeleton, providing further information on their relative and absolute stereochemistry.

Introduction

Nuclear Magnetic Resonance spectroscopy [1] has become the most appreciated technique by the natural product chemists letting to achieve the chemical structures, even complicated and in little amount, of compounds isolated from different sources. Together with Mass Spectrometry, this technique aided us to establish the structures of nine long chain oxygenated polyacetylenes [2] from the Mediterranean sponge *Haliclona fulva* (Case 1) and to describe four cladiellane based diterpenes [3] from the nudibranch mollusc *Tritoniopsis elegans* (Case 2*)* collected in the South China Sea.

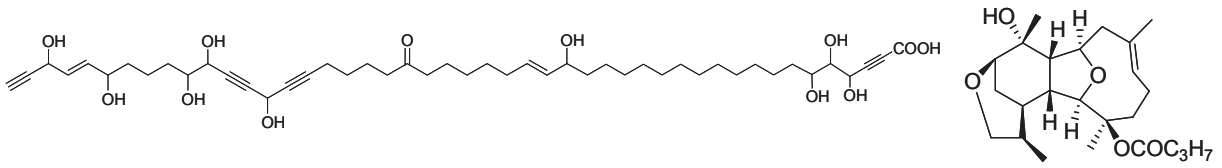

Structures of fulvyne C and tritoniopsin A

The first step

Once obtained a pure compound by using chromatographic means we have to calculate the molecular formula from the high-resolution mass spectrometry (HRMS): it will give the weight and molecular formula of our compounds and information about the presence of unsaturation degrees given by double and triple bonds and eventually by cyclic rings.

The NMR experiments

First, the analysis of the proton spectra of unknown compounds, recorded in a suitable deuterated solvent, can give a series of useful information: a) signals absorbing at different chemical shifts correspond to protons of different functional groups; b) the intensities of the signals are directly proportional to the number of protons generating them; c) the shape of signals (multiplets) gives information about the environment of a given nucleus through the analysis of their coupling constant. Second, the ^{13}C NMR experiments show how many carbons the molecules under investigation contain and which functional groups are present. We can use the ^{13}C-DEPT sequence to obtain important information about the number of CH_3, CH_2 and CH and by difference with the carbon experiment the number of quaternary carbons.

To connect each carbon resonance with the proton directly linked, the HSQC bidimensional experiment has to be performed. The analysis of hetero-nuclear correlation spectra is carried out simply by tracing the coordinates of each cross-peaks with both the proton and the carbon chemical shift scales. Thus a list of correlation between protonated carbons and the attached protons is constructed.

The next step is to carry out a COSY experiment in which you can observe the scalar coupling and so connect geminal and vicinal protons. This experiment appears as a contour plot map with a square diagram symmetric with respect to a diagonal from lower left to upper right. Coupled protons are recognized by an off-diagonal peak at the coordinated corresponding to the chemical shift of the two coupled protons. During the analysis of a COSY spectrum you can draw some partial structures of the compound under investigation. For example in Case 1, these experiments led us to construct the fragments a-e of fulvyne C, as drawn below.

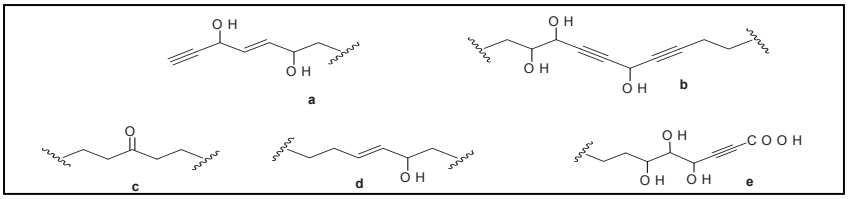

Partial structures deduced by COSY

The HMBC experiment finally gives useful information about the carbons and the protons not directly linked, but 2-4 bonds far. Careful analysis of HMBC spectrum usually allows the connection of the different spin systems identified by COSY correlations whose carbon counterpart has been connected by HSQC.

Further NMR experiments

Sometimes these fundamental NMR sequences are not sufficient to establish unambiguously the chemical structures of new compounds. As example, fulvyne C shows NMR spectra very similar to those of another co-occurring polyacetylene (fulvyne B), therefore they have to possess the same functional groups but located in different fashion along the chain. Analysis of TOCSY experiments recorded on both fulvynes allows to discriminate the two different sequences by defining all proton correlations in a mutually coupled spin system and consequently by connecting the partial structures detected from COSY.

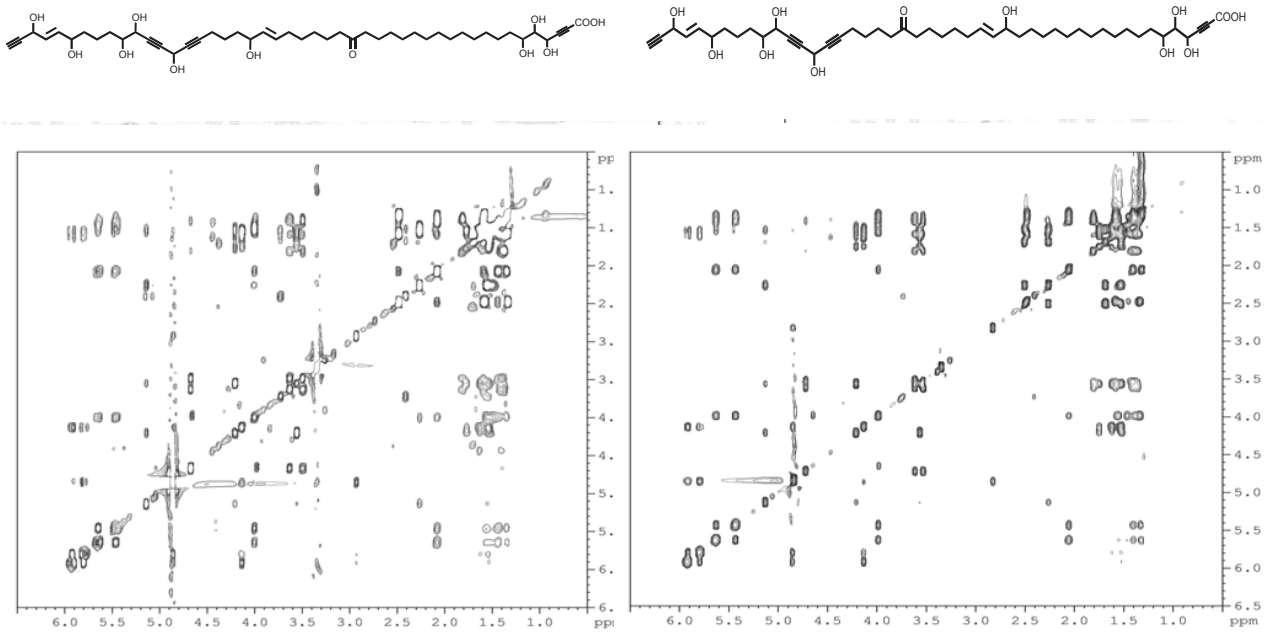

TOCSY spectra for fulvyne C (left) and B (right)

In the second case (tritoniopsin A), once obtained the molecular formula and the number of unsaturation degrees from the HRMS we have carried out the mono-dimensional NMR experiments. From the proton and carbon spectra we immediately get information about the nature of the compound under investigation. Indeed, tritoniopsin A shows a typical terpene pattern due to the presence of several methyls. ^{13}C-NMR and DEPT spectra of tritoniopsin A show 24 carbon resonances (as indicated by the molecular formula), five of which are methyl groups, seven are methylenes, eight are methines and the remaining four are quaternary carbons.

Even in this case, information about which carbons and protons are directly bonded can be obtained by recording the direct hetero-correlation experiment (HSQC).

The spin systems present in the molecule can be deduced from COSY experiment, as shown below, whereas the analysis of HMBC correlations can aid us to connect the corresponding partial structures (main long-range cross-peaks are represented by arrows) and to construct the structure.

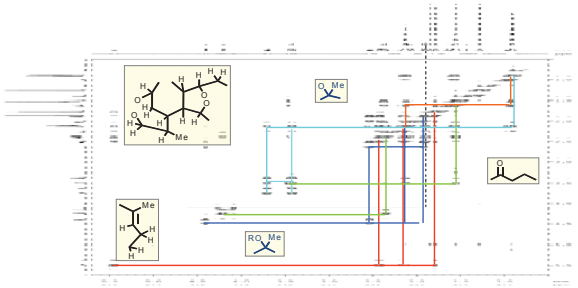

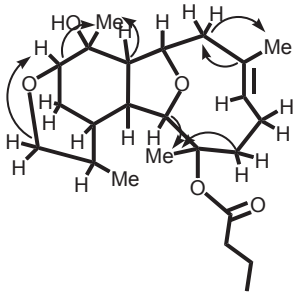

Due to the presence of nine stereogenic centers in tritoniopsin A, the objective is to give correct information on their relative configuration. Some of these can be easily deduced from the analysis of the proton spectrum signals as well as from the carbon chemical shift value. In tritoniopsin A because of the presence of a cyclohexane ring, we can suggest the configuration at two carbons by the shape of the corresponding protons (H-12 and H-14 are equatorially oriented because appear as broad singlets). Moreover, the carbon value of the methyl attached to C-11 on the same ring is consistent with the equatorial position. To confirm these evidences and to establish the configuration of the remaining carbons, mono- and bi-dimensional experiments (nOe diff and NOESY) based on dipole-dipole mechanism (two nuclei not directly linked but spatially close can mutually interact through space) can be carried out obtaining very indicative information.

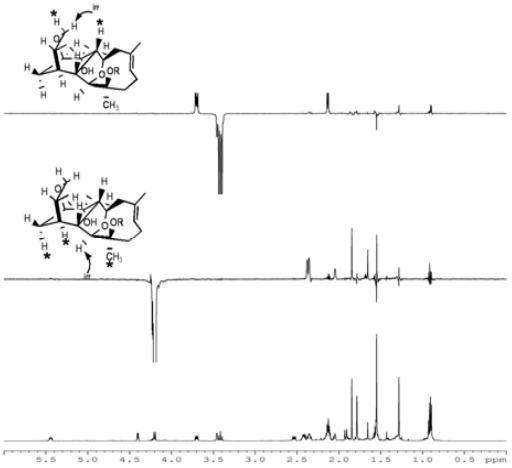

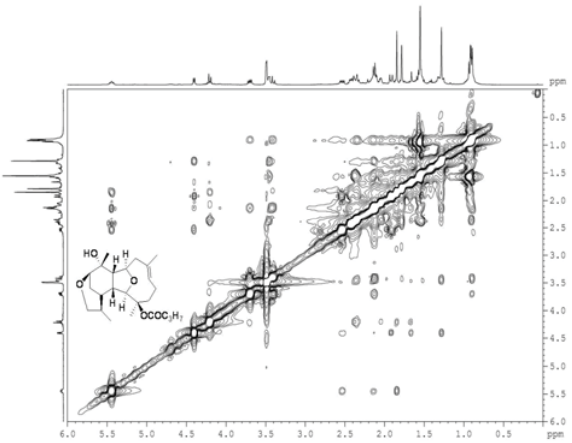

Another example of the versatile use of NMR technique is represented by the application of the Mosher method for the determination of the absolute stereochemistry of tritoniopsins. The presence of a secondary alcohol in one of the isolated tritoniopsins makes this molecule a useful model for the application of the method [4,5] leading to the assignment of the absolute stereochemistry at the carbinol center. The method is based on the conversion of the alcohol into two diastereomeric esters displaying different ^{1}H-NMR spectra. The evaluation of the difference in the chemical shift values of protons in the two esters ($\Delta\delta S$-$\Delta\delta R$) allows the absolute stereochemistry to be established as depicted below.

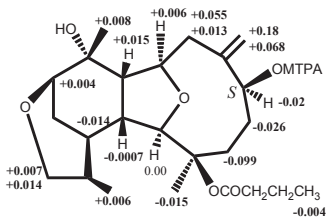

Conclusions

Nuclear Magnetic Resonance techniques represent a powerful tool for the structural determination of organic compounds, particularly in the field of natural products. It requires only minute amount of substance and frequently allows the determination of stereochemical details or even preferred conformation in solution. Nowadays, the variety of experiments available on modern NMR instruments has reduced the time needed for the acquisition data.

Acknowledments. Academy of Sciences (Moldova) and CNR (Italy) are acknowledged for financial support (bilateral project "Novel approaches for the synthesis of optically active cannabinoids with relevant biological activity and therapeutical potential" 2011-2012).

Dr. Maria Letizia Ciavatta was born in 1965 in Naples. She graduated in Pharmacy from University of Naples "Federico II" in 1988 under the supervision of Prof. E. Fattorusso. In 1991 she obtained a master in Officinal Plant Science from University of Naples. After she moved to CNR as a fellow with Professor G. Cimino (ICMIB, Naples, Italy), where she got her training first on some derivatives of cholesterol in food matrix and then on marine natural products. From 1999 she is a researcher of the laboratory of marine natural chemistry, at the Institute of Biomolecular Chemistry, CNR, Italy. Her research interests include the chemical analysis and separation of complex mixtures of natural products of marine, plant and microbial origin with particular attention to structural characterization (NMR and mass) of molecules that show activity as lead-compounds in pharmaceutical field. She is author of more than 60 scientific papers.

References

[1]. For interpretation of basic NMR experiments consult "Spectrometric Identification of Organic Compounds" Silverstein, R.M.; Webster, F.X.; Kiemle, D. Wiley & Sons Inc. Ed., 2005, U.S.

[2]. Nuzzo, G.; Ciavatta, M.L.; Villani, G.; Manzo, E.; Zanfardino, A.; Varcamonti, M.; Gavagnin, M. *Tetrahedron.,* **2012,** *68,* 750-760, *in press*.

[3]. Ciavatta, M.L.; Manzo, E.; Mollo, E.; Mattia, C.A.; Tedesco, C.; Irace, C.; Guo, Y.W.; Li, X.B.; Cimino, G.; Gavagnin, M. *J. Nat. Prod*., **2011**, *74*, 1902-1907.

[4]. Dale, J. A.; Mosher, H. S. *J. Am. Chem. Soc.* **1973**, *95*, 512-515.

[5]. (a) Ohtani, I.; Kusumi, T.; Ishitsuka, M.O.; Kakisawa, H. *Tetrahedron Lett.* **1989**, *30*, 3147-3150. (b) Ohtani, I.; Kusumi, T.; Kashman, Y.; Kakisawa, H. *J. Am. Chem. Soc.* **1991**, *113*, 4092-4096.

SYNTHESIS OF C_6 AND C_7 FUNCTIONALIZED DRIMANES FROM LARIXOL AND SCLAREOL

Alexandru Ciocarlan[b,a*], Pavel F. Vlad[a], Mihai Coltsa[a], Edu Carolina[a], Andrei Biriiac[a], Alina Nicolescu[b,c] and Calin Deleanu[b,c]

[a]*Institute of Chemistry, Academy of Sciences of the Republic of Moldova, Academiei str. 3, MD-2028 Chisinau, Republic of Moldova*
[b]*"Petru Poni" Institute of Macromolecular Chemistry of the Romanian Academy, Aleea Grigore Ghica Voda 41A, RO-700487 Iasi, Romania*
[c]*"Costin D. Nenitescu" Centre of Organic Chemistry of the Romanian Academy, Spl. Independentei 202B, PO Box 35-98, RO-060023 Bucharest, Romania*

[*]*Corresponding author, Tel./fax: + 373-22-739-775; Email: algciocarlan@excite.com*

Abstract: The current communication represents an extended abstract of the presentation delivered on the joint Moldo-Italian seminar "New frontiers in natural product chemistry", held in the Institute of Chemistry, Academy of Sciences of Moldova on 30 September. An overview of the synthetic methods oriented to the synthesis of C_6 and C_7 functionalized euryfurans is provided.

Introduction

Sesquiterpene euryfuran **1** was isolated from several marine organisms such as nudibranches *Hypselodoris californiensis* and *H. Porterae* [1], sponges *Dysidea herbacea* [2] *Euryspongia* species [1] and, from a new genus of a Pacific sponge of the family *Thorectidae* [3]. This natural product has attracted much interest due to its antitumor activity[3] and its potential as synthetic intermediate [4].

Several semisynthetic routes and total synthesis of euryfuran **1** have been published [5-15]. This compound was used as starting material for the syntheses of others natural drimane sesquiterpenes [7-10,16,17].

We will like to report our preliminary results on the syntheses of C_6 and C_7 functionalized euryfurans starting from the abundantly available labdanic diterpenes larixol **2** and sclareol **3**. The side chains of these two labdanes was removed by oxidation to the corresponding 14,15-bisnorlabd-13-ones **4** and **5**, which were transformed by known methods in dienes **6** and **14** [18-20] (Figure 1).

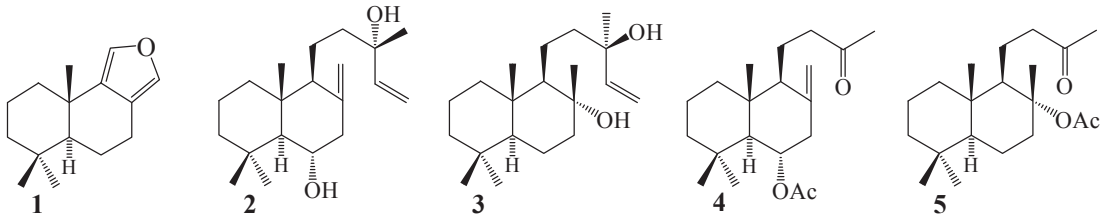

Figure 1

Results and discussion

Diene **6** is an interesting starting material for the synthesis of several C_6 functionalized drimanes. The diene moiety in **6** was submitted to photooxygenation to give the endoperoxyde **7** in high yield, which was converted into acetoxyfuran **8** by treatment with $FeSO_4$. The acetate **8** was hydrolyzed and oxidized to 6-ketofuran **13** in an overall yield of 68%. The same 6-ketofuran **13** was obtained *via* a slightly different sequence of the same transformations of the intermediates **10**, **11** and **12** in 72% overall yield (Figure 2).

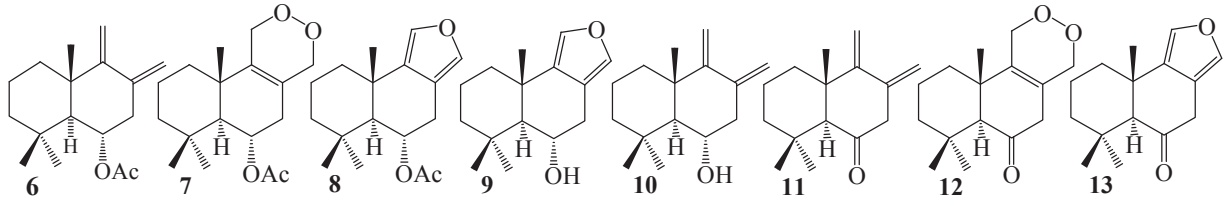

Figure 2

The known endocyclic drim-7,9(11)-diene **14** is a suitable starting material for synthesis of C_7 functionalized drimanes [19,20,22-26]. It is known that olefins with allylic hydrogens give unsaturated hydroperoxydes in the ene-reaction with singlet oxygen [27]. The photooxygenation of diene **14** also shows this ene-reaction to hydroperoxide (**15**) as the main reaction. A 1,4-cycloaddition of singlet oxygen to the exocyclic diene and a rearrangement are responsible for the formation of the two by-products **18** and **19** (Figure 3).

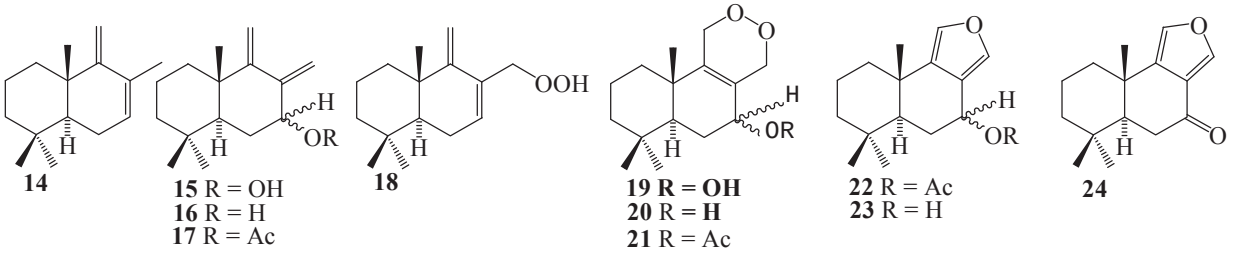

Figure 3

The main product **15** was submitted to reduction with thioureea and acetylation to give a mixture of the C_7-acetates **17**, which was photooxidazed to the acetoxyperoxydes **21** (Figure 3) [28]. The reduction of **21** with ferrous sulphate followed by saponification of the acetate and oxidation gave the 7-ketofuran 24 in 23.4% overall yield. The structures of compounds **19** and **21** were confirmed by X rays analysis. The same compound **24** in 8.7% overall yield was also obtained from side product **19** after reduction of the C_7-peroxide with thioureea, treatment of resulted 7-hydroxyperoxydes **20** with ferrous sulphate and oxidation of the C_7-hydroxy group (Figure 3).

Conclusions

Breakdown of the side chain of (+)-larixol **2** or (+)-sclareol **3** gives an easy access to an exocyclic diene **6** and an endocyclic diene **14** respectively. These two dienes **6** and **14** are excellent starting materials for the syntheses of ring B functionalized drimanes, as it was proved by present syntheses of 6-ketoeuryfuran **13** and of 7-ketoeuryfuran **24**, in respectively 68% and 23.4%.

Acknowledgements

Academy of Sciences (Moldova) and CNR (Italy) are acknowledged for financial support (travel grant 11.820.08.01/ItF). The support from the Project No 264115 (STREAM) in the frame of EU founded FP7-REGPOT-2010-1 call is acknowledged by the authors from the "Petru Poni" Institute".

Dr. Alexandru Ciocarlan was born in 1971. He graduated from Tiraspol State University (Moldova) in 1993 and obtained his Ph.D. degree in 2007 from Institute of Chemistry of Moldova Academy of Sciences, under the supervision of Professor Mihai Coltsa; in 1999 he was researcher in the Institute of Chemistry (Chisinau) of Moldova Academy of Sciences, where he works on the chemical synthesis of terpenic compounds with biological activity. He is the author of more than 25 publications and two patents.

References

[1]. Hochlowski, J.E.; Walker, R.P.; Ireland, C.; Faulkner, D.J. *J. Org. Chem.*, **1982**, *47*, 88-91.
[2]. Dunlop, R.W.; Kazlauskas, R.; March, G.; Murphy, P.T.; Wells, R.J. *Aust. J. Chem.*, **1982**, *35*, 95-103.
[3]. Gulavita, N.K.; Gunasekera, S.P.; Pomponi, S.A. *J. Nat. Prod.*, **1992**, *55(4)*, 506-508.
[4]. Jansen, B.J.M.; deGroot, A. *Nat. Prod. Reports*, **1991**, *8(3)*, 319-337.
[5]. Hueso-Rodriguez, J.A.; Rodriguez, B. *Tetrahedron Lett*., **1989**, *30(7)*, 859-862.
[6]. Nakano, T.; Mailo, M.A. *Synth. commun.,* **1981**, *11(6)*, 463-473.
[7]. Akita, H.; Naito, T.; Oishi, T. *Chem. Lett.,* **1979**, 1365-1368.
[8]. Akita, H.; Naito, T.; Oishi, T. *Chem. Pharm. Bull.,* **1980**, *28,* 2166-2171.
[9]. Ley, S.V.; Mahon, M. *J. Chem. Soc., Perkin Trans. 1*, **1983**, 1379-1381.
[10]. Ley, S.V.; Mahon, M. *Tetrah. Lett.,* **1981**, *22*, 4747.

[11]. Jansen, B.J.M.; Peperzak, R.M.; deGroot, A. *Recl. Trav. Chim. Pays-Bas*, **1987**, *106*, 489-494.
[12]. Jansen, B.J.M.; Peperzak, R.M.; deGroot, A. *Recl. Trav. Chim. Pays-Bas*, **1987**, *106*, 549-553.
[13]. Kanematsu, K.; Soejima, S. *Heterocycles*, **1991**, *32(8)*, 1483-1486.
[14]. Baba, Y.; Sakamoto, T.; Soejima, S.; Kanematsu, K. *Tetrahedron,* **1994**, *50(19)*, 5645-5658.
[15]. Rosales, A.; Lopez-Sanchez, C.; Alvarez-Corral, M.; Muooz-Dorado, M.; Rodriguez-Garcia, I. *Letters in Organic Chemistry*, **2007**, *4(8)*, 553-555.
[16]. Villamizar, J. *Rev. Latinoamer. Quim.*, **1999**, *27(3)*, 96-100.
[17]. Nakano, T.; Villamizar, J.; Mailo, M.A. *J. Chem. Research (S)*, **1998**, 560-561.
[18]. Vlad, P.F.; Ciocarlan, A.G.; Coltsa, M.N.; Deleanu, C.; Costan, O.; Siminov, Yu.A.; Kravtsov, V.C.; Lipkowski, J.; Lis, T.; deGroot, A. *Tetrahedron*, **2006**, *62*, 8489-8497.
[19]. Vlad, P.F.; Aryku, A.N.; Chokyrlan, A.G. *Russ. Chem. Bull.*, **2004**, *53*, 443-446.
[20]. Vlad, P.F.; Ciocarlan, A.G.; Coltsa, M.N.; Baranovsky, A.V.; Khripach, N.B. *Synth. Commun*., **2008**, *38*, 3960-3972.
[21]. Kernan, M.R.; Faulkner, D. J. *J. Org. Chem*., **1988**, *53*, 2773-2776.
[22]. Lithgow, A.M.; Marcos, I.S.; Basabe, P.; Sexmero, J.; Diez, D.; Gomez, A.; Estrella, A.; Urones, J.G. *Nat. Prod. Lett*., **1995**, *6*, 291-294.
[23]. Cortes, M.; Armstrong, V.; Reyes, M.E.; Lopez, J.; Madariaga, E. *Synth. Commun.,* **1996**, *26*, 1995-2002.
[24]. Akyta, H.; Nozawa, M.; Mitsuda, A.; Ohsawa, H. *Tetrahedron: Asymetry*, **2000**, 11, 1375-1388.
[25]. Barrero, A.F.; Alvarez-Manzaneda, E.J.; Chanboun, R. *Tetrahedron*, **1998**, *54*, 5635-5650.
[26]. Alvarez-Manzaneda, E.J.; Chanboun, R.; Torres, E.C.; Alvarez, E.; Alvarez-Manzaneda, R.; Haidour, A.; Ramos, J. *Tetrahedron Lett*., **2004**, *45*, 4453-4455.
[27]. Clennan, E.L.; Pace, A. *Tetrahedron,* **2005**, *61*, 6665-6691.
[28]. Balci, M. *Chem. Rev*., 1981, 81, 91-108.

PHARMACOLOGICAL AND MEDICINAL CHEMISTRY ASPECTS OF CANNABIS COMPOUNDS

Tamara Cotelea

USMF "N. Testemițanu" facultatea Farmacie, str.Malina Mica 66,Chișinau, Republica Moldova,
e-mail: tamara777@bk.ru, phone:+373 22 285979

Abstract: The current communication includes a general overview of the scientific interest and medicianl chemistry aspects of Cannabis compounds. It relates to metabolism, pharmacological action and phisico-chemical analysis of these compounds, as well as of some isomers differing in spatial arrangement of functional groups.

Introduction

Cannabis is one of the first plants utilized by humans as non-food product. Hashish was implimented in nothern China cca. 5000 or 6000 years ago and the plant itself served for textile production. During the first centuries B.C. the first samples of Cannabis paper have ben produced. During the following periods Cannabis was considered in China as a basic crop. It was also used in India in falk medicine, for ritual purposes and also for textile fibers. Aproximatively 1000 yrs. B.C. cannabis appeared in Europe. It was a result of human migrations from Black Sea to Midle Asia and other nearby areas. It was considered a sacred plant in Siria, Egipt and northen Africa. During the midle ages due to its remarcable stability to salted water it was intensively used for marine rope production. It also penetrated America form North to South during the 16-th century. Development of chemical industru during 19-th and 20-th centuries has led to a decline in Cannabis cultivation.

Botanical characterisation

Two basic varieties of Cannabis are known: *Cannabis sativa* and *Cannabis Indica*. They are widely spread in temperate and tropical regions of the Earth. Branching degree depends on the climatic conditions. The size of the composite leaves varies depending on the plant height. Flowers represent masculine (stamen carriers) and feminine (pistils carriers) inflorescents. Masculine inflorescences are tipically more flower-abundant (see pictures below).

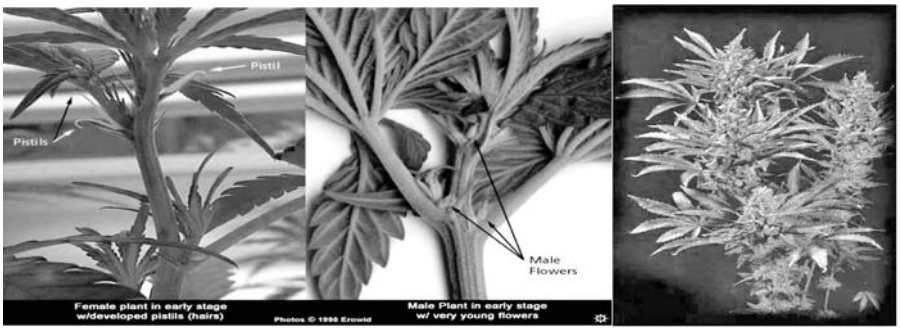

Cannabis halucinogenic compounds

Marijuana represent the finely cut plant, including inflorescents, having the appearence of a usual tea. It can be identified by its specific soil-like smell of crashed Cannabis. Hashish is a brown resin. Usually in drug abuse practices is used in the shape of small balls, called in slang "cakes". It can be smoked or chewed, sometimes it is applyed directly to the gums by friction. Hashish oil represent a plant extract with a more powerfull action, since one drop of oil into a cigarette equivalents to one hashish pipe.

Chemical composition of Cannabis

The basic compounds to cause phisiological efeects are cannabinoids. The plants also contain nitrogen organic substances like proteins, glucoproteins and enzimes. The spectrum of known components also includes simple alcohols, aldehydes, ketones, fatty acids, esters and lactones, terpenes, steroids, fenolic compounds as well as flavonoid glicosides.

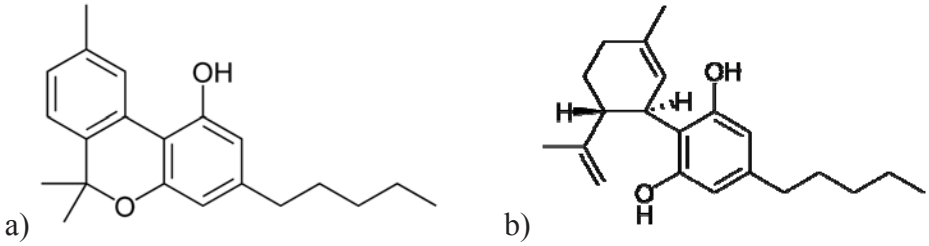

Figure 1

The most abundant components with confirmed activity are cannabinol (a) and cannabidiol (b) (Figure 1). It is considered that canabinol is not a plant catabolism product, but an artefact derived from plant conservation [5]. Tetrahidrocannabinol (THC) is administered under the name Dronabinol and is a part of medical preparations known as Merezine, Marinol. It represent a remedy in the case of anurexia in AIDS patients, conected to abrupt weight loss, nausea and sickness, chemiotherapy side effects in cancer patients where other usual preparations are not effective. For this purpose THC is administered in doses of 2 to 20 mg per day in tablets or capsules for oral usage. THC is absorbed almost entirely (90-95%) after oral administration. Due to combined effects of liver metabolism and encreased lipophylicity only 10-20% of the dose reach the blood stream. THC has a large repartition volume, almost 10l/kg and more then 95%. It is bounded alon with derived metabolites to sanguin proteins. THC elimination phase is caracterized by a bicompartimental model with an initial phase having the elimination period of 4 hours and the β- phase having the elimination period from 25 to 36 hours. Due to the large repartition volume, THC metabolites can be detected in urine at minimal level for a long period of time.

Marijuana intoxication symptoms

Patients of marijuana abuse present chronic coughing, red eyes, fatigue, exagerated appetite, attraction to drugs, drowsiness, sensitivity to viral infections, sclerotic dysfunction, impaired speech, difficulty in communication, abrupt change from passive to aggressive mood, dizziness. The pictures below are sugestive in this context.

Analgesic properties of marijuana compounds

Although the analgesic properties of marijuana are known since 2000 years ago, investigation of anti-nociceptive role of cannabinoids turned out to be difficult, since their receptors were unknown. The interest towards analgesic properties of marijuana has encreased gradually in the 19-th century.

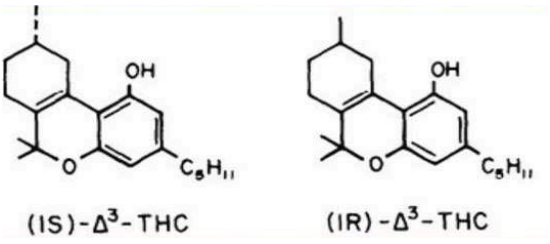

The racemic mixture of enantiomeric cannabinoids 1*S*- Δ^3-THC and 1*R*-Δ^3-THC have been synthesized in 1940. The oral use of cannabis has been reported to sucsessfully alleviate labor pain, as well as other pain-related states. The

systematic study of analgesic compounds and their action mechanism hs been initiated in the late 90-s of the last century and is connected to the discovery of cannabinoid receptors. They are located in the brain (talamus, hippocampus) and spinal cord. A special breakthrough was made in 1992 with the discovery of an endogen compound with the ability to bind to cannabinoid receptors. It is a derivative of arachidonic acid (arachidonyl-ethanol amide) called trivially anandamide (deriving from ancient sanscrit meaning happiness). Its action is similar to that of THC. Besides, a large number of cannabinoids have been produced synthetically. They have proved to be efficient anti-nociceptive agents and inflamation modulators.

THC is metabolized intensively in liver by oxidative degradation processes. The obtained metabolites posess different activity and could be detected in the urine [1,7]. Their elimination takes place via gastro-intestinal and urinary pathways. For analytical detection an extraction step is mandatory, followed by HPLC analysis on RP columns. Hyphenated techniques, such as LC-MS and GC-MS lower the detection limits to 0.05-0.01 ng/ml values [2,3,4,6,8]. Identification of metabolized is confirmed by tandem MS-MS experiments.

Acknowledments. Academy of Sciences (Moldova) and CNR (Italy) are acknowledged for financial support (bilateral project 11.820.08.01/ItF "Novel approaches for the synthesis of optically active cannabinoids with relevant biological activity and therapeutical potential" 2011-2012).

Dr. Tamara Cotelea was born on june 26, 1959 in Butesti village, Glodeni district, Republic of Moldova. She graduated from the Pharmacy Department of „N. Testemitanu" State Medical and Pharmaceutical University and worked as a pharmacist. Starting from 1991 she was a didactic staff of the Pharmacy Department, chair of pharmaceutical and toxicological chemistry. She got the PhD in 2002 with prof. Filip Babelev and in 2005 was appointed Assistant Professor, responsible for teaching courses. In the period 2005-2007 Dr. Cotelea was an expert of Drug Agency, member of the pharmaceutical evaluation and coordination for implementing GMP practices Board. She has contributed with more then 60 papers in the field of drug research. The main research area relates to analytical chemistry, specifically implementation of physico-chemical methods of analysis of drugs in complex matrix. She is a member of the International Association of Forensic Toxicologists.

References

[1]. Balabanova, S.; Arnold, P.J.; Luckow, V.; Brunner, H.; Wolf, H.U. Tetrahydrocannabinole in haar von haschischrauchem. *Z.Rechtsmed.* **1989**, *102*, pp. 503-508.

[2]. Baumgartner, W.A.; Chen-Chih, C.; Donahue, T.D.; Hayes, G.F.; Hill, V.A.; Scholtz, H. Forensic drug testing by mass spectrometric analysis of hair. In: *Forensic applications of mass spectrometry.* Ed. Jehuda Yionon. London, Tokyo. CRC Press: Boca Raton, Ann Arbor, **1995**. pp. 61-94.

[3]. Baumgartner, W.A.; Hill, V.A.; Baer, J.D.; Lyon, I.W.; Charuvastra, V.C. Detection of drug use by analysis of hair. *J. Nucl. Med.* **1988**, *29(* 5), p. 980.

[4]. Crimele, V.; Kintz, P.; Mangin, P. Testing human hair for cannabis. *Forensic. Sci Int.* **1995**, *70*, pp. 175-182.

[5]. Crimele, V.; Satchs, H.; Kintz, P.; Mangin, P. Testing Human Hair for Cannabis. III. Rapid Screening Procedure for the Simultaneous Identification of delta-9-tetrahydrocannabinol, Cannabinol and Cannabidiol. *J.Anal. Toxicol.* **1995**, *20*, pp. 13-16.

[6]. Clarke′s isolation and identification of drugs in pharmaceuticals, body fluids and post-mortem material. Ed. Moffat, A.C. The Pharmaceutical Press. London. **1986**.

[7]. El-Sohly, M.A. Urinalysis and casual handing of marjuana and cocaine. *J.Anal. Toxicol.* **1991**, *15*. p. 46.

[8]. Fihbein, L. Chromatography of environmental hazards. V. IV. Drugs of abuse. Elsevier scietific publishing company. Amsterdam, Oxsford, New York. **1982**.

EXPLORING THE CHEMISTRY OF MARINE OPISTHOBRANCHS: RECENT RESULTS

Margherita Gavagnin

Istituto di Chimica Biomolecolare (ICB),Consiglio Nazionale delle Ricerche,
Via Campi Flegrei, 34, 80078 Pozzuoli (Na), Italy
e-mail: margherita.gavagnin@icb.cnr.it, phone: +39 0818675094, fax: +39 0818041770

Abstract: The current communication is an extended abstract of the presentation delivered on the joint Moldo-Italian seminar "New frontiers in natural product chemistry", held in the Institute of Chemistry, Academy of Sciences of Moldova on 30th September. An overview of the recent studies conducted by our group on opisthobranch molluscs from distinct geographical areas is briefly presented.

Introduction

Marine opisthobranch molluscs are apparently unprotected by the physical constraint of a shell which is either reduced or completely absent in the adults. Their survival is based on a series of defensive strategies, which include the use of deterrent or toxic molecules. Opisthobranchs obtain their chemical "weapons" by either bio-accumulation of selected metabolites from their dietary sources, bio-transformation of dietary compounds, or *de novo* bio-synthesis [1]. Thus they represent a remarkable source of bioactive molecules that have been selected in nature to play fundamental roles for the survival of the species that contain them. This reveals an extraordinary library of compounds that could be considered excellent drug candidates. Among others, a remarkable example is represented by jorumycin (**1**), the defence allomone of the opisthobranch *Jorunna funebris*, which was isolated some years ago by our group from the mantle and the mucus of the mollusc [2]. The synthetic analogue of jorumycin, Zalypsis® (PharmaMar), is now in phase II clinical trial for the treatment of endometrial and cervical tumours [3]. This communication presents an overview of our recent results obtained studying opisthobranchs collected in different sites around the world, in the frame of international collaboration programs.

The chemical investigation of a Chinese population of *J. funebris* [4] has led to the isolation of a series of alkaloids analogues of jorumycin (i.e. **2**-**4**), which were differently distributed in the distinct parts of the animal suggesting possible different biological properties. In the internal organs a plethora of isoquinoline-quinone alkaloids probably derived from the oxidative degradation of renieramycins were also found [4].

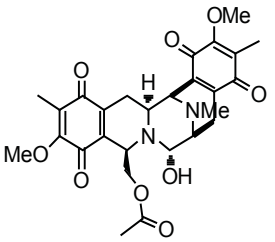

jorumycin (**1**)

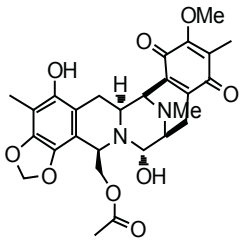

2

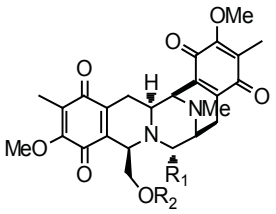

3: R_1= CH_2COCH_3; R_2= H
4: R_1= CH_2COCH_3; R_2= $COCH_3$

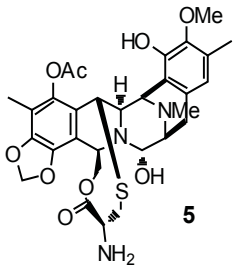

5

A new member of the ecteinascidin family, compound **5**, structurally related to jorumycin and renieramycin series, has been isolated from the external part of some specimens of the eolidacean nudibranch *Phidiana militaris*, collected in South China Sea [4]. In addition, the extract of the mollusc contained two other new and extremely interesting molecules: phidianidine A (**6**) and B (**7**) exhibiting an uncommon carbon skeleton with a 1,2,4-oxadiazole system never reported from marine natural products [5]. This structural moiety has been found only in quisqualic acid isolated from the fruits of a tropical plant. Even though the 1,2,4-oxadiazole system is so rare, there is a wide interest in the synthesis of compounds containing this scaffold due to the broad spectrum of biological properties. The cytotoxicity of phidianidines has been evaluated in terms of cell grow inhibition and the results are very interesting. Both compounds have shown high cytotoxicity against various tumour and non-tumour mammalian cell lines at nanomolar concentration [5]. The specificity towards some cell types relative to others (strongly active against C6 and HeLa cancer cell lines) suggests the existence of specific interactions with biological targets.

Remaining in the eolidacean group, the chemical investigation of two different *Spurilla* species from Argentina and Italy has revealed a different composition of the terpene content of the two molluscs. A new molecule, diterpene **8**,

has been characterized in this study [4]. Very interestingly, bursatellin **9**, structurally related to antibiotic chloramphenicol and previously reported from the anaspidean *Bursatella,* has been found in both species.

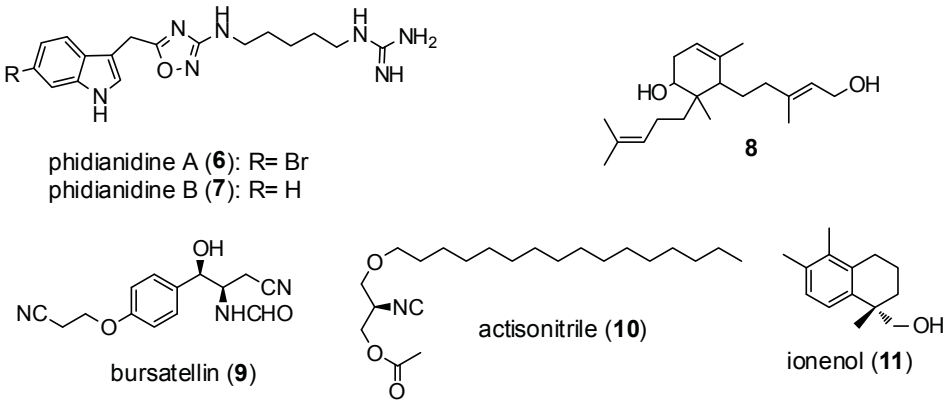

The chemistry of the nudibranch *Actinocyclus papillatus* from South China Sea is very interesting [6]. The main metabolite of the mantle extract is the novel molecule actisonitrile (**10**). This compound is an ether lipid with a glyceryl-like moiety in which the secondary hydroxyl function is replaced by an isocyanide group. Another uncommon compound, methyl-β-ionene alcohol (**11**) has been also found in both mucus and mantle. The two molecules were tested for the cytotoxicity against a series of tumour and non-tumour cell lines. Actisonitrile revealed a moderate activity suggesting to further investigate the pharmacological potential. In this light, it was necessary to complete the structure determination of actisonitrile (**10**) with regards to the assignment of the absolute configuration of the single chiral centre.

The stereospecific synthesis of both enantiomers of actisonitrile was planned with the aim at comparing the optical properties of synthetic products with natural **10** [6]. In Scheme 1 are reported all steps to construct one of the two enantiomers. The enantiomer with the opposite configuration has been prepared in the same way starting from the same precursor with the opposite chirality. The comparison of the optical rotation values and the circular dichroism profiles of synthetic compounds with those of natural product led us to establish that actisonitrile has the *R* configuration.

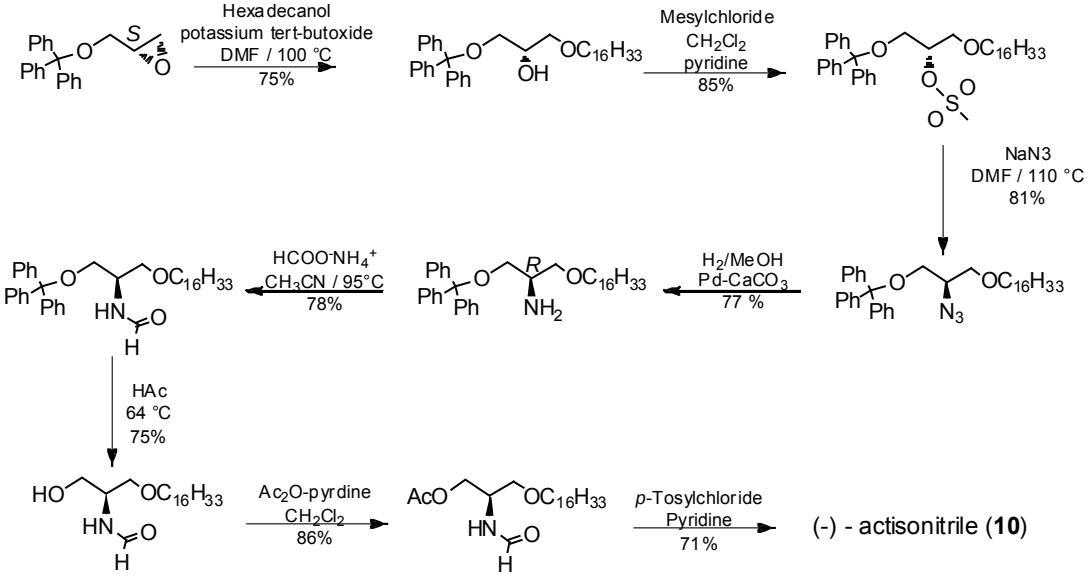

Scheme 1

The family Chromodorididae is the most studied group of nudibranchs from a chemical point of view. Most species belonging to this family contain dietary terpenes which are generally accumulated in the border of the mantle or in mantle dermal formations. Some selected species collected in South China Sea have been analyzed [4]. *Chromodoris reticulata* was found to contain aplyroseol-2 (**12**) as main metabolite along with other two known related diterpenes (**13**,**14**). All three diterpenes have been reported to be cytotoxic being aplyroseol-2 the most active [7]. Aplyroseol-2 has been demonstrated to be also unpalatable for the marine shrimp *Palamon elegans* [4]. This very nice and simple

assay has been performed in our lab [8]. The use of colored pellets allows to observe easily if the food treated with the compound to be tested is accepted or rejected by a generalist predator. Similar diterpene components including aplyroseol-2 (**12**) have been isolated from *Chromodoris sinensis* [4]. In the mantle border of the animal, we were able to detect by ^{1}H-NMR analysis the unstable compound **15** exhibiting two dialdehyde groups that is the precursor of **12**. This molecule is highly reactive and is rapidly converted into the corresponding lactone-hemiacetal derivative **12**. The comparison of the proton spectra of the same sample before and after the filtration on silica-gel clearly demonstrates the rapid transformation [4]. Known degraded spongiane diterpenes (i.e. **16**,**17**) have been isolated from *Chromodoris geometrica* [4]. A correspondence between the ecological and the pharmacological activity could be observed also in this case. Particularly interesting are the pharmacological properties of macfarlandin-E (**16**) and norrisolide (**17**) that exhibit a potent and unique Golgi-modifying activity [9]. Analogously with other *Glossodoris* species, the chemistry of *Glossodoris cincta* is characterized by the presence of sesterterpenes. Heteronemin (**18**) is the main component of the terpene pattern of the nudibranch and is also the most active showing several different biological properties. In particular, it has been recently reported that heteronemin is a potent and promising inhibitor of TNFα-induced NF-kB activation [10].

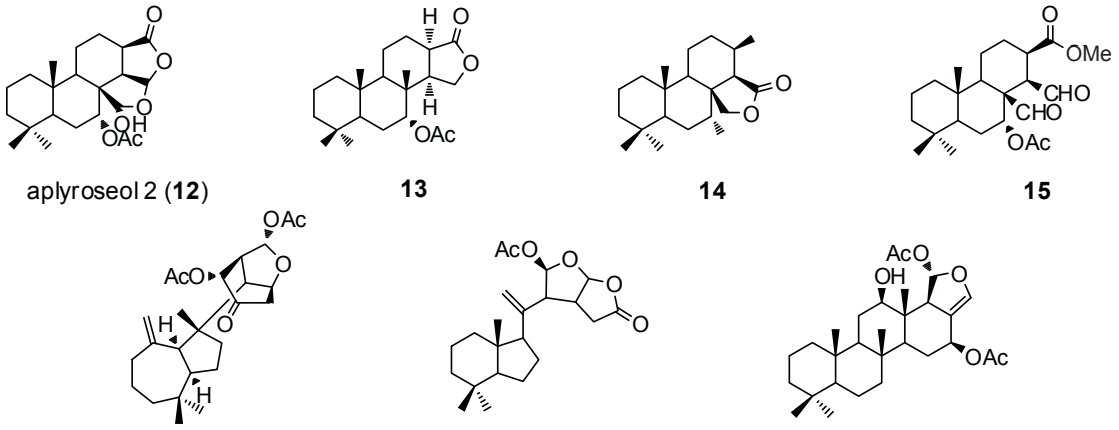

The chemistry of the nudibranch *Dermatobranchus ornatus* from South China Sea has been found to be characterized by some known diterpenes with eunicellin skeleton (i.e. **19**). These molecules are sequestered from a gorgonian of genus *Muricella* and accumulated in the mantle of the animal [11]. Cytotoxic properties have been reported in the literature for some of these compounds [12]. Structurally related molecules, named tritoniopsins (**20**,**21**), characterized the metabolite pattern of a Chinese population of *Tritoniopsis elegans* which was found associated to the soft coral *Cladiella krempfi* [13]. All isolated compounds, which were also detected in the prey, were evaluated for the cytotoxic activity. Tritoniopsin B (**21**) was the most active.

The secondary metabolite pattern of Mediterranean *Discodoris atromaculata* is dominated by a series of long-chain polyacetylenes, named fulvynes (i.e. **22**) all deriving from the sponge *Haliclona fulva* on which the animal feeds [4]. The biological properties of these molecules have not yet been investigated. However, it is interesting to note that they are structurally related to petrocortyne A, which is a potent modulator of the transcription factor NF-kB [14].

The chemistry of the nudibranch *Tambja ceutae* collected at Azores along with the bryozoan *Bugula dentata* was found to be characterized by a series of 4-methoxy-pyrrolic alkaloids belonging to the tambjamine family [15]. Tambjamines are reported to intercalate DNA and facilitate single-strand DNA oxidative cleavage. The new member we isolated (tambjamine K, **23**) has displayed a significant antiproliferative activity against different tumor and non-tumor cell lines.

The chemical studies on a population of circumtropical anaspidean *Syphonota geographica,* collected along the Greek coasts, led us to discover very interesting bioactive natural products [16-19]. The skin metabolites, aplykurodinones (i.e. **24**), are degraded sterols that are typical of different species of the family Aplysiidae from distinct geographical areas [16].

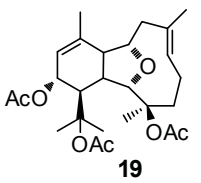

19

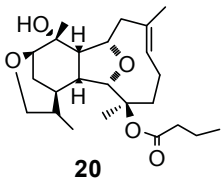

20

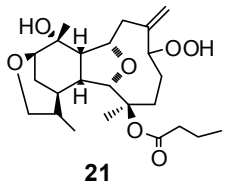

21

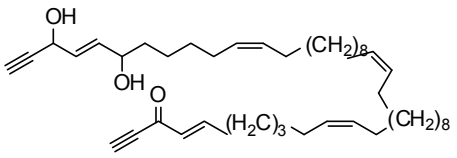

22

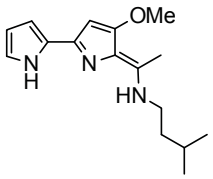

tambjamine K (**23**)

The metabolite pattern of the inner organs was found to be dominated by the presence of syphonoside (**25**), a macrocycle with a unique structure, that inhibits high-density induced apoptosis [17]. This bioactive compound is sequestered from the sea-grass *Halophila stipulacea*, prey of the mollusc. Further studies on both the mollusc and the sea-grass have resulted into the finding of a series of novel minor syphonoside-related compounds (i.e. **26**) [18] as well as of two very rare malonyl flavones (i.e. **27**) [19].

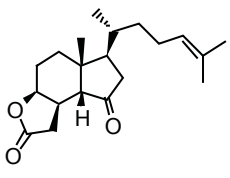

24

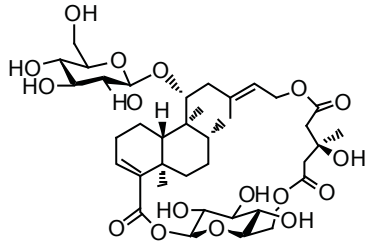

syphonoside (**25**)

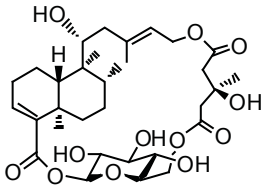

26

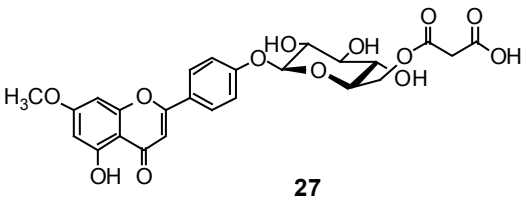

27

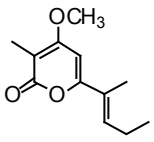

28

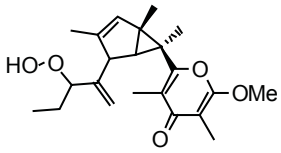

phototridachiapyrone J (**29**)

Finally, a few examples of chemicals isolated from sacoglossans should be mentioned. The Azorean *Aplysiopsis formosa* was found to contain aplysiopsenes (i.e. **28**) [20]. These compounds belong to the sacoglossan polypropionate family and are the smallest members to date isolated. Polypropionates interact with the light by trapping oxygen and therefore protecting the molluscs from sunlight damage. So it has been suggested a possible use as sunscreen in the solar creams [21]. The chemical study on *Elysia patagonica* from Argentina has led to the finding of a new member of elysioidean polypropionates, tridachiapyrone J (**29**) [4]. This molecule is probably formed by a photochemical conversion of a suitable precursor containing the reactive conjugated diene system [21]. However, the main secondary metabolite of *Elysia patagonica* has resulted to be the osmolyte proline betaine [4]. Our studies have demonstrated that this compound, which is accumulated in the mollusc, derives from the diet, the alga *Bryopsis plumosa*. Comparison of the proton spectrum of proline betaine purified from the mollusc extract with that of crude extract of the alga clearly showed the presence of this compound in the alga. In addition, we have also proven that Mediterranean sacoglossans *Ercolanea funerea*, *Caliphylla mediterranea* and *Placida dendritica* all feeding on *Bryopsis plumosa*, analogously with *Elysia patagonica*, are able to sequester proline betaine from the diet and accumulate this molecule in the defensive mucous secretion.

Conclusions. The examples presented here clearly indicate that marine opisthobranch molluscs are a remarkable source of natural products with a high pharmacological potential. The large chemical diversity observed in these organisms reflects their ability of colonizing several different ecological niches and establishing trophic relationships with organisms of different phyla, from which they select bioactive molecules.

Acknowledments. Academy of Sciences (Moldova) and CNR (Italy) are acknowledged for financial support (bilateral project Kulcitki/Gavagnin "Novel approaches for the synthesis of optically active cannabinoids with relevant biological activity and therapeutical potential").

Margherita Gavagnin was born in Naples in 1959. She received her doctoral degree in organic Chemistry in 1983 from Naples University. She spent one postdoctoral year at the Institute of Organic Chemistry of Naples, working in the field of marine natural products. In 1985 she moved, as researcher of the Italian National Council of Research, to the Institute of Chemistry of Molecules of Biological Interest, now Institute of Biomolecular Chemistry, where she has been First Researcher and subsequently Research Director. She has been in charge of research project management in CNR and responsible of several national research projects and bilateral co-operation programmes. She has been member of the Scientific Council of ICMIB and member of ICB Committee. During these years, the scientific activity has been mainly oriented to the chemical characterization of bioactive marine natural products. Most studies have been focused to opisthobranch molluscs, which represent extraordinary models to select lead-compounds for drug development. She is author of more than 130 papers.

References

[1]. G. Cimino, A. Fontana, M. Gavagnin *Curr. Org. Chem*., **1999**, *3*, 327-372; G. Cimino, M.L. Ciavatta, A. Fontana, M. Gavagnin. In C. Tringali (Ed.) Bioactive compounds from natural sources Taylor & Francis, London, **2001**, pp.579-637; G. Cimino, M. Gavagnin (Eds) Molluscs. From Chemo-ecological Study to Biotechnological Application. Vol. 43, Springer **2006**; G. Cimino, A. Fontana, A. Cutignano, M. Gavagnin *Phytochem. Rev*., **2004**, *3*, 285-307.

[2]. A. Fontana, P. Cavaliere, S. Wahidullah, C.G. Naik, G. Cimino *Tetrahedron*, **2000**, *56*, 7305-7308.

[3]. a) G. Cimino, A. Fontana, S. Wahidulla, C. G. Naik, D. G. Gravalos. WO 2000-GB3489-2000/09/11. PCT Int. Appl. 2001:1–9. b) EP20000958872. July 2003. c) WO/2007/052076. May 2007.

[4]. Unpublished results.

[5]. M. Carbone, Y. Li, C. Irace, E. Mollo, F. Castelluccio, A. Di Pascale, G. Cimino, R. Santamaria, Y.-W. Guo, M. Gavagnin, *Org. Letters*, **2011**, *13*, 2516-2519.

[6]. E. Manzo, M. Carbone, E. Mollo, C. Irace, A. Di Pascale, Y. Li, M. L. Ciavatta, G. Cimino, Y.-W. Guo, M. Gavagnin, *Org. Letters*, **2011**, *13*, 1897-1899.

[7]. T. Miyamoto, K. Sakamoto, K. Arao, T. Komori, R. Higuchi, T. Sasaki *Tetrahedron* **1996**, *52*, 8187-8198.

[8]. E. Mollo, M. Gavagnin, M. Carbone, F. Castelluccio, F. Pozone, V. Roussis, J. Templado, M. T. Ghiselin, G. Cimino, *PNAS*, **2008**, *105*, 4582-4586.

[9]. T.P. Brady, E.K. Wallace, S.H. Kim, G. Guizzunti, V. Malhotra, E.A. Theodorakis *Bioorg. Med. Chem. Lett.*, **2004**, 14, 5035-5039.

[10]. M. Schumacher, C. Cerella, S. Eifes, S. Chateauvieux, F. Morceau, M. Jaspars, M. Dicato, M. Diederich, *Biochem. Pharmacology*, **2010**, *79*, 610-622.

[11]. W. Zhang, M. Gavagnin, Y.-W. Guo, E. Mollo, G. Cimino, *Chin. J. Org. Chem*., **2006**, *26*, 1667-1672.

[12]. M. Ochi, K. Yamada, K. Shirase, H. Kotsuki *Heterocycles* **1991**, *32*, 19–21; N. Fusetani, H. Nagata, H. Hirota, T. Tsuyuki *Tetrahedron Lett.* **1989**, *30*, 7079-7082.

[13]. M.L. Ciavatta, E. Manzo, E. Mollo, C. A. Mattia, C. Tedesco, C. Irace, Y.-W. Guo, G. Cimino, M. Gavagnin, *J. Nat. Prod.*, **2011**, *74*, 1902–1907.

[14]. F. Folmer, M. Jaspars, M. Dicato, M. Diederich, *Biochem. Pharmacology*, **2008**, *75*, 603-617.

[15]. M. Carbone, C. Irace, F. Costagliola, F. Castelluccio, G. Villani, G. Calado, V. Padula, G. Cimino, J. L. Cervera, R. Santamaria, M. Gavagnin, *Bioorg. Med. Chem. Lett.*, **2010**, *20*, 2668-2670.

[16]. M. Gavagnin, M. Carbone, M. Nappo, E. Mollo, V. Roussis, G. Cimino, *Tetrahedron*, **2005**, *61*, 617-621.

[17]. M. Gavagnin, M. Carbone, P. Amodeo, E. Mollo, R. M. Vitale, V. Roussis, G. Cimino, *J. Org. Chem.*, **2007**, *72*, 5625-5630.

[18]. M. Carbone, M. Gavagnin, E. Mollo, M. Bidello, V. Roussis, G. Cimino, *Tetrahedron*, **2008**, *64*, 191-196.

[19]. F. . Bitam, M.L. Ciavatta, M. Carbone, E. Manzo, E. Mollo and M. Gavagnin, *Biochem. System. Ecol.*, **2010**, *38*, 686-690.

[20]. M.L. Ciavatta, E. Manzo, G. Nuzzo, G. Villani, J. L. Cervera, G. Cimino, M. Gavagnin, *Tetrahedron Lett.*, **2009**, *50*, 527-529.

[21]. C. Ireland, P.J. Scheuer, *Science.* **1979**, *205*, 922- 923.

SYNTHETIC APPROACHES TO POLIFUNCTIONALIZED PERHYDRINDANES

Veaceslav Kulciţki

Institutul de Chimie al AŞ a RM, str. Academiei, 3, MD-2028, Chişinău, Republica Moldova
e-mail: kulcitki@yahoo.com, phone: +373 22 739769, fax: +373 22 739954

Abstract: The current communication represents an extended abstract of the presentation delivered on the joint Moldo-Italian seminar "New frontiers in natural product chemistry", held in the Institute of Chemistry, Academy of Sciences of Moldova on 31 September. An overview of the synthetic methods oriented to the synthesis of functionalized terpenic perhydrindanes is provided. Different synthetic strategies are considered, including those based on biomimetic approach. The array of obtained new structures can serve as leads in structure-activity studies as well as useful building blocks towards other perhydrindanes.

Introduction

The perhydrindane fragment represents a structural motif broadly found in natural products frequently connected to relevant biological activities. The incorporation of this substructure in the certain molecule can be of two distinct fashions: as a part of a condensed polycyclic system (steroids, giberellins) or as a "stand alone" fragment (vitamine D, rearranged spongiane diterpenoids).

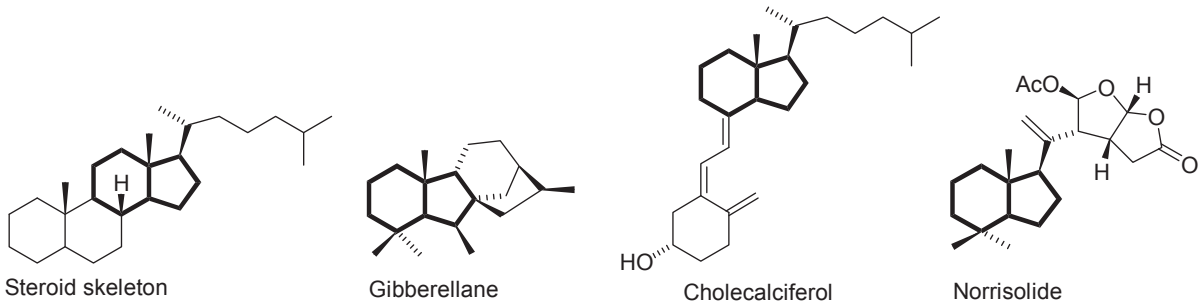

The "stand alone" disposal of perhydrindane moiety is inevitable accompanied by a certain degree of functionalization, and due to the inconveniences connected to the use of this fragment from natural sources, considerably efforts have been undertaken to access functionalized perhydrindanes by synthesis. Different strategies have been reported in the literature, the most proeminent ones are depicted in scheme 1.

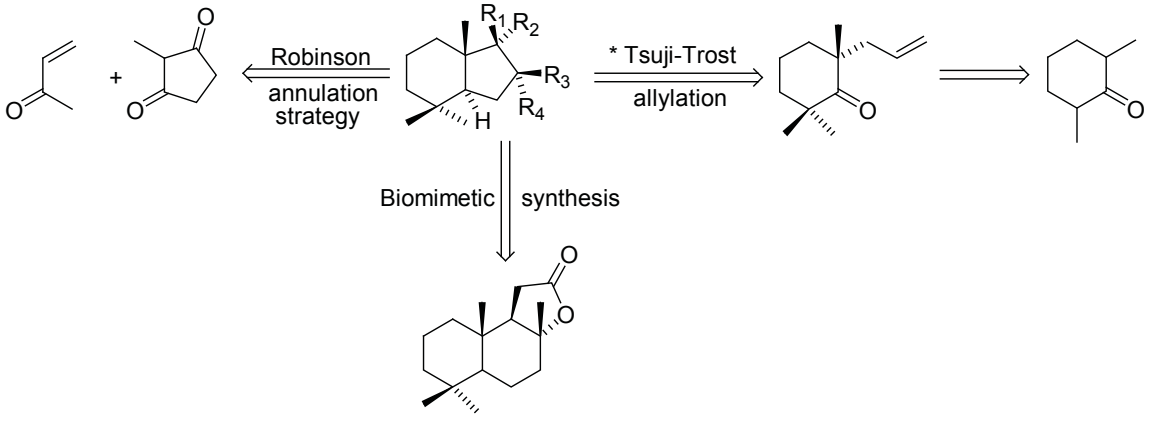

Scheme 1

The current communication presents an outline of synthetic procedures based on different strategies and elaborated in our research group for the synthesis of B-ring functionalized perhydrindanic core.

Biomimetic strategy. The biomimetic strategy in retrosynthetic analysis of perhydrindanic natural products relies on a ring contraction process. Potential substrates are drimanes or homodrimanes, easily accessible from commercial sclareolide. We have used this strategy for the successful synthesis of austrodoral and austrodoric acid - two compounds

of marine origin, isolated by Gavagnin and coworkers from the dorid nudibranch *Austrodoris Kerguelenensis* [1]. The key transformation was a ring contraction of suitable functionalized drimanic or homodrimanic epoxides (scheme 2) [2,3].

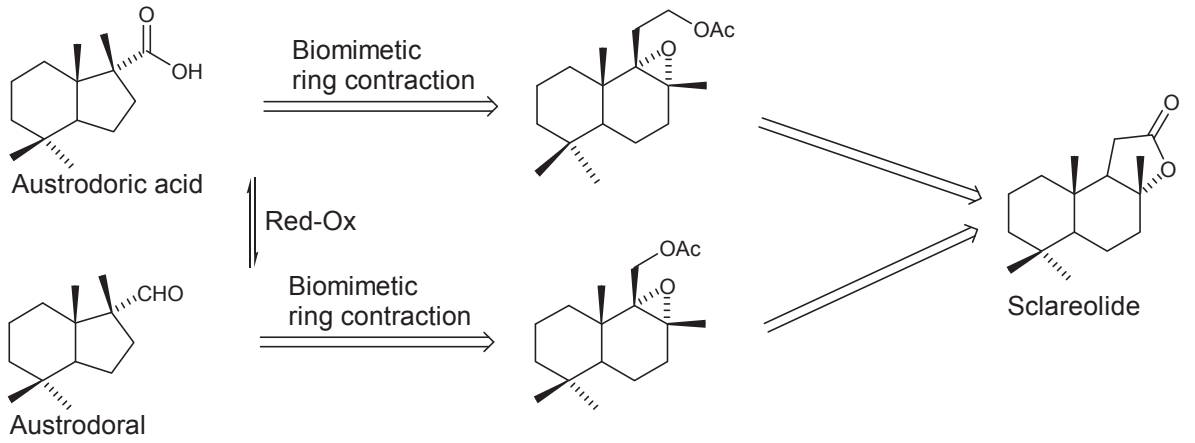

Scheme 2

Tsuji-Trost enantioselective allylation strategy. This strategy has been reported previously by several authors and we have adapted it in order to get a deeper functionalisation of the B-ring. Accordingly, the carboxymethyl group has been introduced by a formylation protocol. The double bond on the A-B junction was selectively reduced by nickel boride to provide the cis-fused perhydrindane (scheme 3).

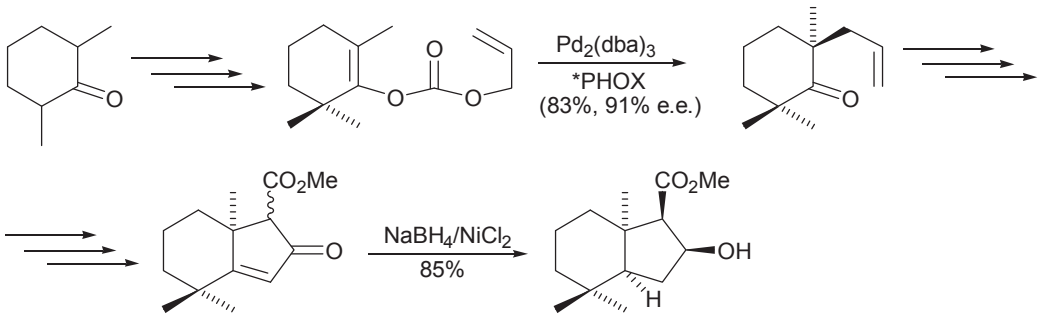

Scheme 3

Intramolecular aldol strategy. The starting material represents the known keto-acid, readily available from sclareolide (scheme 4). The synthetic sequence leading to bicyclic structure includes a oxidative decarboxylation which lead to a primary iodide. Substitution of the iodine for hydroxyl group and Jones oxidation led to the keto-aldehyde, which underwend a smooth intramolecular aldol condensation to provide the functionalized perhydrindane. Further deoxigenation led to the known saturated ketone, used previously for the synthesis of important rearranged spongian terpenes of marine origine [4].

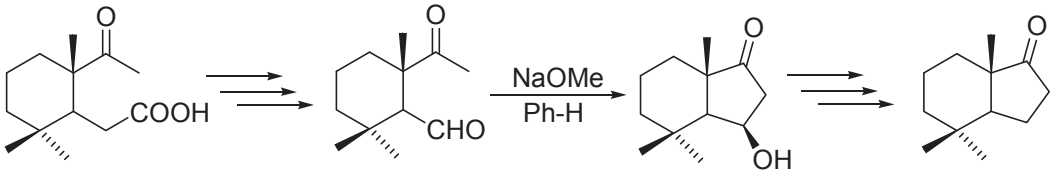

Scheme 4

Conclusions. A whole series of new B-ring functionalized terpenic perhydrindanes have been synthesized using different synthetic strategies. The obtained compounds will be further involved in chemical modification and activity testing studies.

Acknowledments. Academy of Sciences (Moldova) and CNR (Italy) are acknowledged for financial support (travel grant 11.820.08.01/ItF).

Dr. Veaceslav Kulcitki was born in 1969. He graduated from Moldova State University in 1992 and obtained the Ph.D. degree in 1998 from the Institute of Chemistry, Moldova Academy of Sciences, under the supervision of Professor P. F. Vlad and Dr. Sci. N. Ungur. He was a postdoctoral fellow with Professor Guido Cimino (ICB, Naples, Italy) and Professor Oliver Reiser (Regensburg University, Germany) being involved in different projects connected to natural products and synthetic organic chemistry. He is the author of more than 70 publications, including review articles, book chapters and two patents. Dr. Kulcitki has been appointed Associated Professor in 2006 and holds currently the position of a senior scientific researcher at the Institute of Chemistry, Moldova Academy of Sciences. His research interests include synthesis of natural products by biomimetic approaches, including electrophilic cyclisations and molecular rearrangements.

References

[1]. Gavagnin, M.; Carbone, M.; Mollo, E.; Cimino, G. *Tetrahedron Lett.* **2003**, *44*, 1495–1498.
[2]. Kulcitki, V.; Ungur, N.; Gavagnin, M.; Carbone, M.; Cimino, G. *Tetrahedron Asymm.,* **2004**, *15* (3), 423-428.
[3]. Kulciţki, V.; Ungur, N.; Gavagnin, M.; Carbone, M.; Cimino, G. *Eur. J. Org. Chem.,* **2005**, (9), 1816–1822.
[4]. Brady, T.P.; Kim, S.H.; Wen, K.; Theodorakis, E.A. *Angew. Chem.,Int. Ed.,* **2004**, *43*, 739-749.

SYNTHETIC STRATEGY FOR THE PREPARATION OF BIOACTIVE GALACTOGLYCEROLIPIDS

Emiliano Manzo*, Maria Letizia Ciavatta, Dario Pagano and Angelo Fontana.

Institute of Biomolecular Chemistry (National Council of Research), via Campi Flegrei 3-80078, Pozzuoli (Naples-Italy). Email: emanzo@icb.cnr.it

Abstract: The current communication represents an extended abstract of the presentation delivered on the joint Moldo-Italian seminar "New frontiers in natural product chemistry", held in the Institute of Chemistry, Academy of Sciences of Moldova on 30 September. A simple and efficient strategy for the synthesis of galactoglycerolipids is provided.

Introduction

Glycolipids, carbohydrate-linked lipids, are membrane components and are present in all the living organisms kingdoms, i.e. bacteria, plants and animals. They have important roles as energy source and markers for the cellular recognition and communication. Structurally they can be divided in different families like glycoglycerolipids, with acylated glycerol attached to the carbohydrate part, glycosphingolipids with an acylated sphingosine (ceramide) and isoprenoid glycosides, with a terpene alcohol as aglycon. All this kind of molecules are characterized by very important biological activities.[1,2] There is a big interest in both intracellular and extracellular glycolipids. In the last years, members of the family, especially galactosyldiacylglycerols and ceramides, have attracted the interest of the bio-medical community for their properties in cancer chemoprevention[3] and immunology;[4] on the other side sulphoquinovosyldiacylglycerols are characterized by other extensive biological properties as antitumoral,[5] HIV-RT inhibition,[5,6] AIDS-antiviral[7] and DNA polymerase α and β inhibition.[8] The possibility to get these compounds by chemical synthesis is important cause the difficulty in their isolation and purification from natural sources; the synthetic approach can give the opportunity to study the potential activity of these molecules whose structure could be modified in different ways to run SAR analysis. Here we discuss a simple and versatile strategy for the synthesis of galactosyldiacylglycerols.

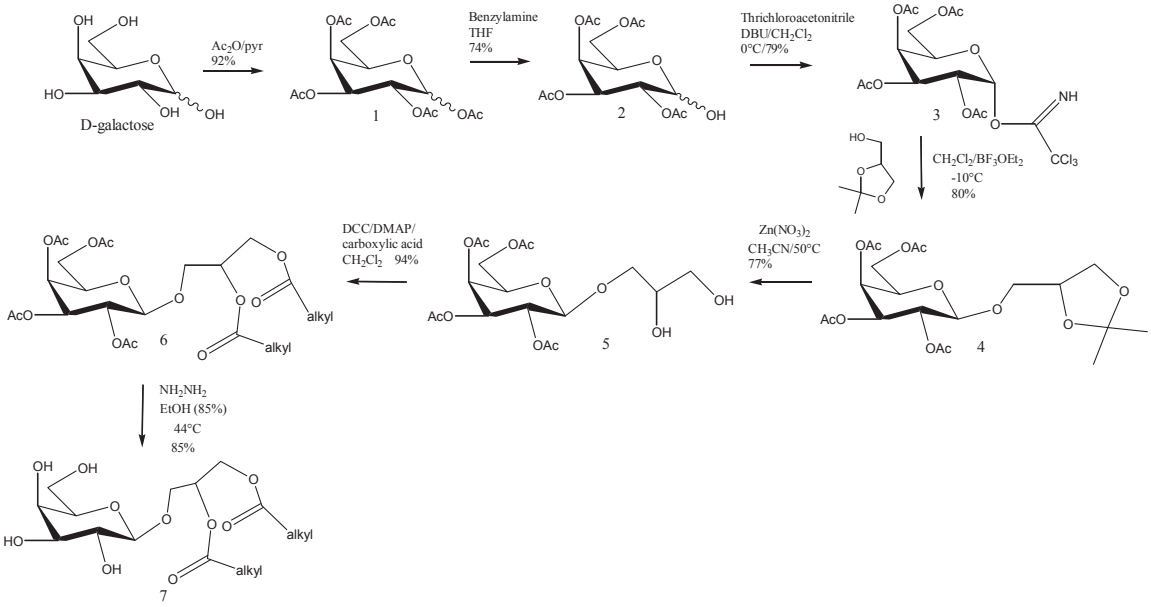

Scheme 1. Synthesis of β- galactosyl-1,2-diacylglycerols

Synthetic strategy (Scheme 1). D-galactose was acetylated (**1**) and the subsequent anomeric deacetylation was performed by benzylamine to get **2**. The hydroxyl anomeric function was derivatized by trichloroacetonitrile in presence of 1,8-Diazabicyclo[5.4.0]undec-7-ene (DBU); the trichloroacetimidate obtained (**3**) was coupled with glycerol 1,2-acetonide (derived by acetonidation of glycerol with 2,2-dimethoxypropane and *p*-toluensulfonic acid in *N,N*-dimethylformamide) to get **4**. After the removal of the isopropylidene protecting group with zinc nitrate in acethonitrile, we obtained compound **5** that was acylated with the carboxylic acids (i.e. linolenic acid) in presence of diciclohexylcarbodiimide and triethylamine; the final step, the deacetylation of **6**, was very important cause the presence

of acyl unsatured moiety that should be unaltered using less amount (in comparison of literature conditions[9]) of hydrazine hydrate at 44°C to get **7**. Using more amount of hydrazine hydrate and increasing the temperature until 55°C, saturation of acyl double bonds happened, and on the other side, partial deacylation yielded to the β-galactosyl-monoacylglycerol (15%) in which the linolenyl residue was on the primary position of the glycerol part.

Conclusions. Synthesis of β-galacto-1,2-diacylglycerols is achieved by a versatile and simple procedure based on the trichloroacetimidate methodology and peracetate sugar precursors. The methodology is tested through stereoselective preparation of β-galacto-lipids representing compounds that have been recently gained great interest as triggers of immune system response. The synthetic strategy is designed to obtain regio- and stereo isomers including derivatives containing poly-unsaturated fatty acids.

Acknowledments. Academy of Sciences (Moldova) and CNR (Italy) are acknowledged for financial support (bilateral project Kulcitki/Gavagnin "Novel approaches for the synthesis of optically active cannabinoids with relevant biological activity and therapeutical potential").

Dr. Emiliano Manzo was born in 1973. He graduated from University of Naples (Italy)-Federico II in 1996 and obtained his Ph.D. degree in 2001 from University of Naples (Italy)-Federico II, Chemistry Department, under the supervision of Professor Michelangelo Parrilli; in 2001 he was researcher in the Institute of Biomolecular Chemistry (Pozzuoli-Naples) of the National Research Council (CNR), where he works on the chemical synthesis of marine natural compounds and on the isolation from marine invertebrates of new compounds with important biological activity and with potential pharmacological applications. He is the author of more than 45 scientific papers and three patents.

References

[1]. Oshida,Y.; Yamada,S.; Matsunaga, K.; Moriya, T.; Ohizumi, Y., *J.Nat.Prod*., **1994**, 57(4), 534-536.

[2]. Nakato,K.; Guo,C-T; Matsufuji,M.; Yoshimoto, A.; Inagaki, M.; Higuchi, R.; Suzuki, Y. *J. Biochem*., **2000**, 127, 191-198.

[3]. a) Matsubara, K.; Matsumoto, H.; Mizushina, Y.; Mori, M.; Nakajima, N.; Fuchigami, M.; Yoshida, H.; Hada, T. *Oncol.Rep.*, **2005**, 14, 157-160.; b) Shirahashi, H.; Murakami, N.; Watanabe, M.; Nagatsu, A.; Sakakibara, J.; Tokuda, H.; Nishino, H.; Iwashima, A. *Chem.Pharm.Bull.*, **1993**, 41, 1664-1666; c) Colombo, D.; Scala, A.; Taiano, I.M.; Toma, L.; Roncheti, F.; Tokuda, H.; Nishino, H.; Sakakibara, J. *Bioorg.Med.Chem.Lett*, **1996**, 6, 1187-1190.; d) Colombo, D.; Franchini, L.; Toma, L.; Ronchetti, F.; Nakabe, N.; Konoshima, T.; Nishino, H.; Tokuda, H. *Eur.J.Med.Chem*, **2005**, 40, 69-.74; e) Nagatsu, A.; Watanabe, M.; Ikemoto, K.; Hashimoto, M.; Murakami, N.; Sakakibara, J.; Tokuda, H.; Nishino, H.; Iwashima, A.; YAzawa, K. *Bioorg. Med. Chem. Lett.*, **1994**, 41, 1619-1622.

[4]. Di Libero, G.; Mori, L. *Nature Rev.* **2005**, 5, 485- 496; Di libero, G. *Science* **2004**, *303*, 485-486.

[5]. Sahara, H.; Ishikawa, M.; Takahaschi, N.; Ohtani, S.; Sato, N.; Gasa, S.; Akino, T.; Kikuchi, K. *J. Cancer*, **1997**, 75, 324-332.

[6]. Ohta, K.; Mizushina, Y.; Hirata, N.; Takemura, M.; Sugawara, F.; Matsukage, A.; Yoshida, S.; Sakaguchi, K. *Chem. Pharm. Bull.*, **1998**, 46, 684;. Ishiyama, H.; Ishibashi, M.; Ogawa, A.; Yoshida, S.; Kobayashi, J. *J. Org. Chem.*, **1997**, 62, 3831-3836; Sun, D.A.; Deng, J.Z.; Shelley, R.S.; Sidney, M.H. *J. Am. Chem. Soc.*, **1999**, 121, 6120-6124; Chen, J.; Zhang, Y.H.; Wang, L.K.; Steven, J.S.; Angela, M.S.; Sidney, M.H. *J. Chem. Soc., Chem. Commun.*, **1998**, 2769-2770.; Deng, J.Z.; Sun, D.A.; Shelley, R.S.; Sidney, M.H.; Ronald, L.C.; John, R.E. *J. Chem. Soc., Perkin Trans. 1,* **1999**, 1147-1149.; Ma, J.; Shelley, R.S.; Sidney, M.H. *J. Nat. Prod.*, **1999**, 62, 1660-1663; Deng, J.Z.; Shelley, R.S.; Sidney, M.H. *J. Nat. Prod.*, **1999**, 62, 1624-1626; Sun, D.A.; Shelley, R.S.; Edward, P.L.; Sidney, M.H. *J. Nat. Prod.,* **1999**, 62, 1110-1113; Deng, J.Z.; Shelley, R.S.; Sidney, M.H.; Carl, F.I.; Mark, E.H. *J. Nat. Prod.,* **1999**, 62, 1000-1002; Deng, J.Z.; Shelley, R.S.; Sidney, M.H. *J. Nat. Prod.,* **1999**, 62, 477-480.; Golik, J.; Dickey, J.K.; Todderud, G.; Lee, D.; Alford, J.; Huang, S.; Klohr, S.; Eustice, D.; Aruffo, A.;

Agler, M.L. *J. Nat. Prod.,* **1997**, 60, 387-389;. Loya, S.; Reshef, V.; Mizrachi, E.; Silberstein, C.; Rachamin, Y.; Carmeli, S.; Hizi, A. *J. Nat. Prod.*, **1998**, 61, 891-895.

[7]. Gustafson, K.R.; Cardellina II, J.H.; Fuller, R.W.; Weislow, O.S.; Kiser, R.F.; Snader, K.M.; Patterson, G.M.L.; Boyd, M.R. *J. Nat. Can. Inst.*, **1989**, 81, 1254-1258.

[8]. Mizushina, Y.; Watanabe, I.; Ohta, K.; Takemura, M.; Sahara, M.; Takahashi, N.; Gasa, S.; Sugawara, F.; Matsukage, A.; Yoshida, S.; Sakaguchi, K. *Biochem. Pharmacol.*, **1998**, 55, 537; Ohta, K.; Mizushina, Y.; Hirata, N.; Sugawara, F.; Matsukage, A.; Yoshida, S.; Sakaguchi, K. *Chem. Pahrm. Bull.*, **1999**, 46, 684; Hanashima, S.; Mizushina, Y.; Takayuki, Y.; Keisuke, U.; Takahashi, S.; Koshino, Y.; Sahara, H.; Sakaguchi, K., Sugawara, F. *Tetrahedron Lett.*, **1999**, 46, 684.

[9]. Janwitayanuchit, W.; Suwanborirux, K.; Patarapanich, C.; Pummangura, S.; Lipipun, V.; Vilaivan, T. *Phytochemistry.*, **2003**, 64, 1253-1264.

TARGET-ORIENTED SYNTHESIS OF SOME TERPENOIDS OF MARINE ORIGIN

Nicon Ungur

Institutul de Chimie al A.Ş.M. str. Academiei 3, MD-2028, Chişinău, Republic of Moldova
E-mail: nicon.ungur@gmail.com, fax: +373 22 739775; tel.: + 373 22 739769.

Abstract: The paper presents an outline of the synthesis of some natural terpenoids of marine origine having diverse carbocyclic skeletons: labdanic, isocopalic, scalaranic, cheilanthanic, drimanic, sacculatanic. Schemes – 6, figures -2. Bibliographic references – 35.

Keywords: marine natural products, terpenoids; glycerol; scalaranes, cheilanthanes, sesterterpenoids, cyclizations, superacids, rearrangements, synthesis.

Terpenoids constitute one of the numerous class of natural products. They represent not only academic interest. Most of them possess biological activity and regulate different vital processess in both vegetal and animal world, including marine and microorganisms [1-3].

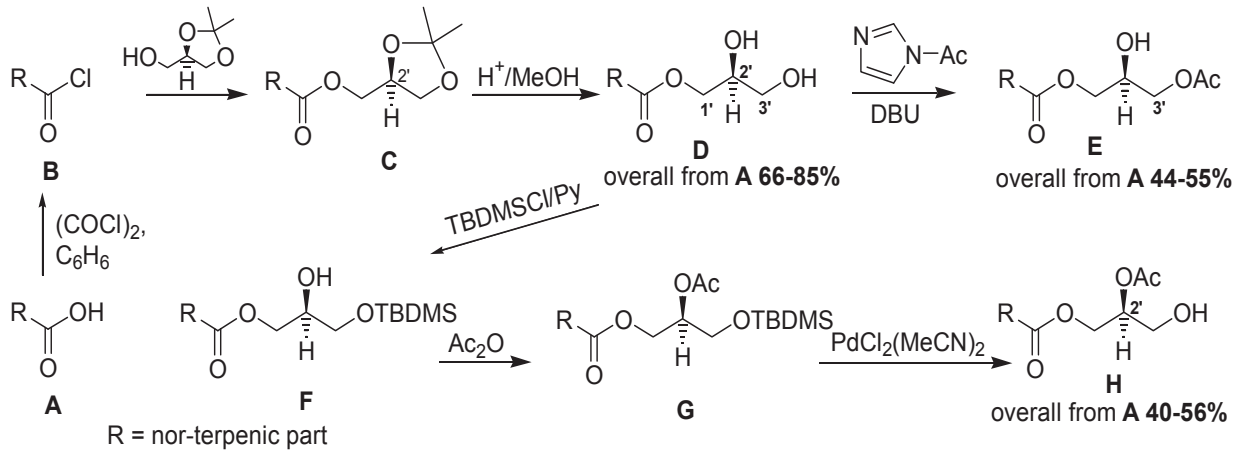

Scheme 1

Terpenoid acylglycerols represent an interesting group of natural bioactive molecules, which could be considered the chemical marker of marine dorid nudibranchs belonging to the related genera *Anisodoris*, *Archidoris*, *Austrodoris*, *Doris* and *Sclerodoris* [4-5].

Synthesis of natural bicyclic and tricyclic diterpenoid diacylglycerols has been performed by regioselective coupling of terpenoid acid with glycerol at 1'-*sn* position. This method may be considered a general approach to obtain optically active acylglycerols. (Scheme 1).

Terpenic acids (**1**-**6**) (Figure 1) have been synthesized from commercially available substances: sclareol (**7**), *E,E*-farnesol (**8**), and copalic acid (**9**) – extracted from commercial "*Copaiva Balsam*" oil.

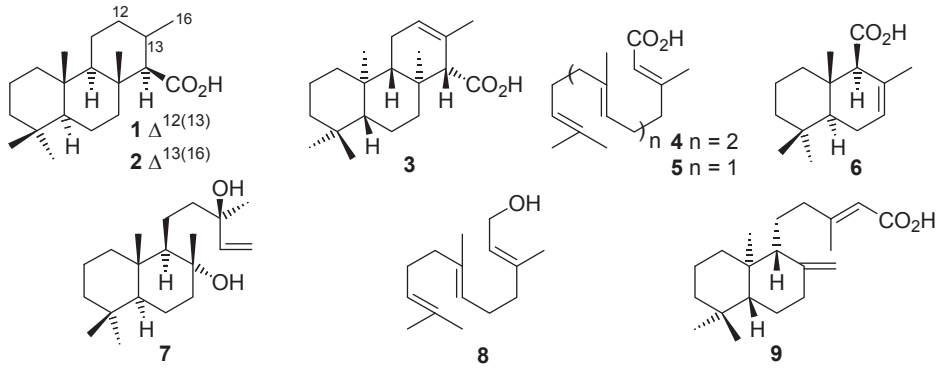

Figure 1

A series of natural di- and sesquiterpenic acylglicerols (**10**-**23**) have been synthesized (Figure 2) according to an elaborated procedure [6-11]. It should be mentioned, that diterpenoid acylglycerols are toxic to fish but also activators of protein kinase C and very active in regenerative test with the fresh water hydrozoan *Hydra vulgaris* [12].

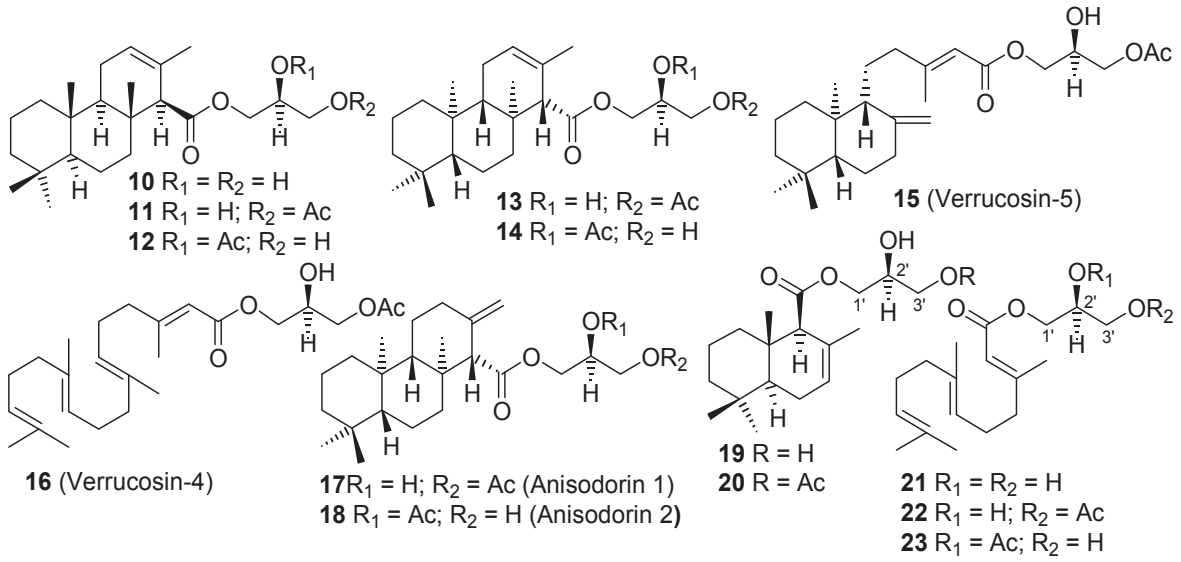

Figure 2

Anisodorid 5 (**24**) has been isolated from *Anisodoris fontaini* molluscs [9]. The absolute stereochemistry of tricyclic diterpenoid **24** was established on comparing with its enantiomer **25**, synthesized by us from the hydroxiacetate **26**, a sclareol (**7**) transformation product (Scheme 2) [14].

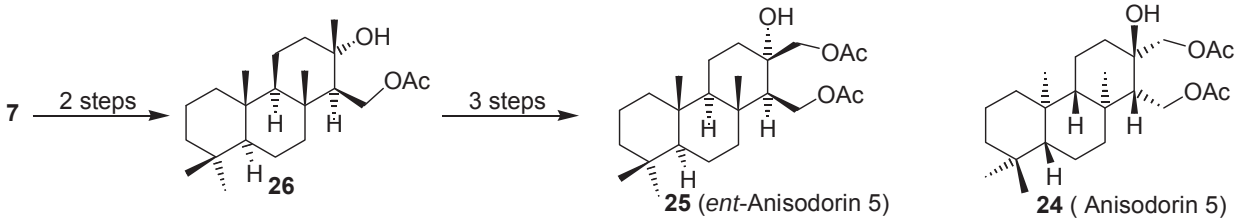

Scheme 2

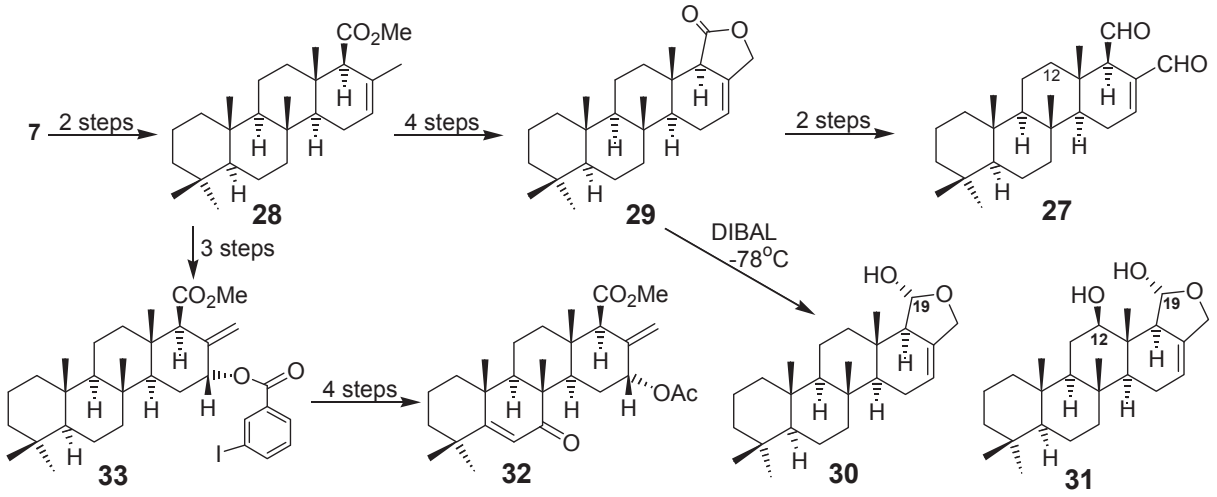

Scheme 3

Scalaranic sesterterpenoids represent a group of natural compounds, isolated basically from marine organisms and which possess diverse biological activity [15]. We have realized the synthesis of natural 12-deacetoxyscalaradial (**27**), isolated previously from the sponge *Cacospongia mollior* [16]. The synthesis started from the scalaranic ester **28** via lactone **29** [17].

Lactol **30**, obtained on the selective reduction of lactone **29** has contributed to the elucidation of stereochemistry at C19 in the natural scalaranic 12-deacetyl-12-*epi*-deoxoscalarin (**31**) [18]. The scalaranic ester **28**, readily available from sclareol (**7**), was successfully used for the synthesis of B-ring functionalized scalarane **32**. The so called Radical Rely Halogenation of the intermediate **33** has served for the specific remote functionalization (Scheme 3) [19]. It is noteworthy mentioning that the synthesis of scalaranic sesterterpenoids, including those with advanced functionalization, has been paid a lot of attention by the scientific comunity [20-26].

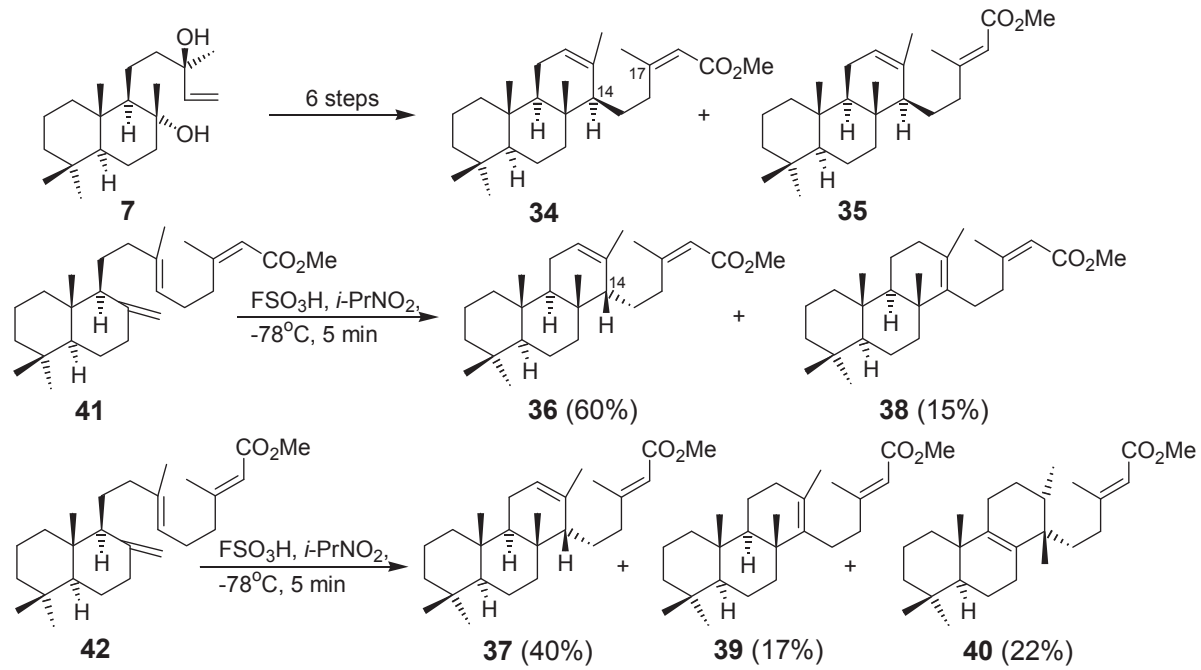

Scheme 4

Natural cheilanthanic sesterterpenoids have been isolated both from marine organisms and plants [27]. They possess a broad spectrum of biological activities and their synthesis represents an actual priority. We have performed a 6-step synthesis of isomeric cheilanthanic esters **34** and **35** [28], starting from sclareol (**7**). The synthesis of cheilanthanic

esters **36** and **37**, which are C14-epimers of esters **34** and **35**, has been performed by superacidic cyclisation of esters **41** and **42** (Scheme 4). It is noteworthy mentioning that in addition to esters **36** and **37**, their C-ring double bond isomers **38** and **39** have been produced, along with substantial amount of rearranged cheilanthane **40** [28,29].

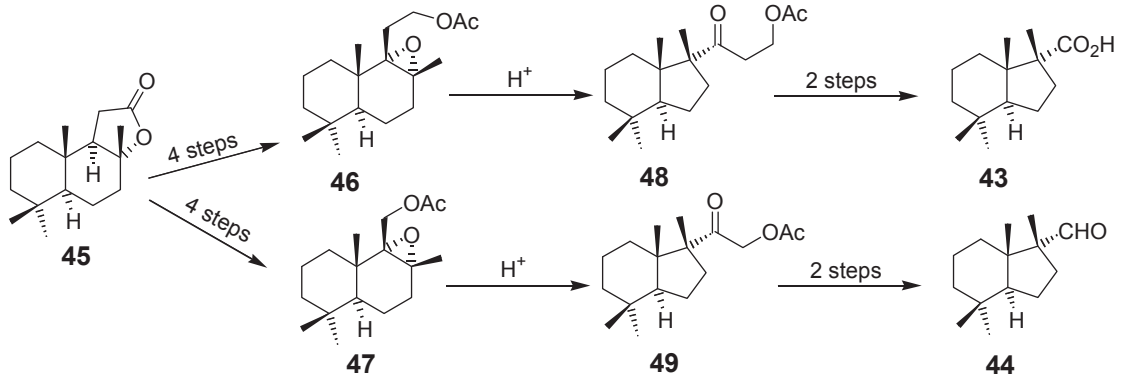

Scheme 5

Austrodoric acid (**43**) and austrodoral (**44**) were isolated from the skin extract of Antarctic dorid nudibranch *Austrodoris kerguelenensis* [30]. We have realized the synthesis of these norsesquiterpenic compounds starting from commercially accessible sclareolide (**45**) (Scheme 5). Lactone **45** was transformed in 4 steps to epoxides **46** or **47**, which rearranged under acidic conditions to the ketoacetates **48** and **49** respectively. These have been converted to austrodoric acid (**43**) [31] and austrodoral (**44**) [32] respectively.

Gem-dimethyl prenylated terpenoids have been isolated from natural sources and showed biological activity [33]. We have elaborated a biomimetic procedure for their synthesis, using as a key step the superacidic cyclisation of open chain α,ω-bifunctionalized terpenes. The starting subsrates **50** and **51** have been obtained from readily available *E,E*-farnesol (**8**) and *E,E,E*-geranyllinalool (**52**) (Scheme 6). On cyclization of bifunctionalized sesquiterpenoid **50** a mixture of two monocyclic compounds **53** and **54** is obtained, while the diterpenic substrate **51** led selectively to sacculatanic diterpenoids **55** and **56** [35].

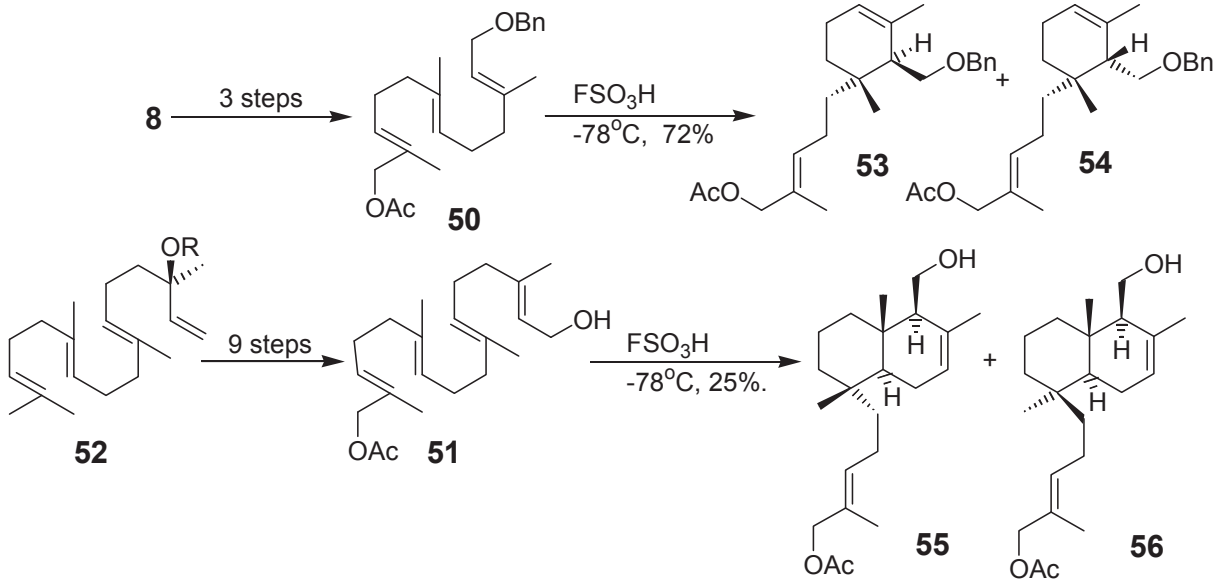

Scheme 6

Conclusions

Our investigations in the field of the synthesis of terpenoids of marine origin have led to:

- elaboration of a general method for the synthesis of natural terpenic mono- and diacylglicerols, as well as of other polifunctionalized isocopalic diterpenoids;
- synthesis of some natural scalaranic sesterterpenoids and some B-ring functionalized ones;

- obtaining of stereoisomeric cheilanthanic sesterterpenoids;
- synthesis of natural nor-sesquiterpenoids – austrodoral and austrodoric acid;
- biomimetic synthesis of terpenoids from sacculatane series.

Acknowledments. Academy of Sciences (Moldova) and CNR (Italy) are acknowledged for financial support (bilateral project 11.820.08.01/ItF "Novel approaches for the synthesis of optically active cannabinoids with relevant biological activity and therapeutical potential" 2011-2012).

Dr. Sci. Nicon Ungur was born in 1954. He graduated from Moldova State University in 1976 and obtained his Ph.D. degree in 1985 from the A. V. Bogatsky Physico-Chemical Institute of the Ukrainian Academy of Sciences, Odessa under the supervision of Professor P. F. Vlad. In 1994, he finished his Habilitation and obtained a Dr. Sci. degree. He was a postdoctoral fellow with Professor G. Cimino (ICB, Naples, Italy), where he got his training in the synthesis of natural terpenoids. He is the author of more than 90 scientific papers including reviews and ten patent applications. He is currently head of the laboratory of terpenoid chemistry, at the Institute of Chemistry, Moldova Academy of Sciences. His research interests include the synthesis of mono-, sesqui-, di- and sesterterpenoids; the electrophilic, superacidic cyclisation and molecular rearrangements of terpenoids; and the synthesis of natural terpenoids, including the biologically active compounds.

References

[1]. Frija, L. M. T.; Frade, R. F. M.; Afonso, C. A. M. *Chem. Rev*., **2011**, *111* (), 4418–4452.
[2]. Awen, B. Z. S.; Nozawa, M.; Hagiwara, H. *Org. Prep. Proced. Int*., **2008**, *40* (4), 317-363.
[3]. Jansen, B. J. M.; De Groot, A. *Nat. Prod. Rep*., **2004**, *21* (), 449–477.
[4]. Faulkner, D. J. *Ecological Roles of Marine Natural Products*; Paul, V. J., Ed.; Comstock Publishing Associates: Ithaca, NY, **1992**, pp 119–163.
[5]. Cimino, G.; Fontana, A.; Gavagnin, M. *Curr. Org. Chem*., **1999**, 3, 327–372.
[6]. Ungur, N.; Gavagnin, M.; Cimino, G. *Tetrahedron Lett.*, **1996**, *37* (20), 3549-3552.
[7]. Fontana, A.; Ungur, N.; Gavagnin, M.; Salierno, C.; Cimino, G. *Tetrahedron Lett.*, **1997**, *38* (23), 4145-4148.
[8]. Gavagnin, M.; Ungur, N.; Castelluccio, F.; Cimino, G. *Tetrahedron*, **1997**, *53* (4), 1491-1504.
[9]. Gavagnin, M.; Ungur, N.; Castelluccio, F.; Munian, C.; Cimino, G. *J. Nat. Prod*., **1999**, *62* (2), 269-274.
[10]. Ungur, N.; Gavagnin, M.; Fontana, A.; Cimino, G. *Tetrahedron Asymm.*, **1999**, *10*, (7), 1263-1273.
[11]. Ungur, N.; Gavagnin, M.; Fontana, A.; Cimino, G. *Tetrahedron*, **2000**, *56* (16), 2503-2512.
[12]. De Petrocellis, L.; Di Marzo, V.; Arca, B.; Gavagnin, M.; Minei, R.; Cimino, G. *Comp. Biochem. Physiol.,* **1991**, *100C*, 603-607.
[13]. Ungur, N.; Gavagnin, M.; Mollo, E.; Cimino, G. *Tetrahedron Asymm.*, **1999**, *10* (9) 1635-1636.
[14]. Vlad, P. F.; Ungur, N. D.; Barba, A. N.; Tatarova, L. E.; Gatilov, Y. V.; Korchagina, D. V.; Bagrianskaya, I. Y.; Gatilova, V. P.; Shmidt, E. N.; Barkhash, V. A. *Zh. Org. Khim*. **1986**, *22*, 2519–2533. [*J. Org. Chem., U.S.S.R.* **1986**, *22*, 2261–2273 (Engl. Transl.)].
[15]. González, M. A. Scalarane Sesterterpenoids. *Curr. Bioact. Compd*., **2010**, *6* (3), 178-206.
[16]. De Rosa, S.; Puliti, R.; Crispino, A. et al. *J. Nat. Prod*., **1994**, *57* (2), 256-262.
[17]. Ungur, N.; Gavagnin, M.; Cimino, G. *Nat. Prod. Lett.*, **1996**, *8* (2), 275-280.
[18]. Fontana, A.; Cavaliere, P.; Ungur, N.; Cimino, G.; D'Sousa, L.; Parameswaram, P. S. *J. Nat. Prod*., **1999**, *62* (10), 1367-1370.
[19]. Kulciţki, V.; Ungur, N.; Gavagnin, M.; Castelluccio, F.; Cimino, G *Tetrahedron*, **2007**, *63* (32), 7617–7623.
[20]. Ungur, N.; Kulciţki, V. *Phytochemistry Review*, **2004**, *3*, (3), 401-415.
[21]. Ungur, N.; Kulciţki, V. In: *Recent Res. Dev. Org. Chem*. **2003**, *7*, 241-258.
[22]. Meng, X.-J.; Liu, Y.; Fan, W.-Y.; Hu, B.; Du, W.; Deng, W.-P. *Tetrahedron Lett*., **2009**, *50* (35), 4983–4985.
[23]. Fan, W.-Y.; Wang, Z.-L.; Zhang, Z.-G.; Li, H.-C.; Deng, W.-P. *Tetrahedron*, **2011**, *67* (31), 5596-5603.
[24]. Wang, Z.-L.; Zhang, Z.-G.; Li, H.-C.; Deng, W.-P. *Tetrahedron*, **2011**, *67* (36), 6939-6943.
[25]. Chen, X.-B.; Yuan, Q.-J.; Wang, J.; Hua, S.-K.; Ren, J.; Zeng, B.-B. *J. Org. Chem*., **2011**, *76* (17), 7216–7221.

[26]. Fan, W.-Y.; Wang, Z.-L.; Li, H.-C.; Fossey, J. S.; Deng, W.-P. *Chem. Commun.,* **2011**, *47* (10), 2961–2963.
[27]. Ungur, N.; Kulcitki, V. *Tetrahedron*, **2009**, *65* (19), 3815–3828.
[28]. Ungur, N.; Kulcitki, V.; Gavagnin, M.; Castelluccio, F.; Cimino, G. *Synthesis*, **2006**, (14), 2385-2391.
[29]. Ungur, N.; Kulcitki, V.; Gavagnin, M.; Castelluccio, F.; Vlad, P. F.; Cimino, G. *Tetrahedron*, **2002**, *58* (51), 10159-10165.
[30]. Gavagnin, M.; Carbone, M.; Mollo, E.; Cimino, G. *Tetrahedron Lett*., **2003**, *44*, 1495–1498.
[31]. Kulcitki, V.; Ungur, N.; Gavagnin, M.; Carbone, M.; Cimino, G. *Tetrahedron Asymm.,* **2004**, *15* (3), 423-428.
[32]. Kulciţki, V.; Ungur, N.; Gavagnin, M.; Carbone, M.; Cimino, G. *Eur. J. Org. Chem*., **2005**, (9), 1816–1822.
[33]. Asakawa, Y. *Phytochemistry*, 2004, 65 (6), 623-669.
[34]. Kulcitki, V.; Ungur, N.; Vlad, P. F.; Gavagnin, M.; Castelluccio, F.; Cimino, G. *Synthesis*, **2000**, (3), 407-410.
[35]. Grinco, M.; Kulciţki, V.; Ungur, N.; Vlad, P. F.; Gavagnin, M.; Castelluccio, F.; Cimino, G. *Helv. Chim. Acta* **2008**, *91* (2), 249-258.

STUDY CONCERNING THE CORROSIVE ACTIVITY PROPERTIES OF MONATOMIC ALCOHOL-GASOLINE BLENDS

Valerian Cerempei

Institute of Agricultural Technics Mecagro, M. Costin str. , 7, Chisinau, MD 2068 R. Moldova
Email: icmea_mecagro@yahoo.com

Abstract: The article studies the corrosive activity of the monatomic alcohol (ethanol, butanol) - gasoline mixtures on the materials from which the internal combustion engines are made. The corrosive influence of these blends was determined in dependence of their composition. It was established that the addition of butanol and triethylamine in the ethanol-gasoline mixture essentially reduces the corrosive activity of this mixture.

Keywords: mixture, butanol, ethanol, corrosion, gasoline, resistance, triethylamine.

Introduction

Based on previous researches [1,2,3] and monographs [4], was determined the corrosive activity of monatomic alcohols and their mixtures with gasoline on certain materials used in internal combustion engines (ICE) construction. However, the existing sources lack specific data concerning the degree of corrosive influence of the specified fuels on different materials, as well as argumentation of inhibitors which significantly reduce the corrosive activity of several substances in fuels compositions.

Consequently, the purpose of our research is to determine the degree of corrosive influence of monatomic alcohols and their blends with gasoline on the materials used in ICE's construction and to argue the substances, which effectively slow down the corrosive activity of these alcohols.

Methodology of the experimental researches

For our researches we used ethanol C_2H_5OH (volume fraction of absolute alcohol - 97.5%), butanol C_4H_9OH C_4H_9OH (absolute alcohol - 99.9% vol.), regular gasoline - 80 (low octane, COR 80), and the following blends: E20 (20% vol. ethanol, 80% vol. gasoline), B20 (20% vol. butanol, 80% vol. gasoline), E16B16 (16% vol. ethanol, 16% vol. butanol, 68% vol. gasoline). We used two types of ethanol: food grade and the ester-aldehydic fraction.

The quality of fuels was assessed according to the determination of acids and alkali soluble in water; organic acids; sulfur; water. The acids and alkali soluble in water were determined as described in the standard procedures of GOST 6307. The concentration of organic acids was assessed according to the neutralization index (GOST 5985), which reflects the quantity in mg of potassium hydroxide, necessary to neutralize the organic acids in 100 mL of fuel. Sulfur content (mg/kg of fuel) was determined according to GOST 19121 - 73, and the presence of water and impurities – according to GOST 2084. The corrosive activity of sulfur compounds was tested on the copper blade (GOST 6321).

The corrosive activity of the mentioned fuels was studied in practice, applying them to the materials, which contact with fuels in internal combustion engines: stee l10, copper, brass, aluminum, membrane polymer from the fuel pump, zinc alloy from the carburetor. Samples of materials for the study of corrosive resistance were prepared from the motor pieces of VAZ and ZMZ type.

Various methods are used to determine the corrosive resistance of materials: gravimetric, resistometric, radiochemical etc. [5,6]. Materials resistance to corrosion was assessed by using microscopes EDNET AG Digital (Germany) and Optical XS – 80 (Guangzhou (Sinosource, China), according to the decimal system. The scale of evaluation of the level of corrosive resistance of materials (table 1) was elaborated according to the recommendations [5,6] and GOST 9.908 – 85. The highest grade (10) was given to the materials, which had no change of the surface state after being kept in the mentioned fluid. The grades have been reduced depending on the share of specific areas showing a pronounced corrosive activity. The periodicity of corrosive resistance evaluation was about a month.

Table 1

The scale of assessment of the corrosive resistance level of materials in biofuels

Group of resistance of materials	Level (note) of:		Lost of shine, %	Points and pits of corrosion		Continuous surface corrosion, %	Depth of de-structured layer of the membrane polymer, mm
	corrosive resistance of materials	corrosive action of fuels		corroded surface, %	depth, mm/ an		
High resistance	10	0	<5	<0.5	<0.001		Lack of significant changes
	9	1	<10	0.5 -1.0	0.001-0.005		
Sufficient resistance	8	2	<20	1.0 - 2.0	0.005 -0.010		
	7	3	<50	2.0 - 5.0	0.010 -0.050		
Reduced resistance	6	4	>50	5.0 - 10	0.050 – 0.1	<5	<0,5
	5	5		10 - 20	0.1 - 0.5	5 - 10	<1,0
Low resistance	4	6		20 - 50	0.5 – 1.0	10 - 20	
	3	7		>50	1.0 – 5.0	20 - 50	
	2	8			5.0 - 10	>50	
Non-resistance	1	9			>10		>1,0

Results and discussions

At the first stage of the research were estimated fuel properties that influence the corrosive activity.

In order to make analysis of the corrosive activity of fuels, their composition was initially studied. Chemical purity butanol and food grade ethanol, used in experiments contain the lowest amounts of impurities, and their composition meets the requirements of the respective standards, as well as the composition of technical ethanol (table 2).

Table 2

Composition of monoatomic alcohols used for the preparation of fuel[1*] measurements

Component	Butanol	Ethanol			
		Food grade (GOST P51723-2001)	Technical (GOST 18300 – 87)	EAF fraction	
				from sweet sorghum	from cereals, grapes
Absolute alcohol, % vol.	99.7	95.0±0.2	96.2	92 – 92.6	93 - 94
Mass concentration, mg/dm^3:	16				
• aldehydes		4.0	4.0 - 10.0	155 - 324	200 - 1600
• fusel oil		8.0	4.0 - 10.0	40 - 400	1200 - 1500
• volatile acids			10.0 – 20.0	140	142 - 190
• esters		15	25.0 - 40.0	70 - 180	760 - 1200
Methylic alcohol, % vol.		0.05	-	0.02	1.0 - 1.4
Dry residue, mg/dm^3			2 - 15	17 - 80	22 - 180
Oxidation test, minute			15 - 10	20	25

The estero-aldehyde fraction (EAF) of ethanol, obtained from different raw material contains large amounts (mg/dm^3 absolute alcohol) of aldehydes (up to 1600), esters (up to 1200), volatile acids (up to 190), fusel oil (up at 1500). Of these substances, only fusel oil practically does not react with the studied metals, and the remaining substances react to form oxides (Cu_2O, CuO), hydroxides [$Fe(OH)_3$, $Al_2(OH)_3$] and other products.

The dry residue reflects primarily the amount of mechanical impurities which don't affect the corrosive activity of the fuel.

[*] The measurements were performed in the laboratory Verification of alcoholic beverages quality of INVV (Accreditation certificate SNC MD CNOO 41007)

It is known [2, 10] that dehydrated alcohols, including ethanol, butanol, don't interact with metals and investigated alloys (Cu, Al, Fe, Zn). The presence in alcohols of aldehydes, esters and acids makes possible the chemical corrosive action of fuels on the metals. And the presence of water significantly increases the electrical conductivity of alcohols, allowing electrochemical corrosion.

The study of monoatomic alcohols composition allows forecasting the highest degree of corrosive activity in the estero-aldehyde fraction of ethanol due to increased concentration of aldehydes, esters, acids. Also the presence of water in alcohol stimulates their interaction with metals. Therefore, the actual degree of corrosive activity can be determined from experiments.

According to [2,4,7,10,11] C_nH_m hydrocarbons from gasoline and dehydrated alcohols, don't interact with ICE materials. But gasoline contaminants (acids, alkali hydroxides, sulfur and sulfur compounds, water) interact with metals. Therefore, was verified the quality of petrol and mixtures monoatomic alcohol - gasoline (table 3).

Table 3

Exploitation properties of fuels

Fuel	Corrosive properties			
	Neutralization index, mgKOH/100cm³	**Sulfur content, mg/kg**	**Copper blade test**	**Presence of water, mechanical impurities**
Gasoline: • normative SM226 • real	 <3 0.12 – 0.53	 <1000 250	 resists resists	 none none
Butanol	0.56	none	resists	none
Ethanol: • EAF • Food grade		 none none		
	Dual mixtures:			
• B10 • B20 • E10 (EAF) • E20 (EAF) • E20 (food grade)	0.14 0.16 0.14 - 0.96 0.18 - 2.45 0.20	 183 164 158	resists resists resists resists resists	none none none none none
	Triple mixture:			
• E16B16	0.2	102	resists	none

Acids and alkalis soluble in water generally interact with metals, so these substances are not allowed in gasoline. Tests of all gasoline samples used in the experiments revealed no water-soluble acids and alkalis. Organic acids interact with metals much weaker than water-soluble acids. Therefore, according to the standards, a limited presence of organic acids norms fuel is allowed. The limit is stipulated by the neutralization index, which reflects the amount of potassium hydroxide needed to neutralize the organic acids, which are contained in 100 cm^3 of fuel. Sufficient corrosive resistance, according to MS 226 is provided, if the neutralization index does not exceed 3 mg KOH/100 cm^3.

In our studies the values of neutralization indices varied, for gasoline, between 0.12-0.53 mg KOH/100 cm^3, for the bio-gasoline E20 (with the estero-aldehyde fraction) – 0.18 - 2.45 and for the mixtures B20, E20 (food grade alcohol), E16B16 (food.) – 0.16-0.20 mg KOH/100 cm^3. The increase of the volume concentration of ethanol (EAF) up to 40% (E40) led to the increase of the neutralization index up to 3.21 mg KOH/100 cm^3.

The results (table 2, 3) demonstrate that the organic acids in alcohols can cause an increased corrosive action of fuel on metals. As to the case of long-term preservation, aldehydes and esters can be transformed in the presence of oxygen in organic acids, which increase the corrosive action.

Sulfur and its compounds, but in particular, their combustion products are the cause drive corrosive materials in contact with. Sulfur content in gasoline (250 mg/kg) does not exceed the norm (1000 mg/kg), and adding alcohol to the gasoline substantially reduces the sulfur content (up to 102 mg/kg). Researches [4] show that adding alcohol to gasoline proportionally decreases the sulfur content in the fuel mixture. This happens due to the lack of visible quantities of sulfur

and its compounds in the studied alcohols. Testing on the copper blade confirms the lack of essential quantities of active sulfur compounds, which promotes corrosive resistance of materials.

The qualitative method used in the study didn't allow detecting the presence of water or mechanical impurities in fuel composition (table 3).

The study of monoatomic alcohols composition (table 2) and corrosive properties of gasoline and of mixtures monoatomic alcohol - gasoline (table 3) allows only forecasting the behavior of materials in long contact with the specified fuels. To assess more accurately the long-term corrosive resistance of materials in biofuels, the next cycle of experiments was conducted.

Study of corrosion properties (table 4) of different materials in regular gasoline - 80, accomplished over a period of 36 months (3 years) showed that the membrane polymer of the fuel pump, aluminum, zinc alloy from the carburetor and steel containing a low-level of carbon have a sufficient corrosion resistance level. After long tests both the polymer and aluminum have suffered practically no change (fig. 1).

On the surface of zinc alloy a thin brown pellicle has formed, and on the steel surface corrosion spots appeared. More pronounced corrosion traces can be observed on the surfaces of copper and copper alloy with zinc.

In ethanol (ether-aldehyde fraction), only the polymer suffered practically no changes (tab. 4, fig. 2), brass surface covered with a thin dark green layer which has good adhesion with the base material. The situation is similar in the case of the zinc alloy. Other materials (aluminum, copper, steel) have insufficient corrosion resistance, which causes damage to their surfaces. The duration of obtaining an acceptable degree of corrosion in ethanol EAF is the lowest for steel (0.5 months), while for aluminum and copper it is equal to 1 month and 3 months, respectively.

Table 4

Long term anti-corrosive properties of materials in fuels with gasoline and monoatomic alcohols (ethanol, butanol)

Fuel	Integral indices of corrosive resistance of materials (note)/duration of obtaining of admissible corrosion level (months)						
	Zn (alloy)	Al	Cu	Brass	Steel	Membrane polymer	Duration, months
Gasoline Normal – 80	8	9	7	7	8	10	36
Ethanol:							
• EAF	7	2/1	4/3	7	2/0.5	9	36
• Food grade	7	9	-	10	10	-	12
Butanol	9	7	10	10	8	-	12
Dual mixtures:							
• E20 (EAF)	4/1.5	4/3	5/6	8	2/0.5	5	36
• E20+triethylamine	9	7	10	10	10	10	36
• E20+pyridine	5/2	5/3	6/8	6/6	1/0.3	6	36
• E20+quinoline	4/1.5	6/4	2/1.5	2/1	6/3	1	36
• B20	10	10	8	10	10	-	12
• B20+H_2O	9	9	8	10	9	-	8
Triple mixtures							
• E16B16	8	8	8	10	8	-	12

In the food grade ethanol (fig. 3), and butanol (fig. 4) all materials showed a high degree of corrosive resistance, which is equal to or higher than for gasoline. The minimal degree of corrosive action of alcohols is due, primarily, to low concentrations of aldehydes, esters, acids (table 2, 3), while the ethanol concentration in water, in EAF and food grade ethanol in the experiments was approximately equal (2-4 % vol). Therefore, in the experimental conditions in the studies on corrosive activity of alcohols the influence of aldehydes, esters, acids is prevailing.

In the blend ethanol- gasoline E20, only the brass showed a sufficient level of resistance (fig. 5) having on the surface corroded points. In comparison with gasoline and ethanol, the blend E20 has higher corrosive activity for the zinc alloy and polymer (tab. 4), on the surface of which a viscous layer is formed. Aluminium and copper in the blend

E20 show higher resistance than in ethanol. Again, the lowest duration of obtaining the limit degree of corrosion was for steel (0.5 months), while for brass – 6 months.

According to the authors [7, 11], introducing certain corrosion inhibitors in the ethanol – gasoline blend allow to form a protective pellicle on the metal surface that prevents the output of metal ions from the surface and their interaction with oxygen or other components.

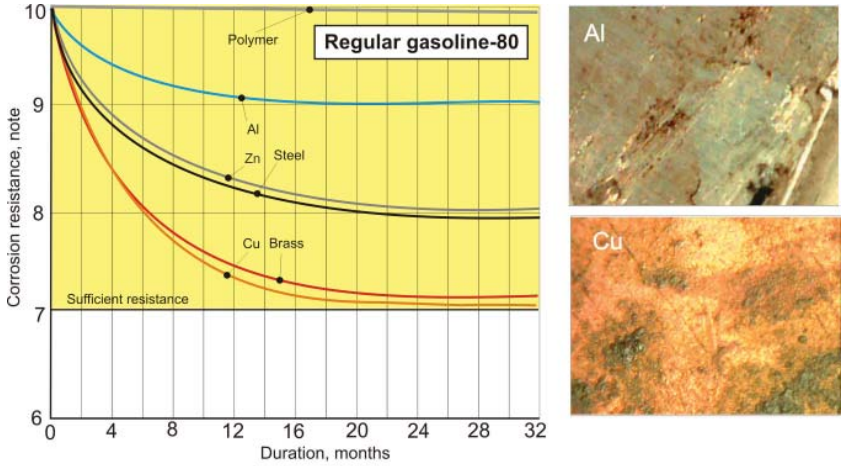

Fig.1 The Evaluation of corrosion resistance of materials in Regular gasoline-80

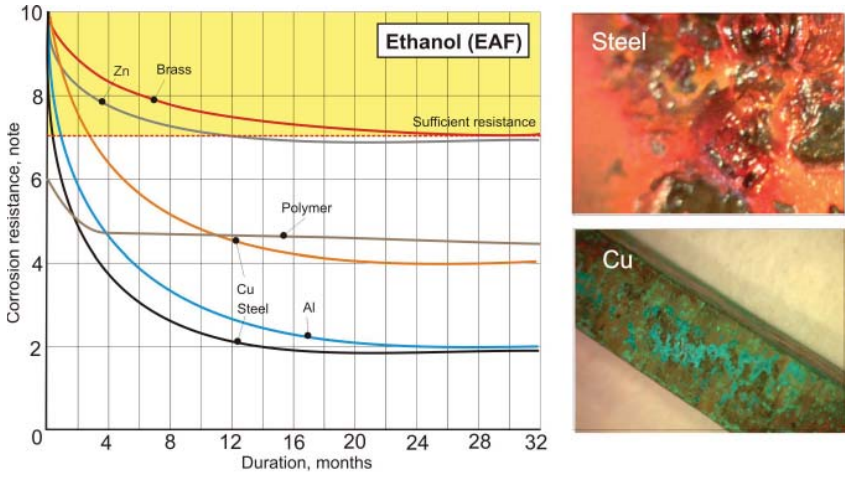

Fig.2 The Evaluation of corrosion resistance of materials in ethanol (EAF)

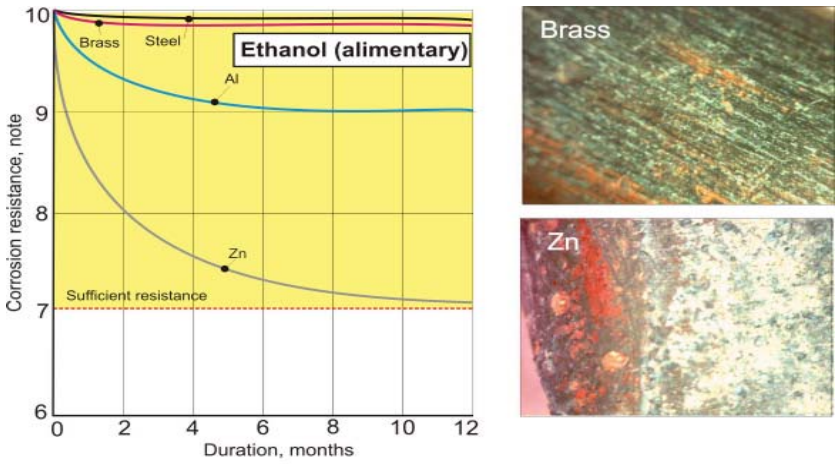

Fig.3 The Evaluation of corrosion resistance of materials in ethanol (alimentary)

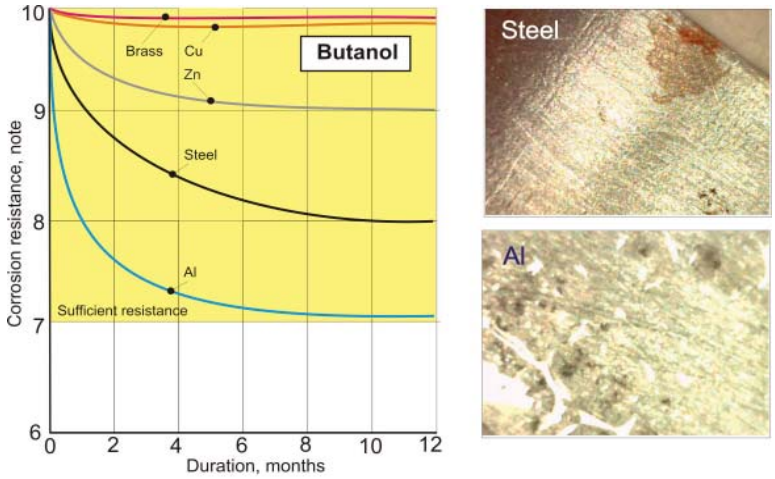

Fig.4 The Evaluation of corrosion resistance of materials in butanol

Among the studied inhibitors (triethylamine, pyridine, quinoline), only the triethylamine allowed an essential increase in corrosion resistance of all materials in the blend E20. This resistance for the zinc alloy (fig. 6, tab. 4), copper, brass and steel, is higher than the one in regular gasoline - 80. Polymer resistance is maintained at a high level. Taking into consideration the mentioned conditions, only aluminum showed a slight decrease of resistance. It is necessary to mention, that practically all materials, over a period of more than three years, maintain a good corrosive resistance level in the blend E20 - triethylamine.

The use of pyridine to reduce the corrosive activity of the blend E20 allowed insignificantly to reach the desired outcome, it was reached in zinc alloy, aluminum, copper and polymer (fig.7, tab.4). On the surfaces of these materials brittle gray or brown pellicles are formed and the liquid decanted sediments of the same color.

Quinoline has substantially increased the corrosion resistance of steel (fig. 8) forming a dark gray pellicle on the metal surface. But copper, brass and polymer decreased the resistance drastically. A smooth green deposition can be observed on metal surfaces: the membrane polymer decomposed.

In the blend butanol - B20, all studied materials showed high resistance (fig.9). The introduction of water in the blend B20 (5% vol.) resulted in its sedimentation, practically not changing materials' corrosive resistance (tab.4). Copper and zinc alloy surfaces turned a bit darker.

In the triple blend of ethanol - butanol - gasoline E16B16 (fig.10), the corrosion resistance of steel is the same as the one in the blend butanol – gasoline B20.

The resistance of zinc alloy, aluminum, copper and brass slightly diminishes, but it is sufficient for practical use (Tab.4) and much higher than in the mixture E20 (EAF). The last phenomenon refers particularly to steel. It is necessary to mention that all studied materials lack sediments in the blend E16B16, the liquid is always transparent.

Thus, butanol in the triple blend with ethanol and gasoline has a positive influence not only on phases' stability, but also on the corrosive resistance of materials, from which the internal combustion engines are made. This fact confirms the results [6,7] obtained earlier. It is necessary to mention that high corrosive activity of ethanol is due to the strong polar group OH^-. The influence of this group decreases essentially in the case of butanol C_4H_9OH.

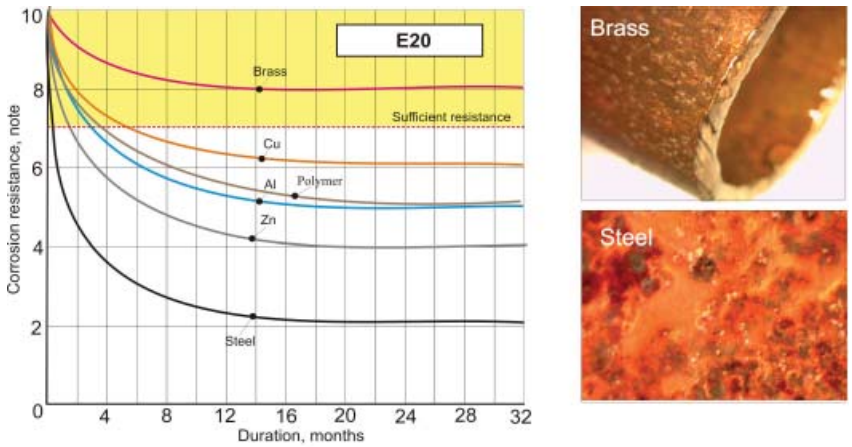

Fig.5 The Evaluation of corrosion resistance of materials in the blend E20

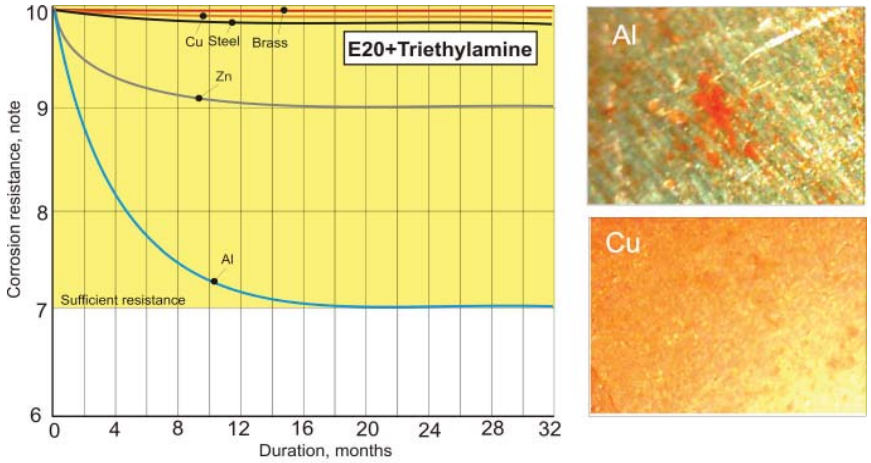

Fig.6 The Evaluation of corrosion resistance of materials in the blend E20+triethylamine

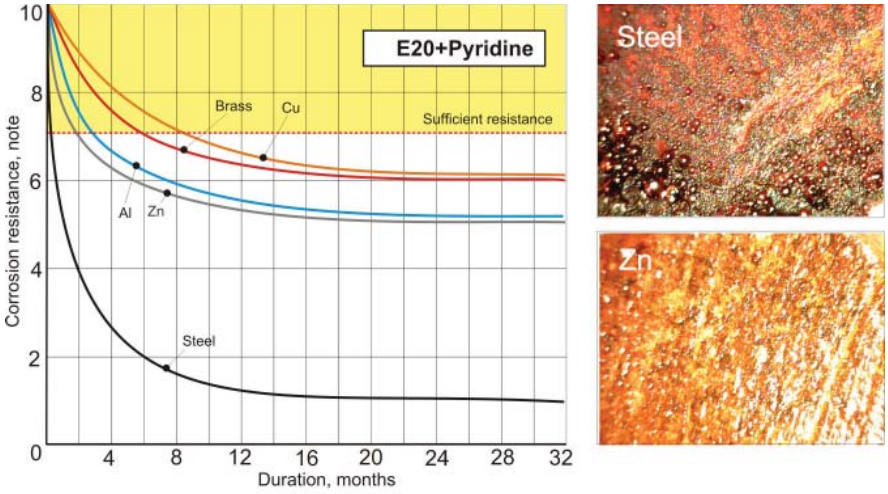

Fig.7 The Evaluation of corrosion resistance of materials in the blend E20+pyridine

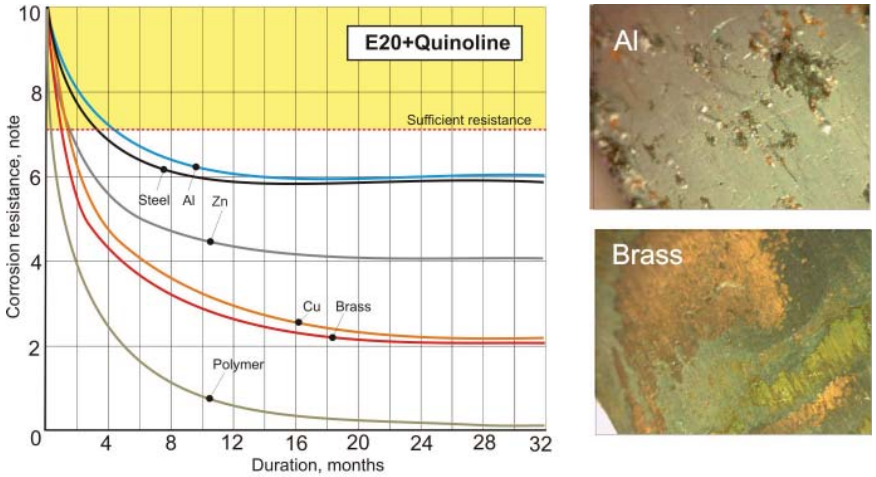

Fig8 The Evaluation of corrosion resistance of materials in the blend E20+quinoline

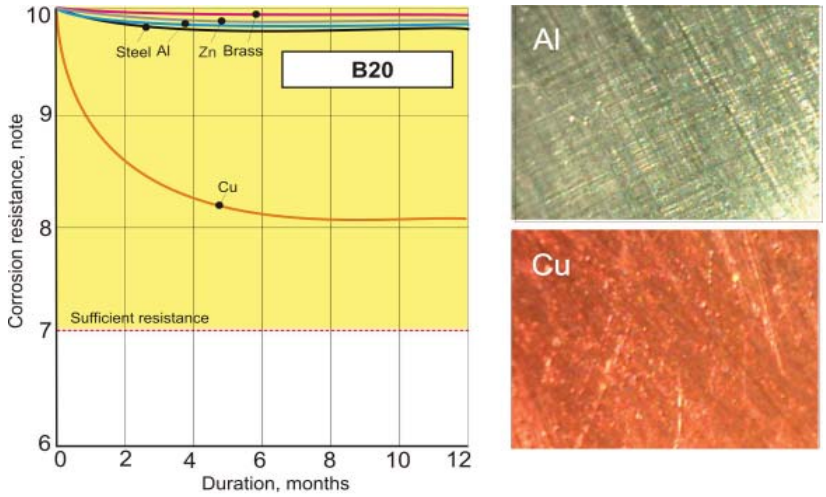

Fig.9 The Evaluation of corrosion resistance of materials in the blend B20

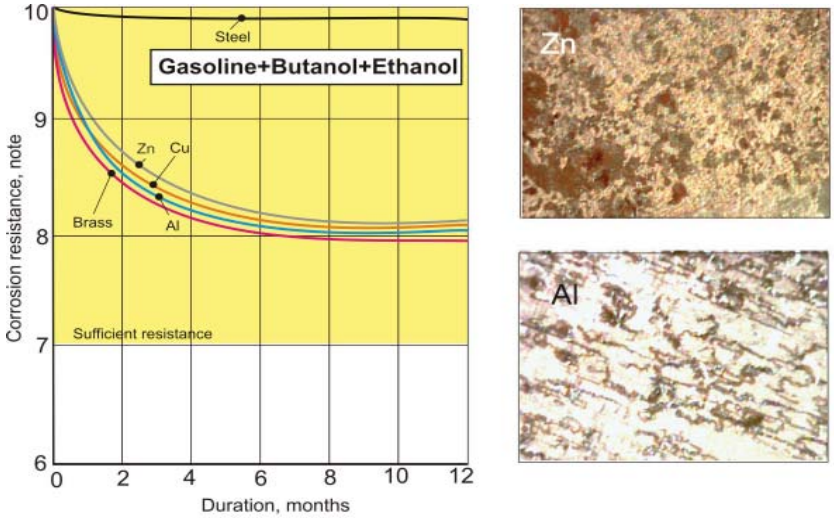

Fig.10 The Evaluation of corrosion resistance of materials in the blend gasoline+ butanol+ethanol

Conclusions

1. The studied compositions and physico-chemical properties of gasoline, butanol, food grade and technical ethanol meet regulatory requirements, which can provide sufficient corrosive resistance to materials of ICE in the mentioned liquids. The estero - aldehyde fractions concentration of ethanol have increased aldehydes, esters, organic acids, which may increase their degree of corrosive activity.
2. The study of anti-corrosion properties of different materials, performed during three years in Normal-80 gasoline, butanol, food grade ethanol showed that all materials in the engine fuel system equipment and tanks have sufficient resistance to corrosion.
3. Ethanol (ethero-aldehyde fraction) and ethanol-gasoline blend E20 diminishes the corrosion resistance of the most studied materials (except for brass). After being kept in ethanol, the aluminum, copper and steel with a low carbon content showed insufficient resistance. And in the blend E20 all materials (except brass) have insufficient resistance.
4. Among the studied inhibitors (triethylamine, pyridine, quinoline), only triethylamine allowed an essential increase of the corrosion resistance of all materials in the blend E20. This resistance for the zinc alloy, copper, brass and steel is higher than that the one in gasoline. Practically all the materials investigated during more than three years have a good anticorrosive resistance in the blend E20. The obtained results do not allow the use of pyridine and quinoline for the reduction of corrosive activity of the blend E20 on the materials from which the internal combustion engine equipment is made.
5. In the blend butanol – gasoline B20, all the studied materials showed high resistance to corrosion. The introduction

of water in the blend B20 (5% vol.) resulted in its sedimentation, practically not changing materials resistance to corrosion.

6. In the triple mixture of ethanol - butanol - gasoline E16B16, the anticorrosive resistance of steel is similar to the one in the blend butanol – gasoline B20. The resistance of zinc alloy, aluminum, copper and brass diminishes in the blend E16B16, but it is sufficient for practical use and is much higher than in the blend E20. In the blend E16B16, all studied materials lack sediment - the liquid is always transparent.

References

[1]. Смаль, Ф. В., Арсенов Е.Е. *Перспективные топлива для автомобилей*. М.: Транспорт, 1979 - 151 с.
[2]. Manea, Gh., Georgescu M. Metanolul – *combustibil neconvenţional*. Bucureşti: Tehnică, 1992 – 84 p.
[3]. Gheorghişor, M. *Carburanţi, lubrifianţi şi materiale auto speciale*. Bucureşti: Paralela, 2003-324 p.
[4]. Energie din biomasă: Tehnologii şi mijloace tehnice/ Ion Hăbăşescu, Valerian Cerempei, Vasile Deleu şi alţ. Chişinău: Bons Offices, 2009-368 p.
[5]. Коррозионная стойкость оборудования химических производств: Способы защиты оборудования от коррозии Под ред. Б.В. Строкана, А.М. Сухотина. – Л.: Химия, 1987 г. – 280 с.
[6]. Игнатьев, Р., Михайлова, А. *Защита техники от коррозии, старения и биоповреждений:* Справочник. – М.: Россельхозиздат, 1987. – 346 с.
[7]. Макаров, В.В., Петрыкин, А.А., Емельянов, В.Е., и др. Спирты как добавки к бензинам. Ж. ”Автомобильная промышленность”, Nr.8, 2005.
[8]. Грандберг, И.И. Органическая химия. М.: Высшая школа, 1974. – 416 с.
[9]. Ольховская, У. *Биотоплива второго поколения: за и против.* The Chemical Journal, 12.2008. – p.38…42.
[10]. http://benzinavto.ru/2009/06/09/korrozya-metallov-pod-dejstviem-spirtovyh-topliv/
[11]. http://chimiegenerala.3x.ro/Capitolul3/Curs/c3_2_3.htm

DETERMINATION OF COPPER AND ZINC IN MINERAL WATERS BY ATOMIC ABSORPTION SPECTROPHOTOMETRY

Tatiana Mitina*, Nadejda Bondarenko, Oxana Bunciuc

Institute of Chemistry of the ASM, 3 Academiei str., Chisinau, Republic of Moldova
Email: mitina_tatiana@mail.ru, Tel: (37322)739977

Abstract: The content of copper and zinc in mineral waters were determined by atomic spectroscopy with preliminary extraction of metals. Validation of the technique was carried out by the method of standard additions and proved the reliability of analytical data.

Keywords: mineral waters, microelements, atomic absorption spectrometry.

Introduction

Mineral waters are natural groundwater, and its origin is associated with the formation of rocks, and the type, structure and chemical composition of the constituent minerals. The action of natural waters on mineral and mountain rocks is accompanied by processes of leaching, exchange and chemical interaction with gaseous media, hydrolysis, hydration, and leads to the formation of mineral waters of different chemical composition. In this paper we assess the content of trace elements (copper and zinc) in some mineral waters on the market of Moldova.

Some microelements (iron, iodine, copper, manganese, zinc, cobalt, molybdenum, selenium, chromium, tin, vanadium, fluorine, silicon and nickel) are essential for life. Very small quantities or traces of metal ions are required for normal growth and metabolism.

Copper is found in many vitamins, hormones, enzymes involved in metabolism and tissue respiration. Zinc is a cofactor of a large group of enzymes involved in protein and other forms of metabolism. However, high amounts of these metals in mineral waters have toxic effects and are regulated by the Governmental Decision No.934 from 15.08.2007 regarding the sanitary standards of natural mineral waters quality. The content of copper ions in mineral waters should not exceed 1 mg/L, for zinc - 5 mg/L.

Ten samples of mineral water were taken in the experiment.

Table 1 shows the general ionic composition and salinity of the analyzed samples.

Table 1

Ionic composition and mineralization of analyzed samples

Nr.	Type of water	Country	General ionic composition, mg/L						
			Ca^{2+}	Mg^{2+}	$K^{+}+Na^{+}$	HCO_3^-	Cl^-	SO_4^{2-}	mineralization
1	Izvoraş	Moldova	85,4	27,8	256,0	634,4	39,8	320,4	1364
2	Varnița Unicum	Moldova	71,0	102,8	284,4	597,8	237,0	383,5	1508
3	Aqualife	Moldova	145,6	85,3	292,1	683,2	83,1	712,0	1817
4	Gura Cainarului	Moldova	172,2	105,0	354,4	701,5	96,7	895,3	2290
5	Gura Izvorului	Moldova	149,8	46,5	77,9	584,8	21,3	176,9	1006
6	Aqua-Plop	Moldova	102,7	49,0	96,7	591,5	21,5	133,0	994,4
7	Borsec	Romania	60,1	30,4	2,8	329,4	-	9,2	431,9
8	Ledianaia Jemciujina	Russia	32,6	10,2	7,8	115,9	10,6	36,8	213,9
9	Esentuchi	Russia	25,3	5,40	2271	4574	841,0	220,3	7937,8
10	Evian	France	79,7	28,0	7,25	378,2	8,78	12,8	446,7

The contents of copper and zinc were determined by atomic absorption spectrometry. The results obtained during the determination of trace elements concentration by atomic absorption spectroscopy can be affected by the macro-composition of the samples. This applies to the determination of copper and zinc in natural waters, especially since the mineralization in the analyzed samples varies over a wide range from 213.9 mg/L to 7937.8

mg/L. To eliminate the influence of the matrix and increase the sensitivity of the method, we used pre-concentration of acidified samples, followed by extraction of metals to be determined in butyl acetate in the form of a complex compound with the complex generator sodium N, N-diethyldithiocarbamate.

Experimental

Determination of metals was carried out by atomic absorption spectrophotometer AAS-3 (Germany) in acetylene-air flame.

Concentration by evaporation:

An aliquot of the sample 100 mL was placed in a 200 mL heat-resistant glass, 1.0 mL of concentrated nitric acid was added, and then slowly heated on a hot plate, preventing the sample from spilling. The contents were evaporated to a volume of 3-5 ml, then cooled, and quantitatively transferred into a 10 ml graduated cylinder.

Concentration by extraction:

Pre-evaporated samples (10 ml of concentrate) were transferred in 100 ml flasks with ground glass stoppers.

The content of the flask was adjusted with distilled water to a volume of 20-25 ml, then 10 ml of 20% citric acid solution is added in each flask, and a few drops of phenolphthalein. Dilute ammonium hydroxide solution was added until a pale pink color of the indicator appeared. In each solution 5 ml of 0.5% sodium N, N-diethyldithiocarbamate and 5 ml of butyl acetate were added. The flasks were closed with ground glass stoppers and shaken for 1 minute. After the phase separation, water was added until the organic phase reached the flask neck. The organic phase was used to determine metal concentrations.

Blank samples for the determination of metals were prepared using the same reagents and in the same amounts as in the preparation of analyzed water samples, but replacing the analyzed water with distilled water. Measurement parameters of the atomic absorption spectrometer AAS-3 for metals determination are presented in table 2.

Table 2

Determination parameters on the atomic absorption spectrometer AAS-3

Determined element	**Cu**	**Zn**
Wavelength, nm	357,9	213,9
Width of slit, mm	0,2	0,2
Current of the hollow cathode lamp, mA	5	5
Integration time, s	4	4
Lag time, s	5	5
Height of the burner, mm	8	8

Concentrations of copper and zinc were calculated from the calibration curves. To draw these graphics, we prepared the stock standard solution with a concentration of 100.0 mg/L from a standard sample of a copper ions solution MSO 0523:2003, or zinc ions solution MSO 0032:1998 with a certified value of 1 mg/cm^3 and a relative error of less than 1% with a probability of 0,95% (Ukraine). From the stock standard solution we prepared the intermediate solution with a concentration of 1.0 mg/L. Working standard solutions were prepared by the method of extraction, like the samples.

For copper and zinc the calibration curve is linear up to 0,05 mg/l. The correlation coefficient for copper is 0,9973, for zinc - 0,9965. The correlation coefficients indicate a good linearity for both microelements.

Results and discussion

Table 3 presents the obtained results for the determination of copper and zinc in mineral waters.

Table 3

Results obtained for copper and zinc determination in mineral waters and the standard deviation of the repeatability

Sample	**Cu, mg/l (means of five determination)**	**Repeatability standard deviation, mg/l**	**Zn, mg/l (means of five determination)**	**Repeatability standard deviation, mg/l**
Izvoraş	0,0078	0,0002	0,010	0,00065
Varnița Unicum	0,0077	0,00019	0,014	0,00052
Aqualife	0,0042	0,0002	0,0078	0,00019
Gura Cainarului	0,0036	0,0005	0,0062	0,0002
Gura Izvorului	0,0042	0,00021	0,0090	0,00057

Aqua-Plop	0,0060	0,00025	0,0090	0,00060
Borsec	0,0047	0,00018	0,0062	0,00045
Ledianaia Jemciujena	0,005	0,00021	0,0062	0,00050
Esentuchi	0,0074	0,00022	0,0093	0,00068
Evian	0,0058	0,00028	0,0160	0,001

The limit of detection (LOD) for copper and zinc was 0,001mg/L. For the determination of the repeatability of the method, copper and zinc were analyzed five times in the same sample.

Validation of the experimental technique was carried out by the method of standard additions. According to the procedure described above, 5 μg/L copper and zinc were introduced in the samples of analyzed water with different salinity, just before the concentration procedure. For this purpose, in 100 ml of sample were introduced 500 μl of 1 mg/L standard solution of copper and zinc. The results of recovery of copper additives are given in table 4, and the extraction of zinc additives - in table 5.

Table 4

Validation of the method of copper determination by standard additions method.

Sample	Mineralization, mg/l	Introduced, mg/L	Determined, mg/L	Recovery, %
Varnița Unicum	1508	0,005	0,0049	98
Esentuchi	7937,8	0,005	0,0052	104
Evian	446,7	0,005	0,0048	96

Table 5

Validation of the method of zinc determination by standard additions method

Sample	Mineralization, mg/l	Introduced, mg/L	Determined, mg/L	Recovery, %
Varnița Unicum	1508	0,005	0,0053	106
Esentuchi	7937,8	0,005	0,0047	94
Evian	446,7	0,005	0,0048	96

Validation by standard addition method showed that the additive is found within 4% of the expected magnitude for copper and 6% for zinc. This demonstrates the absence of losses and influences in the process of concentration for metals determination.

Conclusions

Atomic absorption spectroscopy was used to identify copper and zinc in ten samples of mineral water with different salinity. To eliminate the influence of the matrix and increase the sensitivity of the method, samples were concentrated prior to the analysis, and identified elements were extracted in the form of a complex compound with sodium N, N-diethyldithiocarbamate. Validation of the method showed absence of any systematic error and, therefore, the used technique for determination of copper and zinc in mineral water provides reliable analytical information.

References

[1]. Прайс, В. Аналитическая атомно-абсорбционная спектроскопия. Москва, 1976.
[2]. Babaua, Gabriela-Raluca; Stoica, Anca-Iulia; Capota, Petre; Baiulescu, George-Emil. J. Environmental Geology, 2003,45,58-64.
[3]. Stoica, Anca-Iulia; Babaua, Gabriela-Raluca; Baiulescu, George-Emil. J. Materials and Geoenvironment, 2003, 50, 1, 361-364.
[4]. ISO 5725-(1-6)-2002 Accuracy (trueness and precision) of measurement methods and results.
[5]. SM SR ISO 8288Ş2006 Calitatea apei. Determinarea conţinutului de cobalt, nichel, cupru, zinc, cadmiu şi plumb. Metoda prin spectrometrie de absorbție atomică în flacără.
[6]. CITAC/Eurachem Guide: Guide for quality in Analytical Chemistry, 2002.

PHYSICOCHEMICAL PROPERTIES OF THE GASOLINE AND ALCOHOL BIOFUEL MIXTURES

I. Povar[a],* V. Cerempei[b] and B. Pintilie[a]

[a]*Institute of Chemistry, Academy of Sciences of Moldova*
[b]*Institute of Agricultural Technique "Mecagro"*
e-mail: ipovar@yahoo.ca

Abstract. The influence of added alcohols, ethanol and butanol, on the main biofuel properties, as the specific gravity, Reid saturated vapour pressure and distillation curves have been investigated. These properties are intimately related to the fuel composition and their prediction relies on the knowledge of its components characteristics. This research proves the possibility of obtaining fuels with different levels of resistance to detonation, using gasoline with different chemical components and various fractions of alcohols.

Keywords: alcohol, biofuel, distillation curves, gasoline, Reid saturated vapour pressure, specific gravity.

Introduction

The performance of internal combustion engines significantly depends on the physicochemical characteristics of the fuel, which in turn are determined by their chemical composition. For fuels of petroleum origin the mentioned dependencies have been studied more comprehensive than for biofuels prepared from the gasoline and monatomic alcohols. The purpose of our research has been to study the physicochemical properties and exploiting characteristics of abovementioned biofuels.

Methodology of the experimental researches

The physicochemical properties (the density, saturated vapor pressure, distillation curves, octane number etc.) as well as the exploitation characteristics of such fuels as: (a) Normal-80 gasoline brand, (b) monoatomic alcohols: ethanol C_2H_5OH (produced from sweet sorghum, must of grapes, grain, separated from ether-aldehyde fractions) and n-butanol C_4H_9OH, (c) two-component mixtures of alcohol and gasoline (ethanol-gasoline, butanol-gasoline) in proportions of: 10:90, 20:80, 30:70, 40:60 and 50:50 (% vol), (d) three-component mixtures of alcohols and gasoline (butanol-ethanol-gasoline), have been investigated. The measurements of physicochemical properties and exploitation characteristics have been performed according to the recent technical-normative documents in the Republic of Moldova.

Results and discussions

The obtained results show that the physicochemical properties and exploitation characteristics of the mixtures from alcohols (ethanol or butanol) and gasoline depend on the individual properties of alcohols, as well as on the concentration of each component in the mixture.

The crucial process that occurs in the internal combustion engine

More complete burning of the fuel combustion in engine can occur if the fuel is in a gaseous state being at the same time quite dispersed in its mixture with air. Failing to comply with this requirement makes impossible to function the engine in a good state, consequently it is very important to ensure a more complete evaporation of the fuel. The fuel capacity to move from the liquid state in the gaseous one (at certain values of pressure and temperature) represents its **volatility**, which is typically characterized by the distillation point and saturated vapor pressure.

Distillation

Under current officially authorized regulations, the beginning and end of the gasoline distillation of the "Normal-80" type is within the temperature range of 35 ÷ 215° C. The values obtained for the Normal-80 gasoline sample, taken as the base for subsequent mixtures, are within the range of 42 ÷ 194° C (Table 1).

Table 1

The main characteristics of studied fuels

Fuel characteristics	Values of fuel characteristics								
	Gasoline N-80 (really obtained/ norm of SM 226)	Butanol (N-butane) B 100	B 10	B20	E 20		EAF Ethanol E 100	E18B10	E16B16
					Rect. ethanol	EAF Ethanol			
Distillation:									
- initial temperature of distillation, ºC	42/>35*	110	43	40	40	40	76	38	43
-temperature of distillation, ºC:									
10% vol.	55/<75*	113	55	52	47	48	77	46	53
50% vol.	85/<120*	116	87	89	67	67	78	70	84
90% vol.	154/<190*	116	154	147	143	145	83	131	120
-Final point of distillation, ºC	194/<215*	116	194	192	193	192	95	191	193
-Residue, % vol.	1.3 / <2*	1.0	1.2	1.2	1.1	1.2	0.1	1.3	1.4
-Residue + lost, % vol.	2.5 / <4*	2.0	2.5	2.0	2.0	2.0	0.5	2.0	2.0
Motor octane number MON	75.5	86.5	77.3	78.8	84.8	84.9	91*	84.7	84.6
Density. (20˚C). kg/m^3	728/<775*	797	733	739	745	745	806/ 790*	742	750
Cinematic viscosity (20˚C). mm^2/s	0.57	3.64	0.65	0.73	0.76	0.69	1.52	0.81	0.91
Saturated vapor pressure. kPa	54.3/<80*	4	50.9	47.5	61.2	58.7	23*	54.8	50.9

* According to the normative or informative data; Rect. ethanol - Rectified ethanol, Ethanol EAF - ether-aldehyde fraction of ethanol

By the chromatographic analysis it has established that ethanol, made from the sweet sorghum and used to prepare combustible mixtures, contains 96 - 98% vol. of ethanol, up to 0.1% vol. of methanol and up to 1.4% of the ether-aldehyde fraction, the remaining part (2-3%) being water. In addition it also contains up to 3 g/L of the fusel oil and 0.3 g/L volatile acids.

The initial point of distillation of the gasoline must be not lower than +35°C in order to minimize the loss of light hydrocarbons during the transportation and storage. The values of the initial point of distillation for ethanol-gasoline mixtures increase by 2-6ºC (ethanol = 5-40% vol.) in comparison with the usual changes within the range of 38 - 42°C. The increase of the initial point of distillation for biofuels (ethanol-gasoline mixtures) is determined by the presence of ethanol, whose distillation temperature is 76ºC. In function of the volume fraction of added ethanol, the temperature increases by 2-6°C, being at the level of 38-42°C. From the obtained data one can conclude that the addition of ethanol up to 40-50% vol. conducts to an increase of the initial point of distillation t_{init} for biofuels, so the t_{init} value is established within the range of 38-44°C. The influence of butanol on the values of the initial point of distillation is similar as for ethanol, but still lower, because the polarity of butanol is closer to that of gasoline and, although the distillation temperature of butanol (110°C) is much higher, the addition of butanol does not practically change the respective temperature for the binary mixture (t_{init} varies between 40 and 43ºC) as well as for the ternary mixture of biofuels (t_{init} varies between 38 and 43ºC).

The distillation temperature of 10% vol. is important for the starting capacity of the engine: the temperature is lower, the better are the starting conditions. Although the distillation temperature of 10% vol. of ethanol (t_{10} =77ºC) is higher than that of gasoline A-80 (t_{10}= 55ºC), the presence of ethanol in biofuels with the volume fraction up to 20% decreases the t_{10} value by 1-8°C. The common feature for all ethanol-gasoline blends is the fact that the distillation temperature increases as the ethanol concentration grows. For the ethanol concentrations above 20% vol., the t_{10} value for biofuel exceeds the respective temperature of gasoline by 1-8°C. Regardless of the composition and properties of studied biofuels, an addition up to 20% vol. of ethanol stabilizes the t_{10} value of biofuels within the range of 47-52°C, while with the ethanol concentration increasing up to 50% vol. - within the range of t_{10}= 52 °C -59 °C. The distillation temperature t_{10} of butanol (113°C) is much higher than that of gasoline (55ºC). At the same time, the t_{10} value for the butanol-gasoline mixture (55°C for $C_{butanol}$=10% vol., 52ºC for $C_{butanol}$=20% vol.) is by 1-3°C lower than that of gasoline. This may be explained by molecular interactions, but with a less effect than that for ethanol-gasoline mixtures. The addition of butanol to the ternary mixture E18B10 in proportion of 10% vol. maintains the t_{10} value at 46°C, while for the ratio of 20% vol. the t_{10} value increases up to 53°C.

The distillation temperature of 50% vol. characterizes the fuel capacity to ensure a proper functioning of the engine at different loads and especially in the case of their variation. The excellent function of the spark ignition engine (SIE) is guaranteed when the t_{50} value of gasoline is below 120ºC. In the case of A-80 gasoline, the distillation temperature of 50% vol. is 85°C, while for ethanol is 78°C and for butanol is 116°C. The addition of butanol (10-20% vol.) increases by 2-4°C the t_{50} value when mixed with gasoline and by 3-17ºC in the ternary mixture. In the latter case the largest increase (17°C) occurs at the butanol concentration of 20% vol. in the E16B16 mixture. For the t_{50} value, the synergic influence of butanol is minimal and with increasing the concentration of butanol, especially in the biofuel mixtures, the temperature t_{50} increases substantially, near to that of the gasoline A-80.

The distillation temperature of 90% vol. and the distillation end point describes the complete combustion capacity and the fuel efficiency. For the A-80 gasoline the t_{90} value is equal to 154°C, for ethanol is of 83°C, and for butanol is 116°C. The increase of the ethanol volume fraction up to 30% results in maintaining or lowering the t_{90} value by maximum 11ºC compared to gasoline. The increase of the ethanol volume fraction by more than 30% leads to a more pronounced decrease in the t_{90} value. Thus, for the biofuel E50 the t_{90} value is of 87°C, the decrease being of 72ºC. In the butanol mixtures the decrease of temperature takes also place: in the gasoline blends of up to 7ºC, while in the ternary mixtures up to 34ºC (see table 1).

The distillation endpoint of studied gasoline varies within the range 177-194°C. The addition of alcohol decreases by up to 12ºC the final point of distillation of the ethanol blends and up to 3°C for mixtures with butanol. In both cases this decrease becomes more pronounced with increasing the volume fraction of alcohols in the mixture.
According to [13], the temperature range $\Delta t = t_{final} - t_{90}$ decreasing reflects the diminish of probability of the condensation for heavy fractions of fuel. This range is, respectively: for gasoline A-76, Δt = 18°C; for A-80, Δt = 39-40°C, for ethanol, Δt = 12°C and for butanol, Δt = 0ºC. The addition of ethanol and butanol in the ratio of up to 30-40% vol. changes the temperature difference Δt for the respective gasoline within relative small range: ± 8°C. With increasing the alcohol fraction over 40% vol., the difference Δt increases to 79°C, mostly due the t_{90} value decreasing.

The residue is a non-distilled fraction of fuel, formed from its heavy fractions. The residues remained after the distillation of ethanol (0.1% vol.) and butanol (1.0% vol.) are smaller than those for the respective gasoline (1.3% vol.). In the binary mixtures of ethanol-gasoline and butanol-gasoline there is registered a slight decrease of the residue compared with gasoline of the 0.6 - 1.2% vol. levels.

Distillation losses were 1.2% vol. for gasoline, respectively 0.4% and 1.0% vol. for ethanol and butanol.

The fractional composition (distillation) is reflected by the distillation curves (fig. 1). In the temperature

range of t_{init}-t_{10} the distillation of biofuels (except E50) is practically identical to that of gasoline. The use of ethanol produced from various species of raw material (as sorghum mellitus, ether-aldehyde fraction of grapes or grain) does not essentially influence the distillation temperatures of biofuels. The form of distillation curves shows that the addition of ethanol and butanol to gasoline influences insignificantly on the initial and final distillation point values of mixed fuels, but there is a certain decrease in the intermediate distillation temperatures (t_{10}, t_{50}, t_{90}) for the mixtures of monatomic alcohol and gasoline.

The vapor pressure also influences on the proper engine function. The Reid vapor pressure of the gasoline A-80 is equal to 54.3 kPa, while that for gasoline with the ethanol fraction of 10% vol. and 20% vol. is situated within the 57.0 - 61.2 kPa range. The tendency of increasing pressure with growing the ethanol volume fraction has been registered. Since the vapor pressure of butanol is low (4 kPa), its addition to gasoline with the volume fraction of 10% and 20% reduces the pressure of the A-80 gasoline respectively by 3.4 kPa and 6.8 kPa, while for the biofuel E16B16 respectively by 6.4 and 10.3 kPa.

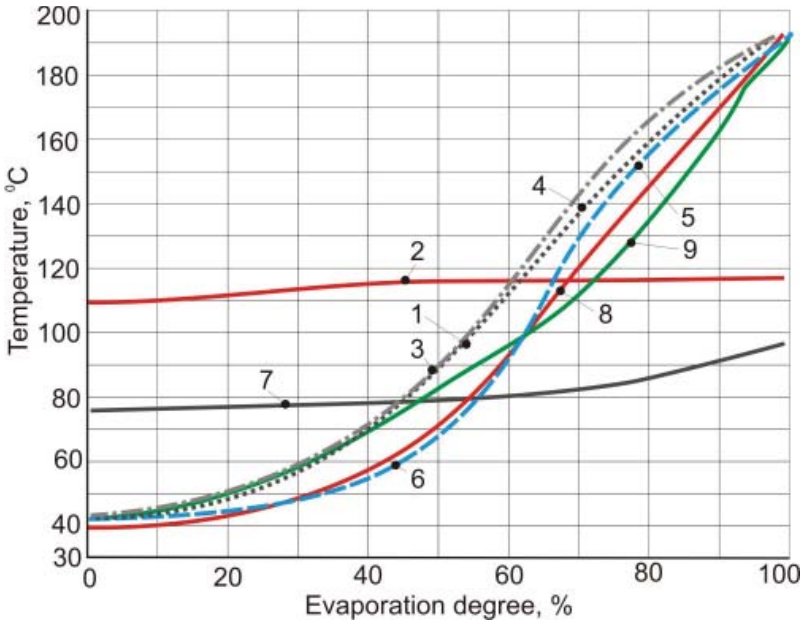

Fig. 1. Modification of the fuel distillation curves: 1 - gasoline A-80, 2 - butanol, 3 - ethanol, 4 - B20 mixture, 5 - biofuel E20 (rectificated) 6 - biofuel E-20 (EAF), 7 - ethanol, 8 - E18B10 mixture, 9-E16B16 mixture

Octane number characterizes the detonation stability and is determined by the Research Method (RON) or Motor Method (MON). It has been established that adding alcohol to gasoline usually increases the octane number (fig. 2). The addition of ethanol causes a higher increase of the octane number (ΔCOM = 0.47 unit /% vol.) than in the case of butanol (ΔCOM = 0.17 unit /% vol.).

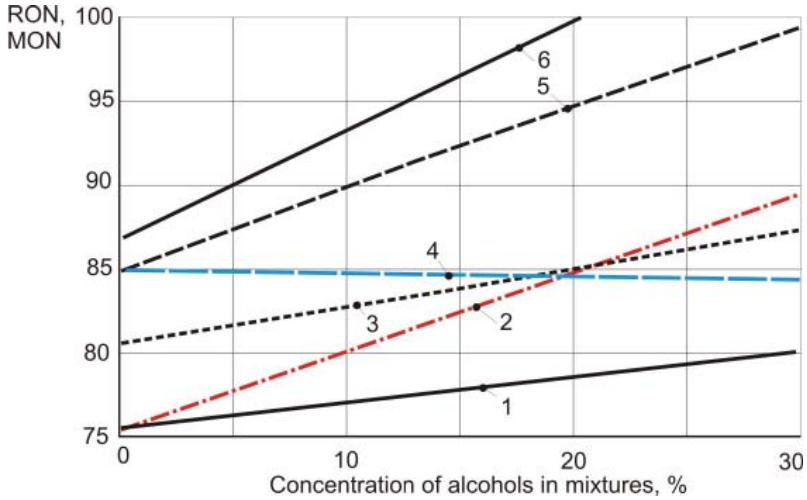

Fig. 2. The dependence of the octane number of biofuel mixtures on the alcohol concentrations: 1, 2, 3, 4 - COM = f (C), 5, 6 - COR = f (C), 1 - butanol + gasoline A-80, 2 - ethanol + gasoline A-76, 3 - ethanol + gasoline A-80, 4 - E16B16 mixture, 5 - ethanol + gasoline A-80, 6 - ethanol + gasoline A-90

Conclusions

1. It has been established that adding ethanol to 40 - 50% vol. has a positive effect on the initial distillation temperature values for biofuels, which are stabilized in a range t_{init} 38 - 44˚C. The influence of butanol on the initial distillation temperature values is identical to that of ethanol. Even the distillation temperature of butanol (t_{init}= 110˚C) is much higher than that for gasoline (t_{init}= 42˚C), adding butanol does not practically change the respective temperature of the binary mixture with gasoline (t_{init}= 40 - 43˚C) as well as for ternary mixture of biofuel (t_{init}= 38 - 43˚C).

2. The addition of alcohols with up to 20% volume fraction in gasoline creates a synergistic effect, reducing that the temperature by 1 - 8˚C. At addition of butanol this effect is lower than for ethanol. The increase of the ethanol content more than 20% vol. results in growing the t_{10} value of biofuel by 1 - 8˚C. The best fuels to start the engine are the mixtures that contain alcohols up to 20 - 30% vol.

3. The ethanol-gasoline blends E5-E50 (with the ethanol fraction of 5 - 50% vol.) have the t_{50} value within 67 - 79˚C, for gasoline - t_{50} = 85 - 95˚C and for ethanol t_{50}=78˚C.. Reducing the temperature t_{50} for biofuel, especially with the ethanol concentration up to 30% vol., has to improve the engine performance at different tasks and is caused by the interaction of component molecules with a synergistic effect. The addition up to 20% vol. of butanol (t_{50} = 116˚C) increases by 2 - 4˚C the temperature t_{50} in the mixture with gasoline and by 3 - 17˚C in the mixture with the biofuel.

4. The alcohols have the temperature t_{90} lower than gasoline (t_{90}= 152 - 159˚C), so for the alcohol-gasoline fuel blends, the 90% distillation temperature has low values. The distillation endpoint drops to 12˚C in the ethanol-gasoline blends and with up to 3˚C in the butanol-gasoline mixtures. The reduction of t_{90} and t_{final} leads to the more complete burning of fuel.

5. The distillation curves show that the addition of monoatomic alcohols in gasoline affects slightly the initial and final points of distillation of mixed fuels, but there is a certain decrease in the intermediate distillation temperature (t_{90}, t_{90}, t_{90}) of the mixtures of alcohols with gasoline.

6. The Reid saturated vapor pressure RVP of studied fuels does not exceed the current normative requirements and technical documents (RVP < 80 kPa). The vapor pressure of the A-80 gasoline is within 49 - 54.3 kPa while that of biofuels with the volumetric fraction of 10% ethanol and 20% vol. is respectively within 57 - 61.2 kPa. The addition of butanol (RVP 4kPa) with the volume fraction 10% and 20% decreases RPV in gasoline by 3.4 and 6.8 kPa respectively, while for the biofuel E20 by 6.4 and 10.3 kPa correspondingly.

7. The addition of ethanol to gasoline (MON 75.5) provides a higher octane number growth (ΔMON = 0.47 unit\% vol.) than in the case of the addition of butanol (ΔMON unit = 0.17 unit\% vol). Under the same conditions, the addition of alcohols leads to an increase in the Research Octane Number higher than for the MON. The addition of up to 20% vol. of butanol does not practically influence the resistance to the detonation of the biofuel E20 (MON 84.8 - 84.6).

8. The carried out research proves the possibility of obtaining fuels with different levels of resistance to detonation, using gasoline with different chemical components and various fractions of alcohol.

Acknowledgments. This work was supported by the "Development and use of the optimized compositions of biofuel mixtures based on physico-chemical modeling" 5393A STCU research project funding.

References

[1]. Manea Gh., Georgescu M. *Methanol – unconventional fuel*. Bucharest, Tehnica, 1992.-84p. (Rom.)
[2]. *Fuel, lubricants and technical liquids* / G.P. Lyshko et al. – 2nd. Ed., Chisinau, GAUM, 1997.-486p. (Rus)
[3]. Apostolache N., Sfinteanu D. *Unconventional fuel car*. Bucureşti, Tehnica, 1989-125p. (Rom.)
[4]. Smali F.V. and Arsenov *Perspective fuel for cars*. Moscow, Transport, 1979.-151p. (Rus)
[5]. Lanzer T., Von Meien O.F., Yamamoto C.I. A *predictive thermodinamic model for the Brazilian gazoline.* Fuel, 84 (2005) – p. 1099.
[6]. Ebert Jessica. *Biobutanol: the next big biofuel* www.bioethanol.ru
[7]. Gheorghişor M. *Fuels, lubricants and special auto equipment.* Ed. Paralela, Bucharest, 2003- 324 p.
[8]. Carlos Coelho de Carvalho Neto, Schulte D.D., Carlo Baldelli, P. Yappoli, Gareth Ellis, Louis Bretton, Ishaia Segal, Hubert E. Stassen Program CPR/88/053, Chine, Shenian, 2002-145p.

STUDY CONCERNING THE POSSIBILITY OF GAMMA-SPECTROSCOPY METHOD TO DETERMINING THE TOTAL POTASSIUM IN SOILS

Leah Tamara[1]*, Lozovaia Zoia[2]

[1]*Institute of Pedology, Agrochemistry and Soil Protection "Nicolae Dimo", Chisinau-2070, Ialoveni str. 100, Moldova; Phone: (+373-22) 28-48-61; Fax: (+373-22) 28-48-55; E-mail: tamaraleah09@gmail.com*
[2]*Institute of Radiology, Gomel-246011, Fediuninschi, 16, Belarus*

Abstract. The paper presents the results of scientific research related to development the specifically express-method for determining total potassium in podzolic soils from Belarus and chernozems from Moldova, based on the use of gamma-spectrometry. Determining the precise of the total content of potassium in the soils can be made directly in the field or laboratory by gamma-spectroscopy method using radiation detection of natural isotope ^{40}K. The conversion coefficient for podzolic soils of Belarus is C=0,00395, for chernozems of Moldova - C=0,00337.

Keywords: gamma-spectrometry, total potassium, ^{40}K, conversion coefficient, chernozems, podzolic soils.

Introduction

Scientific hypothesis of the project was proposed by the Institute of Radiology of Belarus and is based on the following assumptions, resulting from circumstantial evidence or priory expectations and there fore requires experimental validation:

1. Determining the precise total content of potassium in the soils can be made directly in the field or laboratory gamma-spectroscopy method using radiation detection of natural isotope ^{40}K.
2. The content of biologically available forms of potassium in soils is in quantitative relationship to the amount of total potassium in the soil, and this dependence can be expressed by a specific mathematical function, suitable for solving the problem of determination of mobile potassium in the soil in function of total content value.

Research potassium content in soils is an important task in agrochemistry nutrients and soil fertility [1-3]. Preliminary investigations carried out in Belarus and other research institutes have shown that there are all prerequisites for the elaboration and development of laboratory methods and method-express for determining global soil potassium content in the field remote using spectroscopic measurement equipment [4-8].

Gamma-spectroscopic method for determining in the laboratory and field the emission of radionuclide content of potassium-40 in soils was developed in the early of '90 by Scientific Research Institute for Agricultural Radiology of Belarus, now Institute of Radiology [9]. This method was widely used in the practice of Scientific Research Institute to mapping contamination levels post radiate territories with radionuclide from Chernobyl Nuclear Station.

Determination of potassium total by classical analysis method is very expensive. To perform this analysis is necessary to have laboratory platinum dishes and hydrofluoric acid, which is very toxic substance. The price of analysis, performed according to the method varies from $16,5 to $25,0. Using gamma-spectroscopic method (which is cheap and easy) to determine the total potassium will develop the cartograms of potassium content in the soils and preventive measures to reduce reserves of this important element in the arable layer of soil.

Material and methods

The possibility of determination total potassium in soils conforming radioactive isotope content by gamma-spectroscopy method has been studied in soil samples collected from arable and under-arable layers of chernozems from North and Central part of Moldova. Dependence of mobile potassium content by total potassium content in chernozems of Moldova studied within the same samples by determining mobile forms of potassium after Macighin method [10].

The soil samples for develop a method of determining of total potassium in soil in dependence of content of ^{40}K was made with consideration of their genesis and origin of parental rocks. The experimental range included 17 soil samples.

Determination of potassium forms in the soils was carried out according to following methods:

- *Potassium total* – classical method by Berzelius [11], the decompositions of soil with hydrofluoric acid and subsequent determination of potassium by flame photometry method.

- *Potassium global* – gamma-spectroscopic method with subsequent calculation of total potassium content in according to content of ^{40}K isotope (expressed in Becquerel, Bq; 1 Bq = 1 s^{-1}), using the formula: $\mathbf{K_2O, \% = C \cdot A,}$ where: C – conversion coefficient, A – activity of isotope ^{40}K in soil, Bq/kg.

- *Potassium mobile* – Macighin method.

Value of conversion coefficient "C" in some specific cases, depending on sample size, precision analysis of gamma-spectrometry and classical methods, genesis characteristics of soils and parental rocks may be different. According to the calculations of researchers from Belarus the conversion coefficient C=0,00395.

On the base of the difference between the average values of potassium content determined by the classical and the gamma-spectrometry methods (C=0,00395), the value of coefficient was modified using a conversion factor (0,853) for further use in the chernozems, so the used coefficient "C" is equal to 0,00337.

Spectrometric determination was made with "SILENA SNIP 301N" - distant spectrometer. The spectrometer is an information processor for spectroscopy research in environmental radiation monitoring, with high requirements for performing calculation during particularly difficult research and isotopic analysis in the field or laboratory. The spectrometer includes a detector (Nal-Tl) used in gamma-spectroscopy for qualitative and quantitative analysis with high precision and stability. The measures unit is impulse per second (imp/sec).

Data were statistically processed by dispersion and correlation method with software Excel 7.

Results and discussions

High costs and complexity of analytical determination of total potassium limited ability to monitor content of this element in soils and to develop appropriate cartograms. Research goal is to determine the possibility of assessing global potassium in soil in dependence of radioactive potassium-40 isotope content by gamma-spectrometry determination of its in arable and under arable layers samples of chernozems.

To realization of this investigations were carried out in the field and made appropriate statistical samples of homogeneous soil relatively with genesis and originality of parental rocks. Based on laboratory results to determine the total potassium content in arable and under arable layer of soils by classical method (Berzelius, [11]), and gamma-spectroscopic method ranges of variation have been made with the values of these determinations. For each variation series are calculated the average values (X), standard deviation (σ), coefficient of variation (V,%), average error of the mean value (m), relative value of average error (P,%). Correlation coefficients were calculated (r) in conformity by the values of global potassium content, obtained analytically and calculated in accordance of potassium-40 isotope content. Parameters of soil composition and properties of the samples are presented in table 1.

The presented results confirm the proximity degree of investigated soils after composition size and parental rocks origin. The fallow chernozems have excellent physical properties, the arable – satisfactory. Arable soils, as results of agricultural use shall be subject to compaction.

According data presented in table 1, the fallow chernozems are characterized by very high content of humus and excellent chemical and physical properties. These soils are rich in total and mobile forms of potassium. Arable chernozems are moderate humificate and have satisfactory chemical properties. The total potassium content in these soils is high and mobile potassium content is moderate and high.

Correlative dependence between the values of classical determination and calculated values of global potassium (according potassium-40 isotope) is presented in table 2.

The value of the correlation coefficient equals +0,69, which confirms the presence of a large links. Researches confirm that sampling links of connection can be much higher. In this order, in processes of rating the gamma-spectroscopic method for determining radioactive potassium by detection of gamma rays from natural isotope of potassium K-40 and the parallel determination of potassium by classical method, it is necessary:

- to reduce the error of value to determine the isotope K-40 two times, thus reducing the error of determining the value of global potassium from 0,40 % K_2O to 0,20 % K_2O;
- to eliminate of random error analysis of soil samples in 2 or 3 repetition in determining of global potassium;
- a composition of homogeneous samples of soils for statistical processing of obtains results of total potassium determination and corrects to calculate the numerical value of coefficient "C".

Comparing the results of 17 parallel determinations of global potassium content (K_2O, %) in one and the same soil samples with classical and calculated methods (in consideration with radioactive isotope K-40, applying conversion coefficient C=0,00337 for chernozems) has established the following differences:

- Less than 0,1% K_2O – in 9 cases or 53% of the samples;
- From 0,1 to 0,2% K_2O – in 5 cases or 30% of the samples;
- From 0,2 to 0,3% K_2O – in 3 cases or 17% of the samples;

Table 1

Physical properties of soil samples researched for experimental confirmation of possibility to determining total potassium by method of registration the gamma ray of natural isotope K-40

Horizon and depth, cm	Particle size < 0,01mm	pH	Hydrological acidity, me/100g soil	CaCO3,%	Humus, %	Nitrogen total, %	C:N	Phosphor total, %	Phosphor mobile, mg/100g soil	Potassium total, %		Potassium mobile, mg/100g soil
										Classical method	Calculated by content of ^{40}K, C= 0,00337	
Profile 1B. Chernozem typical arable (Bălți Steppe)												
Ahp 0-30	62,8	6,3	2,4	0	4,03	0,216	10,9	0,13	2.0	**2,44**	**2,54**	33
Ah 30-50	62,6	6,5	1,7	0	3,81	0,172	10,1	0,10	0.9	**2,20**	**2,38**	18
Profile 2B. Chernozem typical arable (Bălți Steppe)												
Ahp 0-30	63,3	6,3	2,4	0	4,05	0,193	12,2	0,14	1,3	**2,44**	**2,58**	30
Ah 30-50	63,1	6,5	2,0	0	3,25	0,159	11,9	0,12	0,9	**2,54**	**2,56**	18
Profile 3B. Chernozem typical fallow (Bălți Steppe)												
Ahț1 0-10	65,2	6,5	2,7	0	6,86	0,296	13,5	0,170	2,4	**2,55**	**2,47**	44
Ah 25-50	66,8	6,9	1,6	0	4,61	0,213	12,6	0,130	1,0	**2,52**	**2,50**	24
Profile 62i. Chernozem cambical arable (Hilly part of Codrii)												
Ahp 0-35	57,4	6,6	2,3	0	3,22	0,203	9,2	0,136	2,0	**2,33**	**2,45**	23
Ah 35-50	57,7	6,6	1,7	0	2,86	0,187	8,9	0,102	1,2	**2,46**	**2,52**	13
Profile 14. Chernozem stagnical arable (South-Vest periphery of Prenistru Hilly)												
Ahp 0-34	67,9	7,1	2,2	0	4,53	0,224	11,7	0,116	2,5	**2,38**	**2,30**	39
Ah 34-56	69,1	7,5	1,6	0	3,91	0,177	12,8	0,102	0,9	**2,43**	**2,44**	24
Profile 3 p. Chernozem ordinary arable (Central part of Moldova)												
Ahp 0-22	51,6	7,7	0	6,7	3,24	0,202	9,3	0,160	4,4	**2,21**	**2,29**	33
Ah 22-42	51,5	7,6	0	7,9	2,97	0,188	9,2	0,132	1,8	**2,32**	**2,18**	18
Profile 9 p. Chernozem ordinary arable (Central part of Moldova)												
Ahp 0-33	39,8	8,0	0	12,4	2,80	0,193	8,4	0,146	3,6	**2,18**	**2.00**	18
Ah 3-48	39,5	8,0	0	15,4	2,22	0,160	8,0	0,132	2,0	**2,29**	**2,05**	15
Profile 10.3T Chernozem ordinary fallow (Central part of Moldova)												
Ahț1 0-10	57,3	6,7	2,2	0	7,56	0,366	12,5	0,170	1,4	**2,42**	**2,39**	41
Ahț1 10-21	57,4	6,8	2,0	0	6,81	0,331	12,9	0,131	1,0	**2,41**	**2,64**	29
Ah 21-46	58,8	6,9	1,4	0	4,60	0,223	12,0	0,108	0,6	**2,42**	**2,62**	25

Table 2

Correlation between values of total potassium content in chernozems, determining in parallel in the same samples by classical and gamma-spectroscopy methods

Nr. of profiles	Horizons and depth, cm	K_2O total		Deviation from average value, Δx		Result of deviation from average comparative values
		Gamma-spectroscopy method, C = 0,00337 (1)	Classical method (2)	(1)	(2)	(1x2)
1B	Ahp 0-25	2,54	2,44	+0,13	+0,05	+0,0065
	Ah 25-50	2,38	2,20	-0,03	-0,17	+ 0,0051
2B	Ahp 0-30	2,58	2,44	+0,17	+0,05	+0,0085
	Ah 30-50	2,56	2,54	+0,15	+0,15	+0,0225
3B	Aht1 0-10	2,47	2,55	+0,06	+0,16	+0,0096
	Ah 30-50	2,50	2,52	+0,09	+0,13	+0,0117
62i	Ahp 0-35	2,45	2,40	+0,04	+0,01	+0,0004
	Ah 35-50	2,52	2,46	+0,11	+0,07	+0,0077
14	Ahp 0-34	2,30	2,38	-0,11	-0,01	+0,0011
	Ahk 30-56	2,44	2,43	+0,03	+0,04	+0,0012
3p	Ahpk 0-30	2,29	2,21	-0,12	-0,18	+0,0216
	Ahpk2 30-50	2,18	2,32	-0,23	-0,07	+0,0161
9p	Ahpk1 0-33	2,00	2,18	-0,41	-0,21	+0,0861
	Ahpk2 33-48	2,05	2,29	-0,36	-0,10	+0,0360
10.3T	Aht1 0-10	2,39	2,42	-0,02	+0,03	-0,0006
	Aht2 10-21	2,64	2,41	+0,23	+0,02	+0,0046
	Ah 21-46	2,62	2,42	+0,21	+0,03	+0,0063
Average indexes		**X1=2.41**	**X2=2,39**	**σ=0,19**	**σ=0,11**	**0,2444**

Note: ***C*** *– the coefficient for recalculating the number of Becquerel in total potassium content (K_2O);* ***X*** *– average value;* ***σ*** *– standard deviation squared;* ***r*** *– correlation coefficient;* ***r= + 0,69*** *(high correlation).*

Very high and high coincidence of parallel determination results of global potassium by different methods is found in 83% cases, satisfactory – in 17% cases. Reducing the error in gamma-spectroscopic measurements, excluding the random errors in the determination of potassium in calibration process of new method, conducting research with gamma-spectroscopic method in homogeneous samples of soil, will offer the possibility and opportunity to significantly improve the precision of determining global potassium in soils by the method of calculation as K-40 isotope content.

The results of determining the total potassium in researched soils show that in most cases, the content in the arable layers is lower than in sub-arable layers. This investigation confirms that in case with non application potassium fertilizers, the total reserves of this element in the arable layer of soil will be reduced progressive.

Correlative dependence analysis of results to determine the global and mobile potassium content in chernozems of Moldova have confirmed the total lack of this dependence both in arable and sub-arable soil layers investigated separately.

From scientifically, this phenomenon can be explained. The quantity of total potassium depends essentially only by the content in network of crystalline minerals. This form of potassium is closely linked by mineral network and exchange reactions involved in weak, the element is immobile and inaccessible to plants.

The content of mobile potassium in soil is very small – 20-50 mg/100 g soil, which is equal to 0,02-0,05% of soil mass. These small amounts of mobile potassium in the soil almost no influence the total content of this element. On the other hand, the accumulation of mobile potassium forms in the soils is different. The main components, those participate in the accumulation of mobile potassium in soil are:

- capacity of substances biological circuit;
- intensity of minerals alteration processes;
- the total content of potassium in the crystalline network of soil minerals and its part to involved in cation potassium exchange process;
- anthropogenic factor – the quantity of fertilizes applied in soils.

From the above, it appears that components of replenishment of soil potassium reserves are independent and not depend on each other, and the total content of potassium in the soil.

It must be recognized that the content of potassium mobile forms accessible to plants, is not directly depending on the quantity of total potassium in the soil. Assumed dependence is not statistically confirmed and can not be expressed

by a mathematical function determinate adequate to solve the problem of determining the mobile potassium content in soils on the function of total potassium content value.

Conclusions

Development of a simple and inexpensive gamma-spectroscopy method for determining global potassium in soil will provide an opportunity to draw cartograms of total potassium content and elaborate preventive measures to reduce the reserves of this important physiological element in soils.

The content of biological accessible forms of potassium in the soils is not in direct quantitative dependence to total potassium content and can not be expressed by a specific mathematical function, able to solve the problem of determining the mobile potassium content in function by global value.

Correlative dependence between the values of global potassium obtain by classical and calculated method (in function of K-40 isotope content) estimated by the correlation coefficient, confirms the presence of a large leak links between them.

The link between the results of the determination of global potassium by mentioned method must be much higher. To this end, in the charging gamma-spectroscopy method for determining of potassium in accordance with determination results of potassium by classical method must:

- to reduce the error value to determine the isotope K-40 two times, in this way decrease the value error in determining the global potassium from ±0,40 % K_2O to ±0,20 % K_2O.
- to exclude random errors by determining the 2 or 3 repetitions of total potassium in soil samples used to construct the sample for accurate calculation of the numerical value of the conversion coefficient “C”.

For potassium determinations statistical processing of results is necessary to investigate homogeneous soil samples, composed after this genesis and agricultural use; the origin of the appearance, mineralogical composition of parental rocks.

The results of determining potassium in investigated soils shows that in most cases its content in the arable layers is less than in sub-arable. This confirms that in condition whit non application of potassium fertilizers in soil, the total reserves of potassium in the arable layer of soil will be reduce gradually.

Acknowledgements

This work was supported by the bilateral project 313. BF: “Dependence determination of total and biologic accessible potassium content in podzolic soils of Belarus and chernozems of Moldova”.

References

[1]. Андреева, Е.А. Радиоактивность почв и определение калия радиометрическим методом. Почвоведение, 1960, №5. Активность радионуклидов в объемных образцах. Методика выполнения измерений на гамма-спектрометре: рекомендация: МИ 2143-91: утв. 28.12.1990. 1990.

[2]. Кузнецов, А.В. и др. Методические указания по контролю радиоактивным загрязнением сельскохозяйственных угодий, прилегающих к атомным станциям. М.: ЦИНАО, 1990. 16 с.

[3]. Самохвалов, С.Г. и др. Методические указания по проведению радиологических исследований на контрольных участках. М.: ЦИНАО, 1982. 25 с.

[4]. Вешко, Э.И. Естественная радиоактивность почв Харьковской области. В сб.: Радиоактивность почв и методы её определения. М.: Наука, 1966. С.212-219.

[5]. Инструкции и методические указания по оценке радиационной обстановки на загрязненной территории. В сб.: Межвед. комис. по радиац. контролю природной среды; под ред. Ю.А. Израэля. М., 1989. – 200 с.

[6]. Ковалевский, А. Усовершенствование радиометрического метода определения калия в порошковых пробах. Мин-во геол. и охраны недр СССР. В сб. научно-техн. информации, №5, 1957. 119 с.

[7]. Прохорычева, Н.П.; Агапова Т.Н.; Моторина Л.Н. Содержание калия-40 в почвах берегов водоемов и лугов отдельных районов Калининградской области [Радионуклид]. С.139-145 В сб.: Теоретические и прикладные аспекты биоэкологии. Калинингр. гос. ун-т. Калининград, 2003.

[8]. Сельскохозяйственная радиоэкология / Под ред. Р.М. Алексахина, Н.А. Корнеева. М.: Экология, 1991. 400 с.

[9]. Агеец, В.Ю. Система радиоэкологических контрмер в агросфере Беларуси. Республиканское научно-исследовательское унитарное предприятие «Институт радиологии». МН., 2001. 250 с.

[10]. Аринушкина Е.В. Руководство по химическому анализу почв. М.: Изд-во МГУ, 1970. 470 с.

[11]. Батунер, Л.М., Позин М.Е. Математические методы в химической технике. Л., Гос. н.-т. изд-во хим. литры, 1960.

STUDIES ON THE ANTIOXIDANT ACTIVITY OF THE COMPOUND ENOXIL AND ITS RELATED FORMS

Tudor Lupaşcu*, Alexandru Gonța

Institute of Chemistry, Academy of Sciences of Moldova,
3 Academiei str., MD 2028, Chisinau, Republic of Moldova
E-mail: lupascut@gmail.com

Abstract: Studies of the antioxidant activity of polyphenolic compounds extracted from grape seeds are of considerable interest currently. The compound Enoxil is a mixture of polyphenols, esthers, and carboxylic acids, which could be involved in reducing the risk of diseases associated with oxidative stress. The results of the investigation of antioxidant activity for the compound Enoxil and its forms are presented in this paper. Two distinct methods were used to assess the antioxidant properties of the tested compounds: the radical monocation of 2,2′-azinobis-(3-ethylbenzothiazoline-6-sulfonic acid) ($ABTS^{\bullet+}$ test) and the DPPH method (2,2-diphenyl-1-picrylhydrazyl radical). It can be concluded that acetone-Enoxil has a higher antioxidant activity that other tested compounds.

Keywords: polyphenols, antioxidants, $DPPH^{\bullet}$, $ABTS^{\bullet+}$.

Introduction

A current global problem is the negative influence on the human body of various pathogenic diseases, mutagenic and psychological factors. Among the psychological states that lead to human health disorder is stress, which is a major factor in the emergence of various diseases and abnormalities [1,2].

Scientist study the causes and factors responsible for these effects in the body, to interfere and prevent their harmful action.

One of the causes of disturbances in the body at biological, chemical, genetic and psychological level is the formation of free radicals and oxidative stress [3]. Air pollution, excessive radiation and toxic waste are sources of "primary" radicals derived from the environment. For example, large quantities of free radicals are generated in photolysis processes and water radiolysis [4].

Thus, an antioxidant is a substance that at extremely low concentrations, as compared to the substrate, prevents or significantly delays its oxidation. Antioxidants work properly in close correlation with the structure of free radicals, the harmful agent concentration, with the properties and mode of action in target tissues [5].

Flavonoids are a large class of compounds present in plants, which possess antioxidant properties. These compounds contain phenolic hydroxyl groups in the ring structure, which offer them reducing properties.

The antioxidant activity of polyphenols is determined by the presence of hydroxyl groups in the 3′ and 4′ positions of the B ring and to a lesser extent of the 4′ hydroxyl group in ring B [6]. Flavonols, especially catechins, quercitin, kaemferol and glucosides, are constituents of green and black teas [7], red wine and grape seeds.

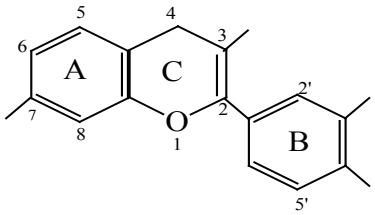

Fig. 1. General chemical structure of flavones [6]

In vitro studies defined the antioxidant potential of polyphenols as a parameter that determines the ability to capture free radicals such as superoxide radicals, singlet oxygen, hydroxyl radical, peroxyl radical (which induce various diseases). Chemical structures that contribute to the antioxidant activity of polyphenols, including a neighboring dihydroxy- or trihydroxy- structure, may chelate metal ions by forming complexes and prevent the generation of free radicals. This structure also allows electron delocalization, conferring high reactivity in free radicals quenching [8].

There is an increasing interest in using natural compounds, such as polyphenols extracted from grape seeds. Various extraction systems were tried to obtain new products such as tannins. Antioxidant, antibacterial and antifungal action exhibited by these compounds is widely studied in the literature. Also due to low solubility in water or alcohol, instability such as oxidation or reduction, these compounds cause problems in the formulation of new drugs [9].

Grape seeds contain a wide range of polyphenolic compounds such as enotannins. In order to improve the

physicochemical properties of these compounds, their structure and physico-chemical properties were modified by oxidation reactions, which resulted in obtaining a new product, Enoxil [10-12].

The obtained preparation presents scientific and practical interest, since manufacturing this product is performed from natural raw materials, sustainable and safe and, unlike other drugs, it does not generate side effects.

Use of antioxidants in cosmetics and pharmaceuticals is widespread. The study of antioxidant properties of the compound Enoxil, used to formulate new cosmetics, has a great importance in stabilizing lipid oxidative processes and other active forms.

For the in vitro evaluation of antioxidant capacity of the isolated compounds, or mixture of compounds, different methods are used, involving the use of various mechanisms for determining the antioxidant activity. The most popular are: the $ABTS^{\bullet+}$ test (2,2′-azinobis-(3-ethyl-6-sulphonate benzothiazoline) radical cation) [13], the test $DPPH^{\bullet}$ (2,2-diphenyl-1-picrylhydrazyl) [14] and the FRAP test, based on the reduction of the ferric tripyridyltriazine complex to the ferrous form to test the total reduction capacity of the antioxidant [15].

Experimental

In our research, we used two methods to determine the antioxidant activity, namely the $DPPH^{\bullet}$ test and the $ABTS^{\bullet+}$ test.

Reagents for the DPPH method

Reagent	**Chemical formula**
DPPH radical, D9132, Aldrich	**2,2-Diphenyl-1-picrylhydrazyl**
Ethanol solution	C_2H_5OH

Reagents for the ABTS method

Reagent	**Chemical formula**
ABTS radical 11557, Fluka, <99% HPLC grade	**2,2′-azino-bis(3-ethylbenzthiazoline-6-sulphonic acid**
Na persulfate S6172, Sigma, >98%BioXtra	$Na_2S_2O_8$
Ethanol solution	C_2H_5OH

Table 1

Enoxil fractions

Fraction	**Color**
Enoxil standard	Yellow
Enoxil –ethanol fraction	Yellowish brown
Enoxil – acetone fraction	Dark yellows
Enoxil - ethylacetate fraction	Pale yellow

Various concentrations were prepared of Enoxil and its forms, in the range 3000-15000 µg/mL and in the final solution to be analyzed (using the ABTS method), the concentrations ranged between 30 and 150 µg/mL.

The $ABTS^{\bullet+}$ radical cation is formed by the reaction of $ABTS^{\bullet+}$ (7 mM solution) and potassium persulfate (2.45 mM, final concentration) for 12-16 hours in the dark at room temperature. The obtained $ABTS^{\bullet+}$ solution (2,2′-azino-bis (3-ethylbenzthiazoline-6-sulfonic acid)) is diluted with 70% ethanol to give an absorbance of 0.700 ± 0.020 at 734 nm. The introduction of 30 *µl* of antioxidant in 3 *ml* $ABTS^{\bullet+}$ should produce an inhibition of 20-80% of the initial solution. The calibration curve is graphed using Trolox standard (0-15 mM range of concentrations) absorbance readings at 734 nm, at 1 and 6 min after mixing [13].

The analysis of antioxidant activity by DPPH method was performed using 3.5 ml of ethanol (70%) solution of $DPPH^{\bullet}$ with the initial concentration of 60 µM, to which was added 0.5 ml antioxidant solution with different concentrations (final concentrations were between 30-150 µg/mL) and the optical density at 517 nm was measured at 1, 5, 10, 20, 30, 60 and 120 minutes with T80 spectrophotometer in 1 cm quartz cuvettes [14].

Results and discussions

Antioxidant properties of the preparation Enoxil were studied using the DPPH test analysis and the interaction with the $ABTS^{\bullet+}$ radical cation, the results are presented in tables and figures below. We studied the antioxidant properties of different Enoxil fractions obtained in the laboratory. According to the method

for determining the antioxidant activity using $ABTS^{\bullet+}$, the consumption of $ABTS^{\bullet+}$ was recorded using the absorbance values after 1 min and 6 min. Using the obtained data, were potted kinetic graphs of $ABTS^{\bullet+}$ reduction at its interaction with different antioxidant fractions of Enoxil used for analysis (fig.1-4).

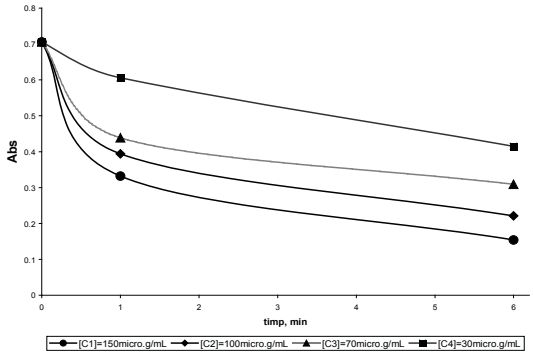

Fig. 1. Reduction of $ABTS^{\bullet+}$ with Enoxil-ethylacetate fraction

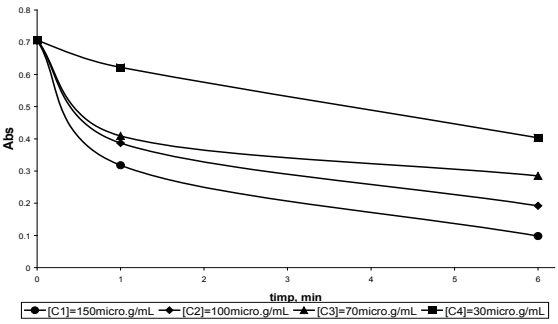

Fig. 2. Reduction of $ABTS^{\bullet+}$ with Enoxil-ethanol fraction

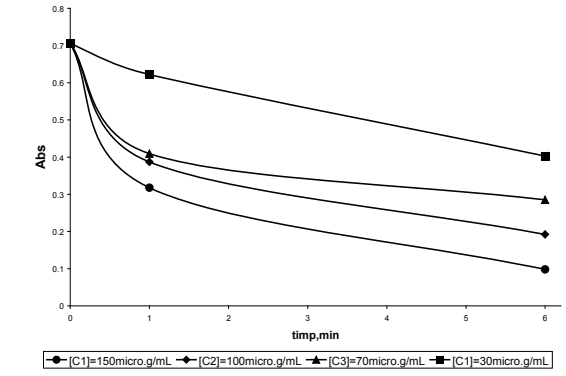

Fig. 3. Reduction of $ABTS^{\bullet+}$ with Enoxil-acetone fraction

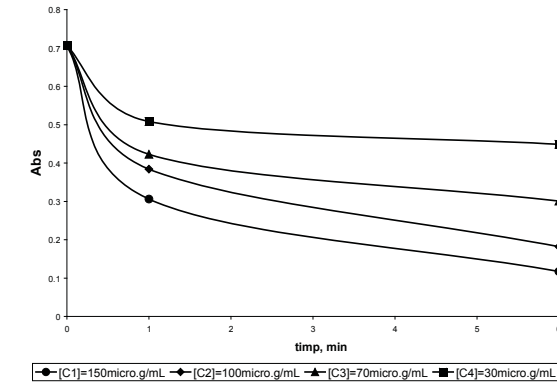

Fig. 4. Reduction of $ABTS^{\bullet+}$ with standard Enoxil

According to the protocol, the antioxidant activity in Trolox equivalents was calculated. For this purpose, Trolox solutions were prepared of known concentrations, which were subjected to oxidation with ABTS, as specified above antioxidant samples. In the next stage, the obtained kinetic experimental data were used to plot graphs (fig. 5) and antioxidant activities were calculated in Trolox equivalents for the studied compounds solutions.

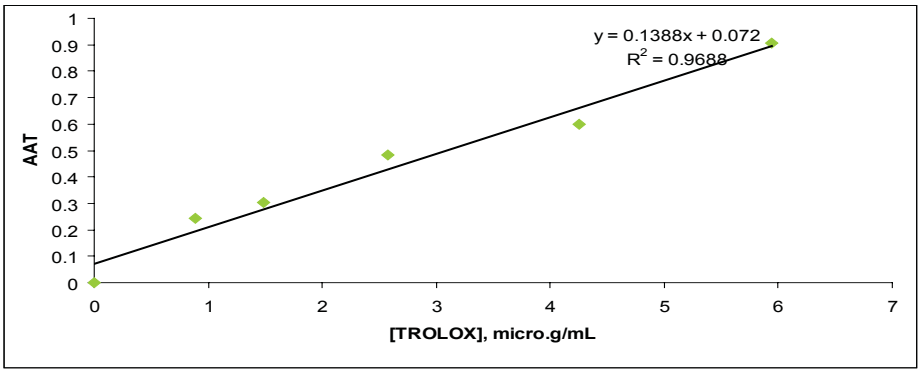

Fig. 5. Total antioxidant activity as function of $[Tx]_0$, determined by the $ABTS^{\bullet+}$ test

Table 2

Dependence of the antioxidant activity, in Trolox equivalents, on the Enoxil-ethyl acetate concentration

Concentration, µg/mL	AAT	Equiv-TROLOX
150	0.521246	3.168
100	0.433428	2.554
70	0.369688	2.090
30	0.260623	1.326

Table 3

Dependence of the antioxidant activity, in Trolox equivalents, on the Enoxil-ethanolic concentration

Concentration, µg/mL	AAT	Equiv-TROLOX
150	0.538244	3.297
100	0.443343	2.623
70	0.398017	2.307
30	0.264873	1.356

Table 4

Dependence of the antioxidant activity, in Trolox equivalents, on the Enoxil-acetone concentration

Concentration, µg/mL	AAT	Equiv -TROLOX
150	0.541076	3.316
100	0.443343	2.623
70	0.412181	2.406
30	0.252125	1.257

Table 5

Dependence of the antioxidant activity, in Trolox equivalents, on the standard Enoxil concentration

Concentration, µg/mL	AAT	Equiv -TROLOX
150	0.531074	3.271
100	0.447592	2.582
70	0.392351	2.282
30	0.271955	1.428

The obtained experimental results show that AAT depends on the concentration of the analyzed Enoxil forms and for the studied concentration range, AAT varies within the range 0.55 - 0.26. The lowest antioxidant activity was observed for the form obtained by ethyl acetate extraction (concentration 150 µg/mL).

From the obtained data we can conclude that for the maximal tested concentration, i.e. 150 µg/mL of antioxidant, the effectiveness of antioxidant activity in the studied fractions decreases in the order: ethyl acetate < standard Enoxil < Enoxil-ethanol fraction < Enoxil-acetone fraction.

Enoxil antioxidant properties are comparable with the antioxidant capacities of catechin, epicatechin, epigalocatechin and others [16].

It is known that mentioned above antioxidants are widely used in experimental research, such as inhibition of cancer development, stopping the cells aging process, protection and regeneration of skin [17].

In general, it is known that the form of obtained kinetic graphs is determined by the molecular structure of the compound under study, involving the stability of the antioxidant radical. Since the molecular structures of Enoxil forms are similar, one would expect similar kinetic graphs.

In polyphenols, the presence of the dihydroxo- group in positions 3′ and 4′ of B ring favors reactions with slow kinetic behavior. However, the presence of compounds with other structures involves a behavior characterized by expression of two stages, the first being fast and the other slow (fig.6), depending on the extraction method.

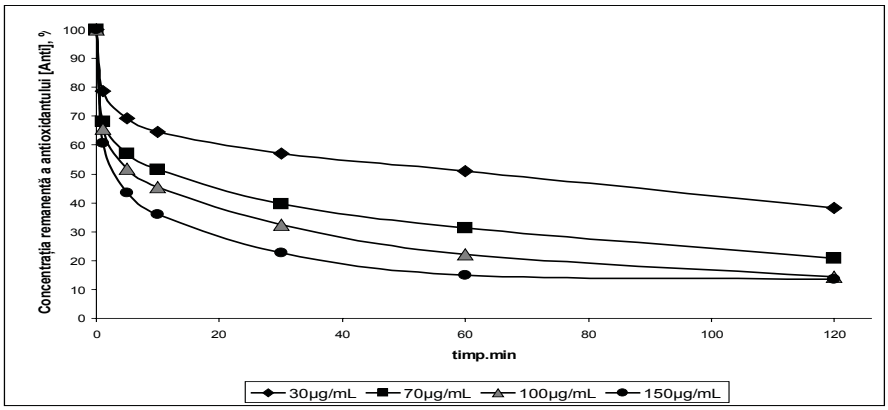

Fig. 6. Kinetic graphs of reduction of Enoxil-ethanol (various concentrations) with DPPH·

The antioxidant/antiradical activity is defined as the antioxidant amount necessary to decrease the initial DPPH· concentration by 50%. It is called the 50% effective concentration (EC_{50}). For simplicity we used the value $1/EC_{50}$ called the antiradical power (PAR) or antiradical activity. Thus, the higher is the PAR value, the more effective is the antioxidant. The antiradical activity is determined from the dependence graph of remaining [DPPH·] (in percent) function of the molar ratio (MR) or mass ratio of the antioxidant and DPPH· (RM= $[ANTI]_0/[DPPH^{\cdot}]_0$). Since the antioxidant activity of test compounds is characterized by two-stage kinetics, the antioxidant activity was determined at the equilibrium. Fig.7 and 8 show the results of experimental determination of EC_{50} for various fractions.

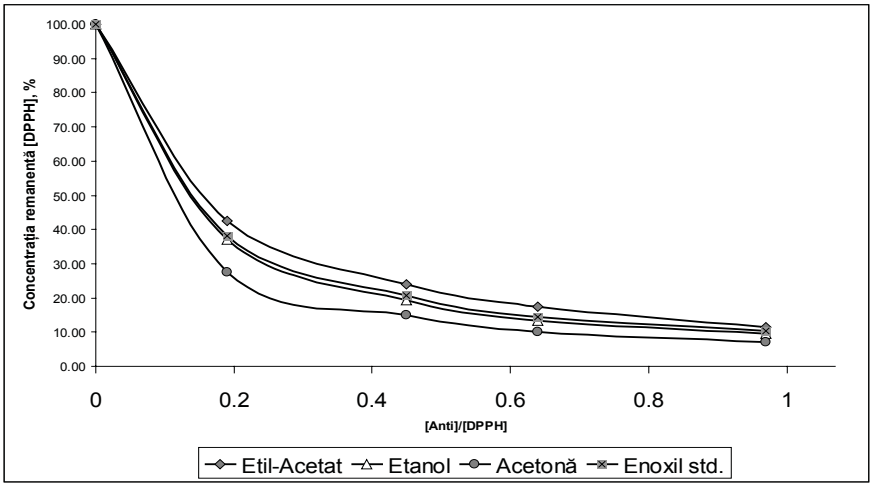

Fig. 7. Kinetic graphs of [DPPH] reduction, % function of the ratio [Anti]/[DPPH·]

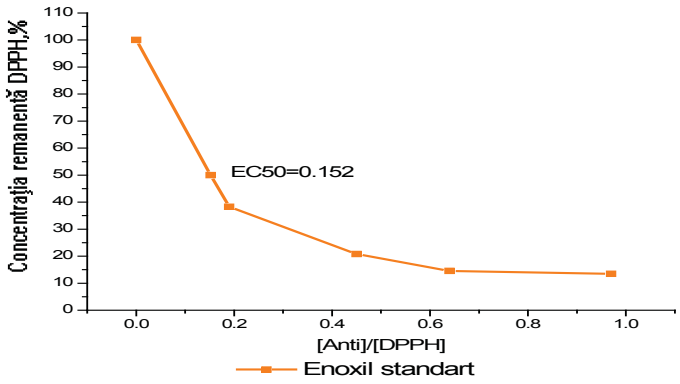

Fig. 8. Kinetic graph of [DPPH·] reduction, % function of the ratio [Anti]/[DPPH]

Thus Enoxil-acetone fraction has the highest antioxidant activity in the reaction with DPPH· (PAR = 7.7), giving a molar ratio EC_{50} of 0.13.

Another parameter for determining the antioxidant activity of antioxidants is the quantity necessary to reduce the initial DPPH· concentration by 100%, i.e. EC_{100}. The stoichiometric relationship can be determined by multiplying the EC_{50} of each antioxidant by 2, which gives the theoretical effective concentration of the antioxidant needed to reduce 100% of DPPH·.

Figure 9 presents the PAR and EC_{50} for Enoxil- acetone fraction compared with other tested antioxidants [18].

Fig. 9. Correlation between PAR and EC_{50} for the tested antioxidants, comparing to other studied antioxidants

Conclusions

- The antioxidant activity of Enoxil fractions was studied using the ABTS·+ test, and the obtained results showed that it depends on the concentration of the analyzed Enoxil forms, and for the investigated concentration range, it varies within the limits 0,55 - 0,26;
- **The antioxidant activity** for various forms doesn't differ significantly, as their chemical composition is similar. The lowest antioxidant activity was registered for the Enoxil –ethyl acetate fraction;
- The obtained results showed that at the maximal investigated concentration of 150 μg/mL of antioxidant, the efficiency of the antioxidant ativity of the fractions decreases in the order:

Enoxil - ethyl acetate < standard Enoxil < Enoxil-ethanol fraction < Enoxil-acetone fraction

- The antioxidant activity of various Enoxil fractions was studied by the DPPH· method, and the analysis of kinetics graphs showed that the tested compounds have two kinetic stages, one fast and the other slow, in the reaction with DPPH·;
- Enoxil-acetone fraction has the highest antioxidant activity in reaction with DPPH· (PAR=7.7), with an EC_{50} value of 0,129.

Acknowledgements: This research was performed with the support of the bilateral collaboration project between the Academy of Sciences of Moldova and the National Authority for Scientific Research of Romania (ANCS) no. **10.820.05.18\RoA.**

References

[1]. Popa, M. Promovarea sănătății și educației pentru sănătate. Școala națională de sănătate publică și management. Public H Press Edition, Bucharest 2006. pp 178-181 (in romanian).

[2]. Goldman, R.; Klatz R. Anti-Aging medicine: An introduction to the World's fastest-growing medical specialty. American Academy of Anti-Aging Medicine, 2002.

[3]. Nitu, R.; Corol, D., Toma, N. Free radicals in biological systems and their cytogenetics effects. Progress in Biotechnology, University from Bucharest, Centrum of Researches in Enzymology, Biotechnology and Bioanalysis, Ed. Ars Docendi, 2002, vol. 2, pp. 17-24.

[4]. Schwarzenbach, R.; Gschwend, P.; Imboden, P. M. Environmental organic chemistry. John Wiley and Sons, 2003, pp. 672-674.

[5]. Valko, M.; Leibfritz, D.; Moncol, J.; Cronin, M.; Mazur, M.; Telser, J. Free radicals and antioxidants in normal physiological functions and human disease. The International Journal of Biochemistry & Cell Biology, 2007, 39, pp. 44–84.

[6]. Halliwell, B. "Are polyphenols antioxidants or pro-oxidants? What do we learn from cell culture and in vivo studies?". Archives of Biochemistry and Biophysics. 2008, 476 (2), pp. 107–112.

[7]. Rietveld, A.; Wiseman, S. Antioxidant effects of tea: evidence from human clinical trials. J. Nutr., 2003, 133 (10), pp. 3285–3292.

[8]. Stohs, S.; Bagchi, D. Oxidative mechanisms in the toxicity of metal ions. Free Radical Biology and Medicine, 2005, 18 (2), pp. 321–36.
[9]. Gonta, A.; Bobeico, V. Activitatea antioxidanta a polifenolilor. Abstract of communication. National scientific conference for young researchers, 10 Edition, Chisinau, 2006, pp. 93-94 (in romanian).
[10]. Chung, K.; Lu, Z.; Chou, M. Mechanism of inhibition of tannic acid and related compounds on the growth of intestinal bacteria. Food and Chemical Toxicology, 1998, 36(12), pp. 1053-1060.
[11]. Kulciţki, V.; Vlad, P.; Duca, Gh. Investigation of grape seed proantocyanidins. Chemistry Journal of Moldova, 2007, 2(1), pp. 36-50.
[12]. Lupascu, T.; Lupascu, L. The obtaining procedure of the water soluble enotannins. MD Patent Nr. 3125. BOPI: 8, 2006.
[13]. Van den Berg, R.; Haenen, G. R.; Van den Berg, H.; Van der Vijgh, W.; Bast, A. The predictive value of the antioxidant capacity of structurally related flavonoids using the Trolox equivalent antioxidant capacity (TEAC) assay. Food Chem., 2000, 70, pp. 391-395.
[14]. Sroka, Z.; Cisowski, W. Hydrogen peroxide scavenging, antioxidant and anti-radical activity of some phenolic acids. Food Chem. Toxicol. 2003, 41, pp. 753-758.
[15]. Benzie, I. F.; Strain, J. J. The ferric reducing ability of plasma (FRAP) as a measure of “antioxidant power”, the FRAP assay. Anal. Biochem., 1996, 239, pp. 70-76.
[16]. Muselík, J.; García-Alonso, M.; Martín-López, M.; Žemlička, M.; Rivas-Gonzalo, J. C. Measurement of antioxidant activity of wine catechins, procyanidins, anthocyanins and pyranoanthocyanins. Int. J. Mol. Sci., 2007, 8, pp. 797-809.
[17]. Diana-Simona, A.; Gabriela, G.; Zeno, G. The anthocyans: Biologically active substances of food and pharmaceutical interest. The Annals of University Dunarea de Jos, Romania, Fascicle IV-Food Technology, 2003, pp. 106-115.
[18]. Porubin, D. Utilizarea compusilor naturali extrasi din produse secundare vinicole in inhibitia N-Nitrozoaminelor. PhD thesis abstract, Chisinau, 2009 (in romanian).

ANALYSIS OF THE PHTHALATE CONTENT LEVELS IN WINE PRODUCTS

Duca Gheorghe[1], Sturza Rodica[2], Gaina Boris[1], Lazacovici Dmitri[2] *

[1] *Academy of Sciences of Moldova, Chisinau, Republic of Moldova*
[2] *National Center for Quality Testing of the Alcoholic Beverages Chisinau, Republic of Moldova*
** dirigiblesina@yahoo.com*

Abstract: The health of the nation is one of the most important concerns of governmental and nongovernmental organizations, ecologists, etc. A number of studies have shown phthalates' potential impact on human health due to their carcinogenic and endocrine-disrupting effects [1]. More than 2000 analyses for determination of phthalates' rests in alcoholic beverages were done in the laboratory of National Center for Quality Testing of the Alcoholic Beverages (Republic of Moldova) using modern method of analysis like GC-MS.

Keywords: phthalates, wine, gas-chromatography, mass-spectrometry, dibutylphthalate.

1. Introduction

Today, in modern, industrialized society people can hardly imagine life without home appliances, communication systems, a convenient plastic packaging, fragrance and cosmetics. Most of these and many other chemical products have their properties such as strength, ductility, durability, incombustibility (incombustibility), etc., owing to a number of synthetic organic chemicals. Phthalates are among the members of this series. Phthalates (esters of phthalic acid) are included in the compositions of almost all types of plastics, rubber, paints and varnishes, giving them elasticity and strength. The most of the phthalates produced used exactly as plasticizers, near 90% (table 1). At perfume and cosmetic products phthalates mainly act as solvents and flavor fixatives.

Table 1

Annual production and consumption of wide-spread phthalates in EU countries.

Phthalate	Abbreviation	Annual production	Annual consumption
Dimethylphthalate	DMP	-	10 000-20 000 [5]
Diethylphthalate	DEP	-	10 000-20 000 [5]
Dibutylphthalate	DBP	26 000 [1]	18 000 [1]
Benzylbutylphthalate	BBP	45 000 [2]	19 500 [4]
Bis(2-ethylhexyl)phthalate	DEHP	595 000 [3]	476 000 [3]

[1] : EU RA DBP 2004; [2]: EU RA BBP 2004; [3]: EU RA DEHP 2001; [4]: EU RA BBP 2007; [5] Harris et al., 1997

The annual production of phthalates was estimated by the World Health Organization (WHO) to approach 8 million pounds (by data on 1992) [2], and 5 billion tons (by data on January 2011) [3]. Approximately 95% of the phthalate enters into the production of polymeric materials, in some of them phthalates' content reaches 50% by weight of the polymer.

Humans always are surrounded by materials containing phthalates, such as linoleum, insulation of wires, pipes, plastic housings of domestic appliances, toys, varnishes and paints.

Most researchers from different organizations suggest that in most cases influence of phthalates upon person is below the tolerable daily intakes (TDI) [2, 4-8]. But it is difficult to determine accurately the dose of exposure as the spreading of phthalates everywhere. According to international studies performed by Center for the Evaluation of Risks to Human Reproduction [7] this factor is in the following ranges (table 2). Women and children are most susceptible to phthalates.

Table 2

Daily dose of phthalate and its effect on different categories of the population

Category/ Age	Age categories				
	Childrens 0-1	**Childrens 1- 3**	**Childrens 4- 10**	**Women 18- 20**	**Men 18- 80**
Daily intakes, µg /kg BW	55- 380	20- 183	5- 54	8- 124	8- 92

(*BW – body weight*)

It is supposed that phthalates accumulate in the human body, which negatively affects its hormones, liver and kidneys may also become the causes of allergies, asthma and cancer, neurodevelopmental disorders and abnormalities in the development of children [8-12]. Molecules of phthalates are not structural elements of the polymer chains and therefore easily stand out in the environment, getting into the human body through food, skin or by inhalation.

In a number of investigated wine-products released by vendors it was detected the presence of phthalates. Particular attention was given to the DBP.

2. Material and Methods

2.1. Methods and reagents

Measuring the concentration of dibutyl phthalate in wine and base-wine based on its elimination by chloroform extraction, chromatographic separation on a capillary column, identify the retention time and mass spectrum, and quantify with the characteristic ion m/z 149. Measuring the concentration of dibutylphthalate in alcoholic beverages such as vodka, brandy, cognac alcohol, rectified ethyl alcohol was based on chromatographic separation of the sample on a capillary column using Aldrin with a purity above 99.3% and supplied by SUPELCO as an internal standard, the identification was made by retention times and mass spectrum, quantification of characteristic ion m/z 149 for DBP, and 66, 261, 263, 265 for Aldrin.

The background solution (synthetic wine) was used to prepare the calibration solutions. It consisted of aqueous solution of 15% ethanol and tartaric acid (5g/dm^3) (tartaric acid, supplied by FLUKA, puriss. p.a. for ion chromatography) and carried to the pH to 3.5 with 5M sodium hydroxide. Synthetic wine was used for calibration standard solutions with concentrations of DBP: 0 - 1,00 mg/dm^3 (dibutylphthalate, PESTANAL from SIGMA-ALDRICH, 99.8%). For the extraction of DBP, 100 ml of sample (calibration solution) was placed in a separatoring funnel of 250 cm^3 with addition of 10 cm^3 of chloroform (Chloroform, LGC PROMOCHEM, for HPLC). Extraction was implemented in 10 min with continuous shaking. After separating the organic layer the bottom layer of chloroform was drained through a paper filter with anhydrous sodium sulfate (sodium sulfate anhydrous, STANCHEM, Spain). Collected 10 ml of the chloroform extract was transferred into a gas chromatography vial, from which was selected 1,0 µl of extract by microsyringe directly for analysis using gas chromatography with mass-spectrometer.

2.2. Instruments

SHIMADZU GCMS-QP-2010S (IS) with a COMBI PAL autosampler (CTC ANALYTICS, Zwingen, Switzerland) equipped with fused silica column RESTEK - Rtx-5MS (30m/0.25mm/0.25µm 100% dimethylpolisiloxane phase) was used to perform injections and gas chromatographic analyses in an automated way.

2.3. *Gas chromatography – mass spectrometry*

The oven program started at an initial temperature of 150^{0}C for 1 min. Temperature was then increased at a rate of 10^{0}C/min to 200^{0}C, maintained for 1 min, then increased at a rate of 20^{0}C/min to 280^{0}C and maintained for 10 min. The carrier gas was helium at 1.0 ml/min (99.9990%), split 5. Ionisation was performed by electron impact (EI), setting the electron multiplier to 1300V. The temperatures used were 260^{0}C for the injector, 280^{0}C for the transfer line, and 200^{0}C for the ion source. The compounds were quantified in selected ion monitoring (SIM) mode. The analyte to internal standard peak area ratio was used as analytical signal for constructing the calibration graphs.

Duration of gas chromatography-mass spectrometric analysis for phthalates constituted 25 minutes.

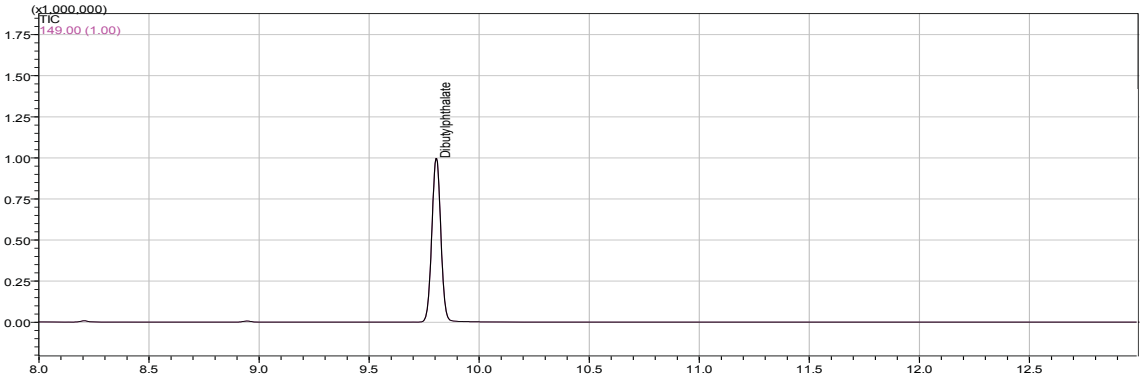

Fig.1. Chromatogram of an extract of a DBP standard solution with concentration 0,10 mg/dm^3

For the analysis of strong alcoholic beverages calibration solutions of DBP were prepared on the basis of 40% water-alcohol mixture with the addition of a solution of aldrin (IS).

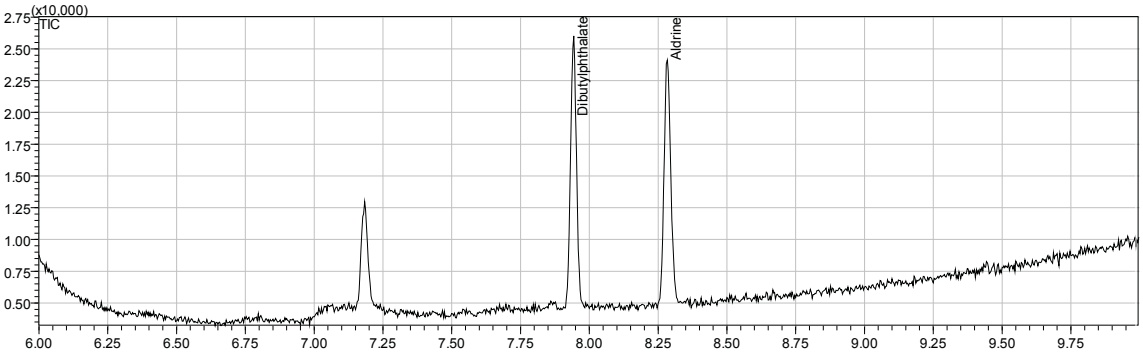

Fig.2. Chromatogram of standard solution of DBP (0,25 mg/dm^3) - Aldrin 0,50 mg/dm^3

3. Results and discussion

The studies conducted in the laboratory of National Center for Quality Testing of the Alcoholic Beverages (Republic of Moldova) included more than 2000 samples of the bottled wine and base-wine for the presence of DBP. The results are shown in table 3.

Table 3

Distribution levels of contamination by DBP in wine production (for base-wine, treated wine and bottled wine)

Product type	DBP concentration, mg/dm^3 (P=0,95)			
	<0,01	**0,01-0,20 / average[1]**	**0,20-0,30/ average [2]**	**>0,30/ average [3]**
Base-wine:				
white	29%	**49%**/ 0,09±0,04	**13%**/0,23±0,03	**9%**/ 0,34±0,07
red	16%	**64%**/ 0,12±0,02	**15%**/0,25±0,04	**5%**/ 0,39±0,11
Treated wine:				
white	9%	**66%**/0,11±0,07	**14%**/0,26±0,04	**11%**/0,32±0,05
red	17%	**57%**/0,17±0,05	**14%**/0,22±0,06	**12%**/0.41±0,07
Bottled wine:				
white	19%	**70%**/0,16±0,05	**9%**/0,22±0,06	**2%**/0,34±0,07
red	16%	**68%**/0,13±0,06	**10%**/0,27±0,05	**6%**/0,37±0,03

[1] - <0,01 - according to the document Hygienic Normatives 2.3.3.972-00 "MCL (Maximum Concentration Limit) of chemicals released from materials, which are in contact with food";

[2] - <0.20, according to the requirements of Hygienic Normatives 2.1.5.1315-03 and changes of Hygienic Normatives 2.1.5.2280-07 "MCL (Maximum Concentration Limit) of chemicals in drinking water, water bodies and cultural-domestic water", for drinking water;

[3] - in accordance with Article 11 of Regulation (CE) 882/2004, LMS = 0,3 mg DBP/kg for the model solutions.

To establish the sources of DBP pollution in wines there were studied 7 samples of sulfitated and concentrated must: <0.01-0.15ppm of DBP was detected. The lowest concentration level of DBP was characteristic for sulfitated must, then concentrated - 0.05-0.15ppm. The results of investigations of 15 grapes samples were negative. In addition, was investigated water at the five wineries used in wine production. It was found that concentration of DBP in natural water is lower than LOQ, while content in flushing water is 0.04-0.05ppm, and 0.09-0.11ppm of DBP in softened water.

Therefore contamination of phthalates has a technogenic character, and it is the result of contact with polymeric materials. In the sequel, we studied samples of different materials, which were in contact with wine production during the winemaking process and storage, such as paints, varnishes, primers, pipes, rubber seals. All these tests were conducted according the Directive 2007/19/EG. Also was investigated migration of DBP to a model solution - 15% aqueous ethanol solution, acidified with tartaric acid. Migration of phthalates from materials, which are in contact with wine, is a continuous process that can continue throughout the period of production or storage. The rate of migration was determined basing on these investigations. Studies have been conducted on materials submitted by Moldovan winemakers and distributors. In addition to fresh paint (intended for contact with food) were analyzed paints, which were in contact with wine during a certain period of time. Fresh (liquid) paint was applied to the flask's inner surface, dried on air in 2-3 days, and then a

model solution was placed into the flask. Content of DBP was determined in the model solution, which was in contact with the dry polymer within 1 day. Ratio of polymer and model was 1:100. Migration took place at the room temperature (20-22^{0}C). The results are presented in tab.4.

Table 4

Migration rate of DBP from the polymer (The ratio of polymer: model = 1:100)

Migration	Paint	Plastic tubes	Rubber seals
mg DBP/kg polymer/day	Fresh paint 867,4[1] 345[2] 339[3] Paint contacted with alcoholic beverage during ~ 1 year 65,7[4] 63,3[5] 63,7[6] 61,2[7] Paint contacted with alcoholic beverage during 2-3 years 33,2[8] 35,1[9] Paint contacted with alcoholic beverage during >5 years 0,7[10] 3,4[11] 6,9[12]	Non-used in the making process 142[13] have been in contact with product 33,5[14]	Non-used in the making process 506[15] have been in contact with product 31,5[16]

[1-16] - materials obtained from various wineries, average of two parallel measurements.

In order to optimize the extraction process of DBP during presampling were investigated some dependencies:

a) Effect of pH on the level of recovery was established. Samples of synthetic wine with different values of pH (3.5, 4.0, 4.5, 5.0, 5.5, 6.0, 6.5, 7.0) were contaminated by DBP. The level of recuperation for a solution with pH = 7.0 was taken as 100%. The results are expressed in fig. 3.

b) Similarly, the influence of sugar content on the extractability of DBP was investigated with Synthetic wine (2.1). Sugar concentration in the samples was formed using concentrated must (C (DBP) <0.01mg/dm^3). DBP was added to the obtained model solutions with concentrations of sugars: 0, 30, 50, 100 and 150 g/dm^3. Chloroform extracts of these samples were analyzed. The results are expressed in fig. 3.

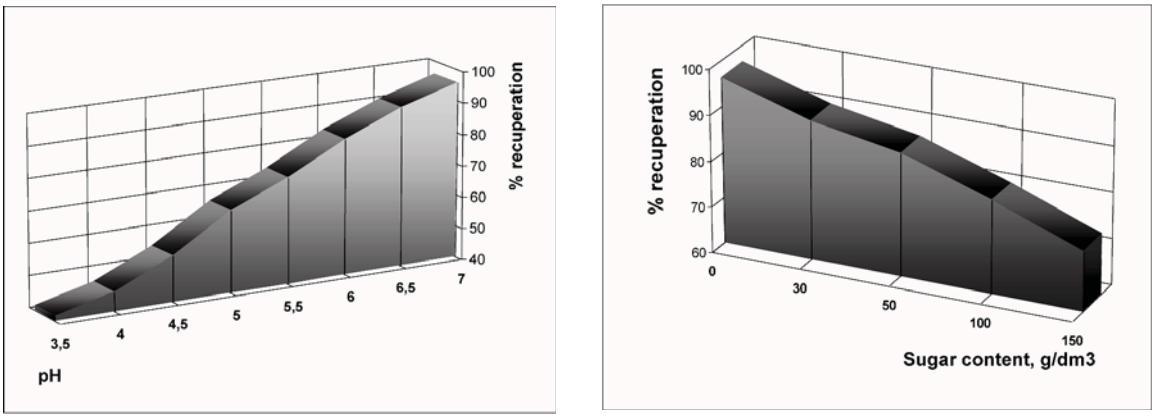

Fig.3. Effect of pH and sugar's content on the recuperation level of DBP

c) Effect of alcohol content on the extractability of DBP was also investigated using synthetic wine (2.1). Alcohol content in the samples was formed by ethyl alcohol (C (DBP) <0.01mg/dm^3). DBP was added to the obtained model solutions with concentrations of alcohol: 6, 9, 12, 15, 18 and 21% v/v. Chloroform extracts of these samples were tested. As it follows from the results of investigation alcohol content doesn't influence significantly on the level of recovery (fig. 4).

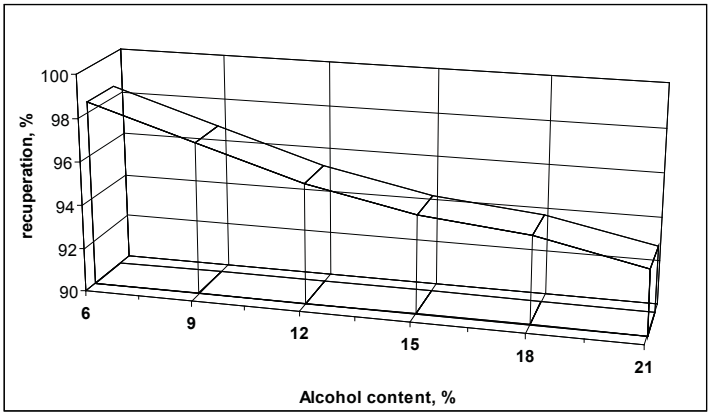

Fig. 4. Effect of alcohol content on the recuperation level of DBP

4. Conclusions

In the context of studies conducted in the laboratory of National Center for Quality Testing of the Alcoholic Beverages (Republic of Moldova) were included more than 2000 samples of the bottled wine and base-wine for the presence of most widespread and toxic phthalate – dibutylphthalate. Results display presences DBP in 85 % of studied samples of wines, i.e. a content of DBP more than LOQ (0.01mg/dm^3). Samples of sulfitated and concentrated must, natural and softened water and grapes samples were studied to establish the sources of DBP pollution in wines. Has been determined that contamination of phthalates has a technogenic character, and it is the result of contact with polymeric materials. Optimum conditions of extraction DBP from liquid samples were obtained. Also has been established, that significant influence on extractability is performed by pH value and sugars content value, the alcohol contents in synthetic wine has not displayed significant effect. In addition migration DBP from polymeric materials has been learnt. In the nearest future we plan to research plugs and other materials used in winemaking process on presence of DBP and its migration.

Acknowledgments

Authors would like to acknowledge Moldavian wineries and distributors for the represented samples and the required information.

References

[1]. Peakall DB. Phthalate esters: occurrence and biological effects. Residue Rev 1975, 54: 1 – 41.
[2]. WHO 1992: Diethylhexyl phthalate, Environmental Health Criteria 131.
[3]. Phthalates and Their Alternatives:Health and Environmental Concerns. Universisty of Massachusetts Lowell. 2011, 4.
[4]. CE : The Scientific Committee on Medicinal Products and Medical Devices : Opinion on Medical Devices Containing DEHP Plasticised PVC.
[5]. EU RA DBP 2004.
[6]. Communication 2006/C 90/04 du 13 avril 2006 de la commission européenne.
[7]. CE JRC Institut of health and Consumer protection Toxicology and chemical substance. Phthalates Risk assessment report – 2008.
[8]. CEHRH. Center for the Evaluation of Risks to Human Reproduction. NTPCERHR expert panel.
[9]. CSTEE. Scientific Committee on Toxicity, Ecotoxicity and the Environment. Opinion on the results of a second risk assessment of phthalates in human health part. Brussels: European Commission, 2004.
[10]. T. Lovekamp-Swan, B.J. Davis, Environ. Health Perspect. 111 (2003) 139.
[11]. Caroline Sablayrolles, Mireille Montr´ejaud-Vignoles, David Benanou, Lucie Patria, Michel Treilhou. Development and validation of methods for the trace determination of phthalates in sludge and vegetables. Journal of Chromatography A, 1072 (2005) 233–242.
[12]. Barnabé S, Beauchesne I, Cooper DG, Nicell JA. Plasticizers and their degradation products in the process streams of a large urban physicochemical sewage treatment plant. Water Res 2008, 42: 153- 162.

COORDINATION COMPOUNDS OF NICKEL(II), COPPER(II) AND COBALT(II) BASED ON S-METHYLISOTHIOSEMICARBAZIDE AS DYES FOR THERMOPLASTIC POLYMERS

Ştefan Manole, Maria Cocu*

Institute of Chemistry, Academy of Sciences of Moldova, str. Academiei, 3, MD-2028, Chişinău, Republic of Moldova
Tel. +373 22 73 99 63; E-mail: mariacocu@gmail.com

Abstract: We have researched the color properties of coordination compounds synthesized by us previously [1] (8-(1′,2′-naphthyl)-1-R3-methyl-6-thiomethyl-4,5,7-triazaocta-1,3,5,7-tetraenato-1,1′-diolato(-)O, O′, N^4, N^7-M(II), where R=CH_3, C_6H_5, M=Ni, Co, Cu), which can be used for coloring thermoplastic masses. They meet the requirements for use as a pigment for coloring thermoplastic masses [2]. Colors of colored products have a high photostability (7 points), thermostability (>250 °C) and intensity of color that give a low consumption (0.004 to 0.008 g medium tone, a 0.040-0.080 g to 100 g polystyrene intense tone and 0.002 to 0.008 g medium tone and 0.010-0.030 g intense tone for 100 g polyethylene). Compounds of nickel (II) stained polystyrene and polyethylene in red, cobalt (II) - in green with a yellow tinge, copper (II) - in deep red with a yellow tint.

Keywords: coordination compounds, transition metals, dyes, thermoplastic polymers.

Introduction

Synthesis of coordination compounds containing active functional groups capable of forming chelate compounds remains a current problem of preparative chemistry. The interest in the synthesis of compounds with such properties is stimulated by both theoretical and practical issues. They possess biological properties [3], catalytic properties [4], and can be used as dyes [5-10].

A special role in the synthesis of coordination compounds has the template method, where the central ion guides the assembly of polydentate ligands [11]. Authors [12-17] have shown that thiosemicarbazide and their derivatives easily condense with polydentate organic ligands, polyfunctional possessing different types of coordination especially with transition metals. Metal organizes the assembly of ligands.

For example, 2,2-difluor-9-alkylthio-5,6-di(α-furyl)-12-methyl-1,3-dioxa-4,7,8,10,11,14-hexaaza-2-boracyclotetradeca-4,6,8,11,13-pentaenato-N^4,N^7,N^{10},N^{14}-nickel(II) with coordination node to the central atom N_4, which has a dark brown color, stained polyethylene and polystyrene in green color with brown tint [5]. In [6], where the fragment >BF_2 is replaced with H, it is demonstrated that mentioned polymers don't change their color when used for coloring. In the study of color properties of polymer (9-(1′,2′-naphthyl)-4-methyl-7-alkylthio-5,6,8-triazanon-2,4,6,8-tetraenato(-)-1′,2-diolato-O^1, O^2, N^5, N^8-nickel(II), where the coordinative node is N_2O_2, a color change of coordination polymers has been observed from green with brown tint [5, 6] to bordeaux. In this case, like in those previously mentioned, no visible influence of alkyl radical on the color of polymers is observed.

Of great interest is the influence of metal in this type of compounds at coloring of plastics masses.

Results and discussion

Using these methods, we proceeded to the synthesis of new compounds of this type. As a result of the interaction of methanol solutions of acetyl(benzoyl)acetone S-methylisothiosemicarbazone with 1-hydroxy-2-naphthaldehyde and $M(CH_3COO)_2 \cdot XH_2O$ were obtained coordination compounds: 8-(1′,2′-naphthyl)-1-R-3-methyl-6-thiomethyl-4,5,7-triazaocta-1,3,5,7-tetraenato-1,1′-diolato(-)O, O', N^4, N^7-M(II), where R=CH_3, C_6H_5, M=Ni, Co, Cu, with general formula:

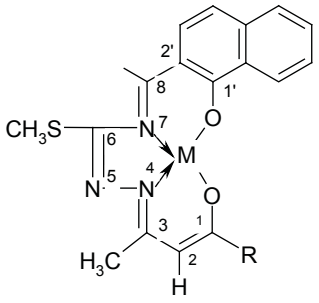

Where R=CH_3, M=Ni (1), Co(2), Cu(3)
R=C_6H_5, M=Ni (4), Co(5), Cu(6) (table 1).

Composition of substances and their structures have been established and confirmed by physico-chemical methods of analysis (IR spectroscopy, UV-Vis, ^{1}H, ^{13}C NMR, mass spectrometry, magnetochemistry and X-ray crystallography) [1].

Compounds are in the form of fine dark-brown crystalline powder, insoluble in water, alcohol, slightly soluble in chloroform, soluble in dimethylsulphoxide. Some practical properties of the mentioned compounds have been studied, which proved to be promising. For example, compounds of nickel(II) and copper(II) activate biological processes which is manifested by stimulating the biosynthesis of pectolytic enzymes of fungal strain (~ 50%) and increased biomass accumulation (10-15%) compared to the control [14].

Table 1

Characteristics of dyes 1-6

Dye			Thermostability, °C	Color of polystyrene	Color of polyethylene	Photostability, points	Uniformity of color	Consumption dyes, g /100 g polymer							
								Polystyrene				Polyethylene			
								Block type		Emulsion, suspension		High density		Low density	
M	R	No.						Middle tone	Intense tone	Middle tone	Intense tone	Middle tone	Intense tone	Middle tone	Intense tone
Ni	CH_3	1	250	Claret	Claret	7	Uniformly	0.004 - 0.008	0.040 – 0.080	0.008 – 0.010	0.020 – 0.050	0.002 - 0.004	0.010 - 0.030	0.002 - 0.004	0.010 – 0.030
Ni	C_6H_5	2	320	Claret	Claret										
Co	CH_3	3	250	Green with yellow tint	Green with yellow tint										
Co	C_6H_5	4	365	Green with yellow tint	Green with yellow tint										
Cu	CH_3	5	250	Claret with yellow tint	Claret with yellow tint										
Cu	C_6H_5	6	360	Claret with yellow tint	Claret with yellow tint										

Bearing a high thermostability (>250 ° C), photostability (7 points), migration luminescence, stability and physical-mechanical processing, given the diversity and intensity of color, the produced compounds meet the requirements [2] for use as plastics dyes.

We tried testing these compounds as pigments for coloring polystyrene block, suspension, emulsion and high and low density polyethylene. Experiments conducted under laboratory conditions received promising results.

Coordination compounds 1 and 2 color polystyrene and polyethylene in claret, compounds 3 and 4 - green with yellow tint, compounds 5 and 6 - deep red with yellow tint. Thus, the metal bears a decisive influence on the color of plastic parts. The influence of the radical R on the color change of plastic parts is not visually observed, but analysis data of the absorption spectra from the visible region suggests a insignificant influence.

It should be noted, that the amount of dyes used for coloring polystyrene (block, emulsion or suspension) and low or high density polyethylene is very low (0.004 to 0.008 g medium tone, 0.040 to 0.080 g intense tone to 100 g polystyrene and 0.002 - 0.008 g medium tone, 0.010-0.030 g intense tone to 100 g polyethylene) (Table 1).

Varying the dye concentration, transparent plastic parts with different shades or non-transparent ones can be obtained. The obtained pieces are colored evenly, possess a high photostability, and stable towards physico-mechanical processing.

Due to the accession of compounds 1-6 to polystyrene, their use as dyes for thermoplastic masses does not require additional staff to process grain, in this case the dye consumption is reduced significantly.

Conclusions

Polystyrene and polyethylene colored with products of condensation of acetyl(benzoyl)acetone S-alkylisothiosemicarbazones and organic polydentate ligands usually have a high thermostability, migration luminescence, stabilized photostability at physical and mechanical processing and pronounced color intensity. Polymers are color-enteritis due to metal, S-alkylisothiosemicarbazone and polydentate aducts, but no alkyl radical influence is observed.

Experimental

Prior to coloring, polystyrene in block, emulsion or suspension granulated is mixed in a reactor supplied with a thermometer, a stirrer and a tap to release the reactor content into the mold. At stirring, the mixture in the reactor is heated up until the components melt; afterwards they are fused as required. In the case of coloring polyethylene, a more intense stirring is required, as the adherence of the dye to polyethylene is lower than for polystyrene.

References

[1]. Cocu, M. Sinteza templata si studiul compusilor coordinativi ai unor 3d-elemente cu liganzi tetradentati in baza tiosemicarbazidei alchilate. PhD thesis abstract. Chişinău 2007, 24 p. (in romanian).
[2]. Gordon, P.; Gregori, P. Organicescaia himia crasitelei. Moscow, Mir, 1986, p. 158 (in russian).
[3]. Dugas, H. Bioorganic chemistry. New York, 1996, pp. 338-460 (ISBN 0-387-94494-X (hardcover), ISBN 0-387-98910-2 (softcover)).
[4]. Bush, D. Uspehi Khim., 1969, v. 38, № 6, p.822-853 (in russian).
[5]. Patent MD 1206 G2, 30.04.1999.
[6]. Patent SU 1808845 A1.
[7]. Patent MD 2881 G2, 10.31.2005.
[8]. Khatirinejad-Fard, S.; Khanlou, M. New method of synthesis for the substituted aromatic di-carbonyl pigments. Abstracts of Papers, 234th ACS National Meeting, Boston, MA, United States, August 19-23, 2007.
[9]. Alexandrescu, G. Industria Usoara. Bucharest, 1965, 12, pp. 7-11(in romanian).
[10]. Patent DE2728864 A1.
[11]. Gerbeleu, N. V., Arion, V. B.; Burgess, John. Template Synthesis of Macrocyclic Compounds. Wiley-VCH, 1999 ISBN: 3527295593, 567 p.
[12]. Gărbălău, N.V.; Revenco, M.D. J. Neorg. Khim., 1971, v. 16, p. 1046; 1972, v. 17, p. 2126; 1973, v. 18, p. 2397 (Russian Journal of Inorganic Chemistry, in russian).
[13]. Iampoliskaia, M.A.; Shova, S.G.; Gărbălău, N.V. and all. J. Neorg. Khim., 1982, v. 27, p. 2551 (Russian Journal of Inorganic Chemistry, in russian).
[14]. Arion, V. B.; Gărbălău, N.V.; Indricean, C.M. J. Neorg. Khim., 1986, v. 31, p. 126 (Russian Journal of Inorganic Chemistry, in russian).
[15]. Cocu, M.A.; Grădinaru, J.I.; Revenco, M.D.; Rybak-Akimova, E.; Gărbălău, N.V. Chem. J. of Moldova, 2008, 3(2), pp. 38-46.
[16]. Bourosh, P.N.; Simonov, Yu.A.; Arion, V.B.; Sobolev, A.N.; Gărbălău, N.V.; Pahopol, V.S. Kristallographiya, 1989, v. 34, p. 637-641 (Crystallography Reports (Kristallografiya), in russian).
[17]. Cocu, M.A.; Clapco, S.; Gărbălău, N.V.; Grădinaru, J.I. Romanian International Conference on Chemistry and Chemical Engineering- RICCCE XIV. Bucharest, Romania, September 22nd – 24th, 2005, p. S01-51 - S01-53.

SYNTHESIS AND SPECTROSCOPIC STUDY OF SOME COORDINATIVE COMPOUNDS OF Co(III), Ni(II) AND Cu(II) WITH DIANILINE- AND DISULFANILAMIDEGLYOXIME

Andrei Rija*, Ion Bulhac, Eduard Coropceanu, Elena Gorincioi, Elena Calmîc, Alic Barbă, Olga Bologa

Institute of Chemistry, Academy of Sciences of Moldova, 3 Academiei st., MD-2028, Chisinau, Moldova
E-mail: andreirija@yahoo.com, tel/fax (373) 22 739611

Abstract: Directed synthesis of dianiline- ($DAnH_2$) and disulfanilamideglyoximes ($DSamH_2$) has been accomplished by condensation of dichloroglyoxime with aniline or sulfanilamide in 1:2 molar ratio, as well as their corresponding Co(III), Ni(II) and Cu(II) coordinative compounds. Composition, structure and some properties of dioximes and complexes have been established by using elemental analysis, UV-Vis, IR and NMR- spectroscopies. Dioxime coordination at the central atom and structure of complexes depends on pH of reaction medium: at pH=5-6 - *bis*-dioximates, whilst at pH=2 – *tris*-dioximines are obtained. In the case of the corresponding *tris*-dioximines increment of the functional groups number in dioxime fragments, which can form intermolecular hydrogen bonds, leads to the augment of the stability of complexes.

Keywords: α-dioximes, coordinative compounds, 3d metals, spectroscopy.

Introduction

Actually *vic*-dioximates are appreciated as coordinative compounds possessing a broad spectrum of applications in branches as: analytical, biological, medicinal and pigment's chemistries. *vic*-Dioximes and the important role of their complexes, especially with 1.2-dioxime, have been widely investigated, while the substitution of some fragments of dioxime can significantly influence the structure and stability of complexes [1-4].

On interaction of amines or thiols with dichloroglyoxime or cianogen-di-N-oxide different symmetrically substituted derivatives of diamine- or dithioglyoxime have been obtained. New optically active *vic*-dioximes have been described and the syntheses of mono- and dinuclear complexes on their basis have been performed [5, 6].

Cobaloximes containing *bis*-(thiophenyl)glyoxime in equatorial plane have been studied [7]. It has been noted that the orientation of thiophenyl groups with respect to the dioximine plane varies depending on the size of axial ligand and influences the values of chemical shifts in NMR-spectra. The *cis*-position of thiodioxime from the equatorial plane reflects upon Co–C bond reactivity in these complexes. A study with the use of cyclic voltametry has demonstrated that reduction Co(III)/Co(II) and Co(II)/Co(I) occurs easier in $ClCo(dSPhgH)_2Py$ (dSPhgH – dithiophenylglyoxime) in comparison with other chlorocobaloximes (gH - glyoxime, dmgH -dimethylglyoxime, dpgH - diphenylglyoxime). Thus, the general investigations in this field clearly suggest that many of the axial ligand's chemical properties: spectroscopic, geometry, kinetics significantly depend on the changes in equatorial ligand.

Gumus *et. al.* [8] have shown that inclusion of hexilamine radical in dioxime fragment permits to obtain Ni(II) and Pd(II) dioximates and in their crystalline structure tubular channels with diameter ~16 Å were found.

Recent investigations have demonstrated the biostimulator activity of Co(III) dioximates upon fungi [9,10]. Supplementation the nutritive medium of these microorganisms with the mentioned compounds causes an enhancement of the outcome of enzime production and in some cases the technological cycle of cultivation the producer has been diminished [11].

On the basis of biostimulator effects in enzymogenesis processes of Co(III) complexes containing aniline or sulfanylamide on axial coordinate, their inclusion in dioximine moiety has been considered, aimed at obtaining the new dioximates of transition metals, which will accentuate these properties, as expected. Furthermore, the mobility of the „wings" of these dioximes can open interesting structural opportunities for obtaining the supramolecular systems. Preparation of dioximates with bulky ligands could make possible the formation of gaps in the crystalline structure [8], which is favourable for the intake of small molecules.

Materials and methods

Composition, structure and properties of oximes and complexes have been established on the basis of elemental analysis, as well as IR, UV-Vis and NMR spectroscopies data. IR-spectra of compounds were recorded at FT-IR Perkin Elmer ***Spectrometer 100*** in vaseline oil at 4000–400 cm^{-1} and ATR at 4000–650 cm^{-1}. UV-Vis spectra were recorded at Perkin Elmer ***Lambda 25*** spectrophotometer in water solutions of compounds of $0.5 \cdot 10^{-4}$ mol/L. NMR-spectra were recorded on a Bruker spectrometer at 400.13 MHz for ^1H and 100.61 MHz for ^{13}C in DMSO-d_6 using TMS as an internal reference. Chemical shifts (δ) are reported in parts per million (ppm) and are referenced to the residual non-deuterated solvent peak (2.49 for ^1H and 39.70 for ^{13}C).

Experimental part

Synthesis of coordinative reagents

Glyoxime has been synthesized according to the literature procedure [12] in 67% yield.

Dichloroglyoxime has been prepared as reported by Dutta *et al.* [7] in ~35% overall yield. Compound is soluble in alcohols, DMF, DMSO.

Disulfanilamideglyoxime ($DSamH_2$). The solution of 3.14 g (0.02 mol) dichloroglyoxime in 15 ml ethanol was added to a solution of 6.89 g (0.04 mol) sulfanilamide in 40 ml ethanol at room temperature (rt) under continuous stirring. The reaction mixture was cooled in ice bath for 10 min, and then 3.20 g (0.03 mol) sodium carbonate was added. The mixture was stirred for 6 hr, then diluted with 20 ml water and left in refrigerator for the next day. The obtained precipitate was filtered off, washed with cold water and dried in air. Yield: 63%. Found, %: C 39.14; H 3.58; N 19.54. Calculated for $C_{14}H_{16}N_6O_6S_2$, %: C 39.25; H 3.76; N 19.62.

Dianilineglyoxime ($DAnH_2$) was prepared, in 93% yield, according to the procedure as described for preparation of disulfanilamideglyoxime. Found, %: C 62.15; H 5.09; N 20.66. Calculated for $C_{14}H_{14}N_4O_2$, %: C 62.21; H 5.22; N 20.73.

Synthesis of coordinative compounds.

$[Ni(DAnH_2)_3]Cl_2 \cdot 6CH_3OH$ (1). To the warm solution of 0.27 g (1.0 mmol) $DAnH_2$ in 30 ml methanol the solution of 0.12 g (0.5 mmol) $NiCl_2 \cdot 6H_2O$ in 20 ml methanol was added. The obtained mixture was stirred for 5-10 min, then filtered and left at rt. After 2-3 days the crystals have appeared in solution of emerald color. The crystals are soluble in diethyl ether, alcohols, DMSO and DMF. The reaction yield constituted 46 %. Found, %: C 50.78; H 5.81; N 14.76. Calculated for $C_{48}H_{66}Cl_2N_{12}NiO_{12}$, %: C 50.90; H 5.87; N 14.84.

$[Ni(DAnH)_2] \cdot H_2O$ (2). A solution of 0.27 g (1.0 mmol) $DAnH_2$ in 30 ml methanol was added to a solution of 0.12 g (0.5 mmol) $NiCl_2 \cdot 6H_2O$ in 20 ml methanol and the mixture was stirred for 10 min at 40-50°C. Ammonia (1-2 drops, 25%) was added while stirring. The color of solution changed from green to brown and a precipitate of the same color has been formed. The precipitate was filtered off, washed with cold methanol, ether and dried at rt. The reaction yield constituted 56%. The complex is soluble in DMF and weakly soluble in methanol and DMSO. Found, %: C 54.59; H 4.45; N 18.09. Calculated for $C_{28}H_{28}N_8NiO_5$, %: C 54.66; H 4.59; N 18.21.

$[Cu(DAnH_2)_3]SO_4 \cdot 3H_2O$ (3). For the synthesis of this complex similar conditions as for compound (**1**) were applied, but the solubilisation of Cu(II) salt in a minimal amount of water has preceded the addition of methanol. The reaction yield constituted 42%. Compound is soluble in DMSO, DMF and alcohols. Found, %: C 49.16; H 4.67; N 16.32. Calculated for $C_{42}H_{48}CuN_{12}O_{13}S$, %: C 49.24; H 4.72; N 16.41.

$[Co(DAnH)_2(Thio)_2]_2[TiF_6] \cdot 2DMF \cdot H_2O$ (4). Dianilineglyoxime, 0.27g (1.0 mmol) and thiocarbamide, 0.08 g (1.0 mmol) were dissolved in a mixture of 10 ml DMF and 40 ml methanol. The mixture was refluxed at ~60°C, under stirring. Chrystallohydrate $CoTiF_6 \cdot 6H_2O$, 0.17 g (0.5 mmol) was dissolved in 10 ml water and added by dropping funnel (~ 1 drop in 4-5 sec.) to the initial solution and stirring was continued for 3 hr. Ammonia solution (1:4) was dropped into reaction to adjust its pH to ~5 and this value was maintained till the end of reaction. The stirring was stopped and the reaction medium was left for slow evaporation. Dark brown monocrystalls were obtained that were unstable at air. Reaction yield constituted 19%. Compound is soluble in DMF, DMSO and less soluble in alcohols. Found, %: C 43.31; H 4.52; N 19.81. Calculated for $C_{66}H_{84}Co_2F_6N_{26}O_{11}S_4Ti$, %: C 43.42; H 4.64; N 19.95.

$[Co(DAnH_2)_3]_2[TiF_6]_3 \cdot 1.5DMF$ (5). This compound has been synthesized as afore-described for **(4)**, without the addition of ammonia solution. The results of investigations have shown that thiocarbamide moiety does not enter the complex and three molecules of non-deprotonated dioxime are bound to the central atom. Reaction yield constituted 32%. Product is soluble in alcohols, DMF and DMSO. Found, %: C 45.38; H 3.96; N 15.11. Calculated for $C_{88.5}H_{94.5}Co_2F_{18}N_{25.5}O_{13.5}Ti_3$, %: C 45.53; H 4.08; N 15.30.

$[Ni(DSamH)_2] \cdot 2H_2O$ (6). To the warm solution of 0.21 g (0.50 mmol) disulfanilamideglyoxime in 30 ml methanol 0.06 g (0.25 mmol) $NiCl_2 \cdot 6H_2O$ in 15 ml methanol were added and the mixture was stirred for 15 min at 60°C. While stirring few drops of ammonia was added and a brown precipitate appeared that was separated, washed with cold methanol then diethyl ether and dried at air. Reaction yield constituted 43%. Complex is soluble in DMF and DMSO and weakly soluble in methanol. Found, %: C 35.41; H 3.54; N 17.62. Calculated for $C_{28}H_{34}N_{12}NiO_{14}S_4$, %: C 35.41; H 3.61; N 17.70.

$[Cu(DSamH_2)_3]SO_4 \cdot 5H_2O$ (7). Disulfanilamideglyoxime, 0.21 g (0.50 mmol) was dissolved in 40 ml methanol and heated in water bath at 60°C. Crystallohydrate $CuSO_4 \cdot 5H_2O$, 0.06 g (0.25 mmol) dissolved in a minimum amount of water and 20 ml methanol was added dropwise to the solution of ligand, then heating was removed and the solution was left at rt. The slow evaporation gave dark-brown crystals. Reaction yield constituted 52%. Compound is soluble in DMF and DMSO. Found, %: C 32.72; H 3.71; N 16.34. Calculated for $C_{42}H_{58}CuN_{18}O_{27}S_7$, %: C 32.86; H 3.81; N 16.42.

$[Co(DSamH)_2(Thio)_2]_2[ZrF_6] \cdot DMF \cdot H_2O$ (8). A mixture of 0.21 g (0.5 mmol) disulfanilamideglyoxime in 30 ml methanol and 0.04 g (0.5 mmol) thiocarbamide in 10 ml methanol was refluxed at 60°C with stirring. To this mixture a solution of 0.1 g (0.25 mmol) $CoZrF_6 \cdot 6H_2O$ in 20 ml of water/methanol (1:1) was added. The reaction mixture was stirred for 3 hrs, while maintaining the pH of solution at 4.5-5.5 value by dropping ammonia solution (1:3). A

dark brown precipitate was formed that was filtered off, washed with cold methanol and diethyl ether. Reaction yield constituted 36%. Compound is soluble in methanol, DMF and DMSO. Found, %: C 31.02; H 3.46; N 18.91. Calculated for $C_{63}H_{85}Co_2F_6N_{33}O_{26}S_{12}ZrS$, %: C 31.16; H 3.53; N 19.03.

$[Co(DSamH)_2(Thio)_2]_2[TiF_6]\cdot 1.5DMF\cdot 2H_2O$ (9). This compound was prepared according to the procedure as described for preparation of compound **8**, by using $CoTiF_6\cdot 6H_2O$ instead of Zr crystallohydrate. Found, %: C 31.64; H 3.61; N 19.08. Calculated for $C_{64.5}H_{90.5}Co_2F_6N_{33.5}O_{27.5}S_{12}Ti$, %: C 31.75; H 3.74; N 19.23.

Results and discussion

As a result of the condensation between dichloroglyoxime and various organic amines, a series of α-aminodioximes can be obtained, according to the following scheme:

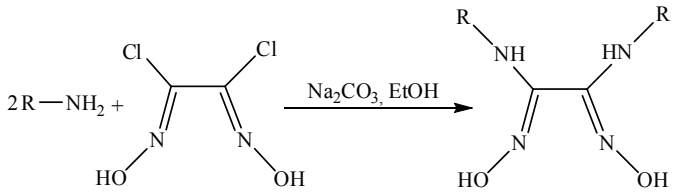

R-NH_2 - aniline or sulfanilamide

This approach served as basic for the obtaining of $DAnH_2$ and $DSamH_2$, the latter being synthesized for the first time. The prepared compounds were identified by elemental analysis, UV-Vis, IR and NMR spectroscopies. UV-Vis spectrum of $DAnH_2$ contains two absorbtion bands at 205 and 260 nm belonging to the aromatic ring, whilst the corresponding UV-Vis spectrum of $DSamH_2$ is characterized by the adsorption band at 281 nm.

In the IR-spectrum of $DAnH_2$ the following absorption bands are present: ν(OH)=3390, ν(NH)=3369, ν(C=N)=1637, $\nu(CC)_{arom.}$=1596 cm^{-1}. The ν(NO)=972 cm^{-1} band is characteristic for unprotonated oxime group, while $\delta(CH)_{arom.}$=752 and 689 cm^{-1} is attributed to monosubstituted aromatic ring. The presence of intensive bands: ν(NO) and δ(CH), as well as disappearance of ν(CCl) band at 850 cm^{-1} demonstrates that the condensation between dichloroglyoxime and aniline has occurred. In IR-spectrum of $DSamH_2$ the absorption bands of ν(NH)= 3424, 3357, 3283 cm^{-1} are present and ν(OH)=3076 cm^{-1} as well, which is shifted to lower values due to the formed by oxime OH molecular associates. The bands of ν(C=N)=1642 cm^{-1}, $\nu(CC)_{arom}$=1592 cm^{-1}, ν(SO)=1302, 1150 cm^{-1}, ν(NO)=935 cm^{-1} and δ(CH)=767, 725 cm^{-1} are also characteristic for this spectrum.

The ^1H NMR spectrum of $DAnH_2$ contains the multiplets in 6.79 – 7.09 ppm region that attest the presence of aromatic ring in compound, a singlet at 8.16 ppm that is characteristic for the NH group proton and a singlet at 10.43 ppm confirming the presence of oxime group. Integration of the peaks in this spectrum has shown that both chlorine atoms of initial dichloroglyoxime were substituted by aniline radicals. The presence of 5 resonances in ^{13}C NMR spectrum, including quaternary atom of oxime group (δ_C 142.66), quaternary atom (δ_C 139.70) and tertiary atoms of aromatic ring (δ_C 128.16, 121.23 and 118.92) were ascribed to $DAnH_2$.

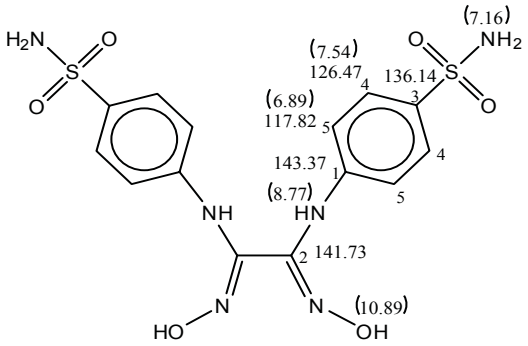

Disulfanilamideglyoxime

Fig. 1. Disulfanilamideglyoxime with its ^1H and ^{13}C values.

The ^1H NMR spectrum of $DSamH_2$ (Figure 1) contains two doublets belonging to the aromatic ring at 7.54 ppm (2H, J=8.78 Hz) and 6.89 ppm (2H, J=8.78 Hz), a singlet at 7.16 ppm (NH_2 protons) and a singlet at 8.77 ppm (NH proton). Oxime group protons give a peak at 10.89 ppm. In ^{13}C NMR spectrum the presence of tertiary carbon resonances (δ_C 117.82 and 126.47), quaternary atoms of aromatic ring (δ_C 136.14 and 143.37) and oxime carbon atom (δ_C 141.73) has been attested. It was found that protons and carbons signals appear downfield in disulfanilamideglyoxime, as compared to the sulfanilamide (Figure 2). Only quaternary carbon of aromatic ring close to NH group is upfield shifted by condensation. Both proton and carbon signals of oxime group are shifted to higher field as compared to the dichloroglyoxime. The attribution of the peaks for the carbon atoms has been performed on the basis of 2D NMR techniques: HSQC and HMBC (Figure 3). Also, in 2D HMBC experiment, the protons of NH and OH groups have a cross peaks at the shift of C^2, that proves the condensation of sulfanilamide with dicloroglyoxime. As it can be concluded from these spectra, sulfanilamide condenses *via* amino group of aromatic ring: it suffers the biggest downfield shift and integration of the peaks confirms the loss of one proton from this group.

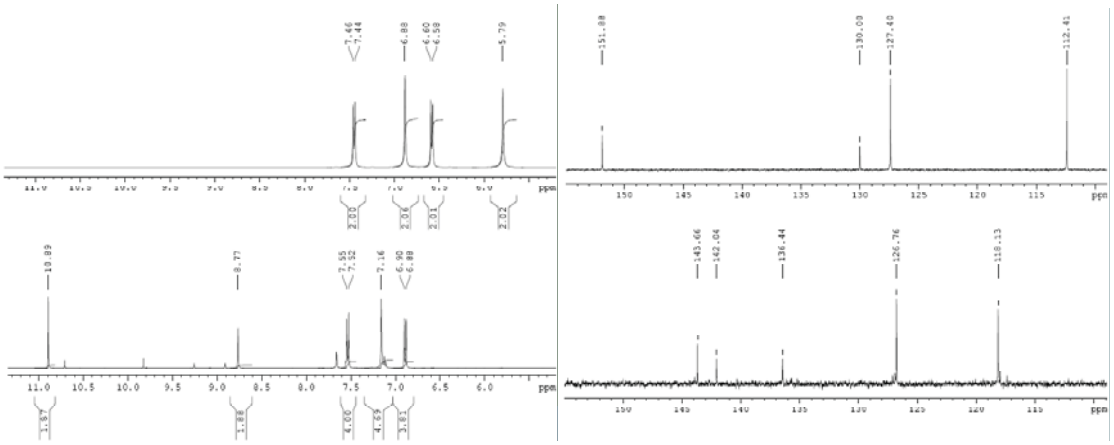

Fig. 2. ^{1}H and $^{<}$C NMR spectra of sulfanilamide (a, b) and disuflanilamideglyoxime (c, d).

On interaction of a Co(II), Ni(II) or Cu(II) salt with the described dioximes in a 1:2 molar ratio, *bis*-dioximates or *tris*-dioximines of the corresponding metals were obtained, depending on the conditions of synthesis. The pH~2 is more favourable for the obtaining of *tris*-dioximines, while at pH~5-6 *bis*-dioximates of the respective metals are preferentially formed. Variation of the pH value was achieved by adding 1-2 drops of ammonia solution or hydrochloric acid. Methanol, water and dimethylformamide were used as solvents. A part of obtained complexes are unstable at air.

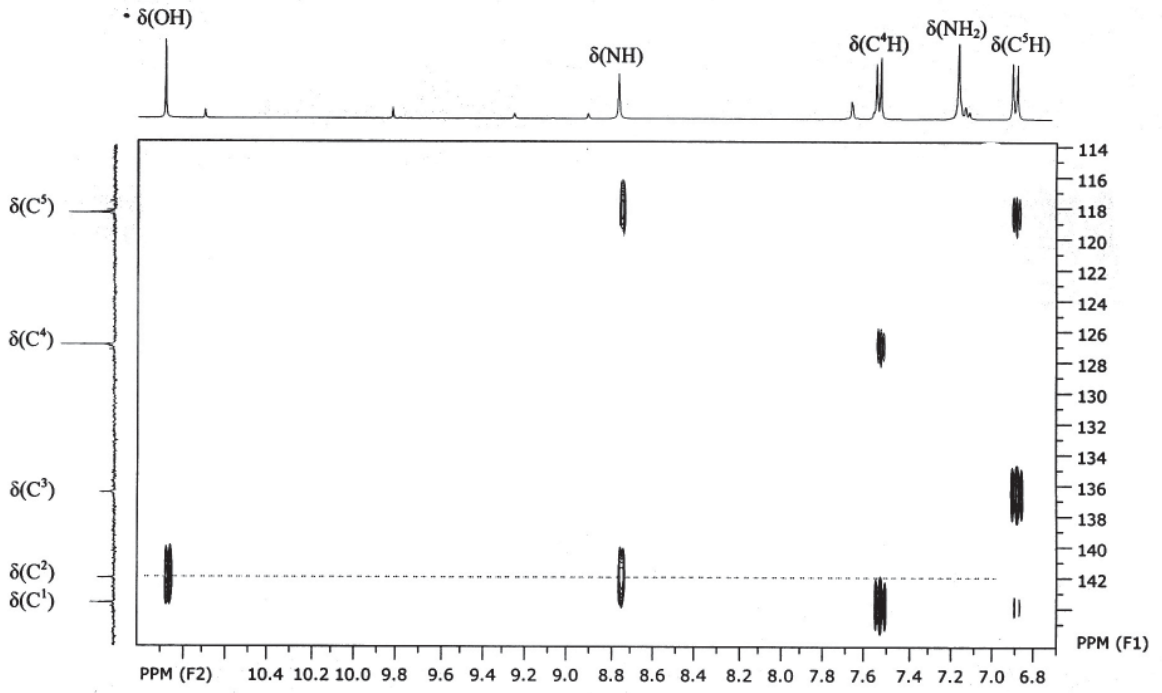

Fig. 3. 2D HMBC experiment of disulfanilamideglyoxime.

In UV-Vis spectra of Ni(II) and Cu(II) complexes containing $DAnH_2$ characteristic bands of aromatic ring are noted at ~205 and 260 nm, which certify the presence of this ligand in complex. In the case of *bis*-dianilineglyoximate of Ni(II) it has been observed that the corresponding absorption band at 260 nm is less intensive then the band at 205 nm, as compared to *tris*-dianilineglyoximine. Furthermore, a new band appeared at 378 nm (Figure 4). The following explanation seems plausible: the composed band at 260 nm reflects two electronic transitions and the formation of *trans*-dioximates is accompanied by the disappearance of one transition as a result of an electron shift. In the case of complex $[Co(DAnH)_2Thio]_2[TiF_6]$ three absorption bands were recorded: at 202 nm, characteristic for aromatic ring; at 243 nm probably distinguishing π-π^* transitions in chelate ring and a band at 321 nm that is attributed to the molecules of coordinated thiocarbamide.

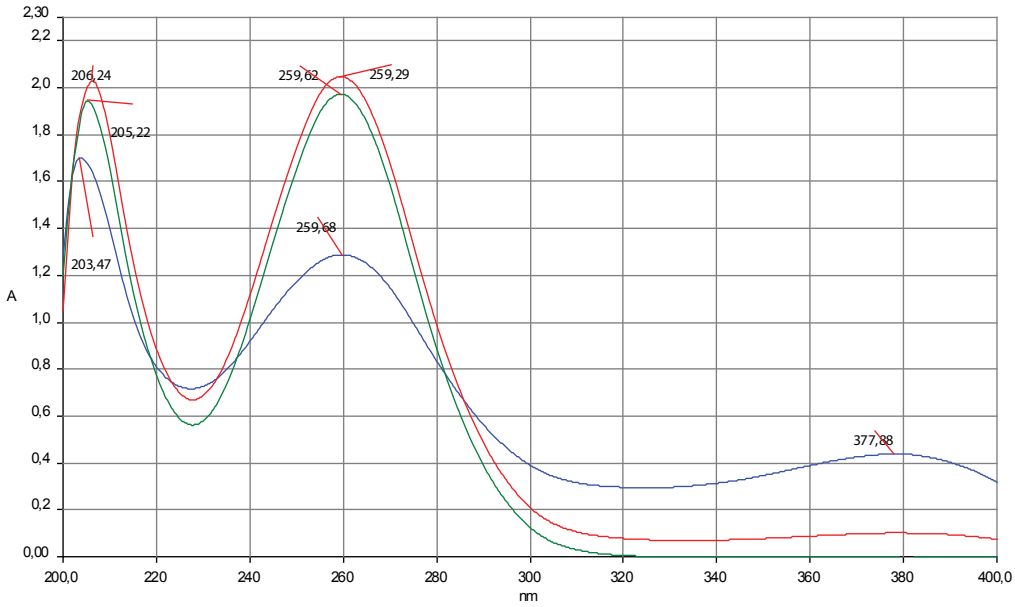

Fig. 4. UV-Vis spectra of compounds
$DAnH_2$ (1), $[Ni(DAnH_2)_3]Cl_2$ (2), $[Ni(DAnH)_2]$ (3)

In the case of Ni(II) and Co(II) dioximates containing $DSamH_2$ the presence of this ligand in the corresponding complexes has been certified by the absorption bands at 202 and 275-282 nm. Also in the case of these compounds it has been noted that the addition of one drop of ammonia, which favors the formation of *bis*-dioximates, causes the decrease in intensity of absorption band at 280 nm. The generation of intramolecular hydrogen bonds contributes to the electron density shift from the aromatic ring towards metal-cycle, which could cause intensity diminution of the respective band.

In IR-spectra of $DAnH_2$-containing *tris*-dioximines the absorption bands ν(NH)+ν(OH)=3331-3380, ν(C=N)=1647-1655 and $\nu(CC)_{arom.}$=1596 cm^{-1} are present. The presence of ν(NO)=970-998 cm^{-1} band, as well as the lack of characteristic ionized ν(NO) at ~1240 and ~1080 cm^{-1} demonstrates the absence of O–H···O intramolecular hydrogen bonds, proving the *tris*- character of these dioximines of 3d-metals. The absorption bands of vibrations δ(CH) that characterizes the aromatic monosubstituted ring are found at 752-755 and 691-695 cm^{-1} region. In *bis*-dioximates of Co(III), Cu(II) and Ni(II) with dianilineglyoxime the bands of valence vibrations ν(NH)+ν(OH)=3209-3312 cm^{-1} are shifted to lower fields than in the free $DAnH_2$ molecule. The bands ν(C=N) at 1647-1652 and $\nu(CC)_{arom.}$ at 1592-1594 cm^{-1} regions are present. Decrease in intensity of 972 cm^{-1} band, as well as appearance of the bands belonging to the ionized N–OH group at 1234-1241 cm^{-1} and 1075-1093 cm^{-1} regions implies the formation of O–H···O intramolecular hydrogen bonds. Bands δ(CH) are present at 747-753 and 689-694 cm^{-1} regions, characterizing the aromatic monosubstituted ring.

In IR-spectra of *tris*-dioximines containing $DSamH_2$ the bands ν(NH)=3469-3208, ν(OH)=3071-3075, ν(C=N)=1643-1646, $\nu(C\text{-}C)_{arom.}$=1588-1595, ν(NO)=900-913 and δ(CH)=741-747 cm^{-1} are found. In IR-spectra of *bis*-disulfanilamideglyoximates of Co(III) and Ni(II), as in the similar complexes with $DAnH_2$, the majority of the aforementioned bands are present. Decrease in intensity of the band from 935 cm^{-1} region has been established and the bands of oxime N–OH ionized group at 1255-1258 and 1093-1096 cm^{-1} appeared, which prove the formation of O–H···O intramolecular hydrogen bonds.

In the case of Co(III) dioximates containing on axial coordinate the molecules of thiocarbamide the presence of ligand in complex is ascertained by the pronounced band ν(C=S)=1396-1408 cm^{-1}.

In ^1H NMR spectrum of complex $[Co(DAnH_2)_3]_2[TiF_6]_3 \cdot 4DMF$ the peak of oxime proton is more shielded (9.10 ppm), as compared with the free ligand peak at 10.43 ppm. The peak of NH group does not suffer any chemical shift with respect to the case of free ligand, being found at 8.15 ppm. The peaks of aromatic ring of $DAnH_2$, a doublet and two triplets are found in 6.70-7.16 ppm region, as in the spectrum of free ligand. The only upfield chemical shift of the oxime proton peak is probably caused by an electronic density migration from metal to chelate ring. The peaks at 2.73 and 2.89 ppm characterize the methyl groups and at 7.95 ppm the methine group of dimethylformamide molecules from complex.

In ^{13}C NMR spectrum of this complex the peak of oxime carbon atom is upfield too, being found at 142.37 ppm, thus confirming the supposition on an electronic density migration from metal to chelate ring. The chemical shifts of aromatic carbon atoms at 118-140 ppm do not essentially vary from the corresponding values in the spectrum of the free

ligand. Despite the introduction of the Thio ligand in the reaction medium, neither IR nor NMR spectra could certify its presence. The upfield shift of the oxime proton peak, as well as integration of the peaks in ^{1}H NMR spectrum, rule out the supposition on deprotonation of oxime group, thus constituting a further evidence (along with the elemental analysis, UV-Vis and IR- data) about Co(III) *tris*-dianilineglyoximine formation. The *tris*-dioximines of Ni(II) and Cu(II) were also obtained when the reactions were performed in the absence of ammonia or sodium acetate, according to the IR, UV-Vis and elemental analysis data. When an ammonia solution is added to the reaction medium, the formation of respective *bis*-dioximates occurred that has been ascertained by the chemical shift of oxime proton at ~17-18 ppm in ^{1}H NMR spectrum, proving the intramolecular hydrogen bond formation.

In the case of ^{1}H NMR spectrum of Co(III) *tris*-disulfanilamideglyoximine the oxime proton peak is also upfield with ~1 ppm (from 10.89 ppm in the free ligand to 9.79-9.69 ppm). The chemical shift assigned to NH group is slightly upfield (8.36-8.25 ppm) with respect to the peak of free oxime at 8.76 ppm. These upfield shifts are attributed to an electron density migration from metal to the chelate ring, similarly to the afore-mentioned case of *tris*-form of dianilineglyoxime complexes. The two doublets assigned to the aromatic ring protons at 7.64 and 6.81 ppm are placed approximately in the same region, as compared with the free disulfanilamideglyoxime. The peak of NH_2 group does not essentially move in the spectrum, being found at 7.16 ppm, as well.

Considering the ^{1}H NMR spectrum of $[Ni(DSamH)_2]\cdot 2H_2O$ complex, the peak of oxime proton is downfield at 17.32 ppm, which confirms the intramolecular hydrogen bond formation between dioxime monoanions. The proton peaks of NH (9.84 ppm) and vicinal to it CH (7.84 ppm) groups are also downfield, being shifted with ~1 ppm, as compared with the free ligand (8.77 and 6.89 ppm, respectively). The other peaks (CH remote from oxime group at 7.69 ppm and NH_2 at 7.27 ppm) do not markedly differentiate as compared with the free ligand. In ^{13}C NMR spectrum the most downfield chemical shift belongs to the peak of the quaternary oxime carbon at 146.11 ppm (141.73 ppm in the free ligand). Since ^{1}H NMR operates in a through-bond as well as through-space manner but ^{13}C NMR operates mainly through-bond, any shift in ^{13}C δ(C=N) will be due to cobalt anisotropy or Sam fragment (if is considered as an acceptor group of electron density). The peaks of quaternary carbon atom and methine close to SO_2 group are slightly downfield with 1.0-1.2 ppm, the corresponding nuclei resonating at 136.81 and 127.39 ppm. The chemical shift of the other methine group is upfield, as compared with the free ligand (116.57 ppm *versus* 117.82 ppm, respectively).

^{1}H and ^{13}C NMR spectra of the other synthesized *bis*-disulfanilamideglyoximates do not essentially differ from the spectra of $[Ni(DSamH)_2]\cdot 2H_2O$ complex.

To summarize, $DAnH_2$ and $DSamH_2$ behave differently from the dimethylglyoxime, diphenylglyoxime or 1.2-cilcohexandiondioxime. In reaction with Co(II), Ni(II) and Cu(II) salt, $DAnH_2$ and $DSamH_2$ are prone to form *tris*-dioximines and not *bis*-dioximates like traditional dioximes. The *tris*-dioximine complexes with $DSamH_2$ are most stable than those with $DAnH_2$ due to a larger number of functional group that can participate to a hydrogen bond linkage. The new complexes may be effective as stimulators in biosynthetic processes of enzymes in some fungi strains.

References

[1]. Underhill, A. E.; Watkins, D. M. and Petring R., *Inorg. Nucl. Chem.Lett.,* 9, 1269, (1973).
[2]. İrez, G. and Bekaroğlu, Ö. *Synth. React. Inorg. M.,* 13, 781, (1983).
[3]. Serin, S. and Bekaroğlu, Ö. *Z. Anorg. Allg. Chem.,* 496, 197, (1983).
[4]. Gök, Y. and Serin, S., *Synth. React. Inorg. M.,* 18, 975, (1988).
[5]. Koçak, M., Bekaroglu, Ö. J. *Coord. Chem.*, 47, Issue 2, 359, (1999).
[6]. Gürsoy, S. et. al. *Transition Metal Chemistry*, 25, 474, (2000).
[7]. Dutta, G.; Kumar K. and Gupta, B. D.. *Organometallics, 28,* 3485, (2009).
[8]. Gulay Gumus, et. al., *New J. Chem*., 28, 177, 2004.
[9]. Десятник А.А., и. др. *Коорд. химия*. Т.28, №2, 144, 2002.
[10]. Coropceanu, E. ş.a. *Bul. Instit. Politehnic din Iaşi*. T. XLIX (LIII). Fasc. 5, 293, (2003).
[11]. Deseatnic, A., ş.a., 2009.07.31, BOPI nr. 7/2009.
[12]. http://www.sciencemadness.org/member_publications/energetic_glyoxime_and_diaminofurazan_derivatives.pdf

SYNTHESIS AND PHOTOOXYGENATION OF THE METHYL ESTER OF 11-HOMODRIM-6,8(9)-DIENE-12-OIC ACID

Andrei Bîrîiac

Institute of Chemistry of the Academy of Sciences of Moldova, Academy str. 3, MD-2028, Chisinau, Moldova
Tel: +37322739769, Fax: +37322739775, E-mail: andreib84@gmail.com

Abstract: Starting with the methyl 11-homodrim-8-ene-7-oxo-12-oate a two steps synthesis of methyl-11-homodrim-6,8(9)-diene-12-oate was accomplished in 87% overall yield, which on photooxygenation in the presence of tetraphenylporphyrin gave a mixture of methyl esters of 11-homodrim-7-ene-6α,9α-peroxy-12-oic and 11-homodrim-5,8-diene-7-oxo-12-oic acids 21% and 54% yields, respectively.

Keywords: homodrimanes, synthesis, photooxygenation.

1. Introduction

Drimanic sesquiterpenoids represent one of the largest groups of sesquiterpenoids, which continues to attract the attention of scientists due to their interesting and varied biological activity [1, 2]. Commonly, polyfunctional compounds are more active, especially those with functional groups at the atoms C-6 and C-9, *e.g.* pereniporin A **1** and B **2** [3], cinnamodial (ugandensidial) **3** [4], cinnamosmolide **4** [5], mukaadial **5** [6] and albrassitriol **6** [7], than monofunctional ones (Figure 1).

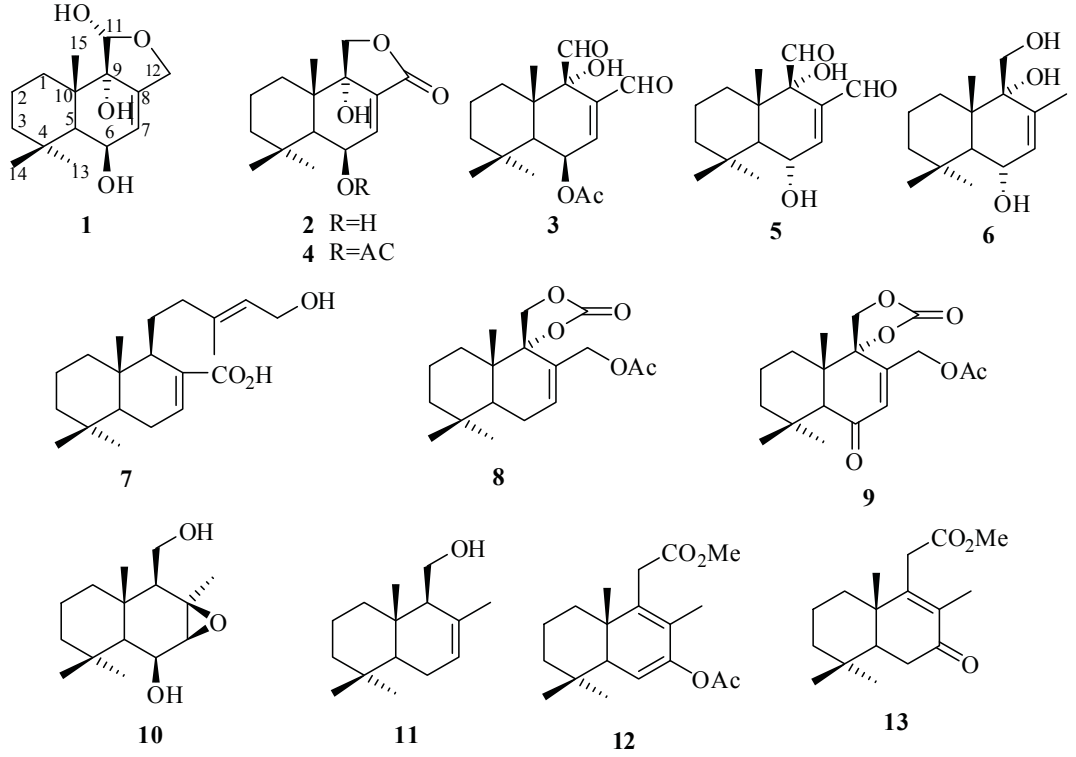

Figure 1

Because of the low content of sesquiterpenoids **1-6** and related compounds in natural sources, the interest of chemists turned to their synthetic preparation from easily available predecessors. However, it should be noted that carbon atoms C-6 and, especially, C-9 are sterically hindered and their direct functionalization is difficult. This is possible to do *via* complicated synthesis in moderate overall yields. For example, pereniporin A **1** was obtained in 11 steps from available zamoranic acid **7** in 4% overall yield [8]. The introduction of keto group in position C-6 was possible only in some cases, for example, in compound **8**, which was oxidized with CrO_3 in acetic acid in compound **9** in a moderate yield (52%) [9].

Thus, the authors [10] on synthesis of uvidine C **10** from drimenol **11** introduced hydroxyl group in position C-6 in 8 steps.

Considering the above, we attempted to develop a method of simultaneous functionalization of atoms C-6 and C-9 in the cycle B of an available norlabdanic compound, containing conjugated 1,3-dienic system at C-6-C-7 and C-8-C-9 carbon atoms, using the reaction of photolytic [4+2] cycloaddition of singlet oxygen to dienic system.

2. Results and discussion

Earlier, for elaboration of a short method of simultaneous functionalization of the carbon atoms C-6 and C-9 in the series of 11-homodrimanic compounds, the photooxygenation reaction of the enolacetate **12**, prepared from ketoester **13**, was studied [11]. The latter one was prepared by oxidation of the mixture of known esters **14** [12, 13].

According to literature data 1,3-dienic compounds react with singlet oxygen giving endoperoxides by [4+2] cycloaddition reaction [14-16]. However, the reaction product of enolester **12** with singlet oxygen was not the expected endoperoxide **15** but the dienone **16**. This result can be explained by the fact that the dienic system of compound **12** contains the electron-reach C-6-C-7 double bond, which reacts with electrophilic singlet oxygen giving the perepoxyde **17**. The addition of the singlet oxygen to this double bond occurs from sterically more accesible α-side of the molecule (see Figure 2).

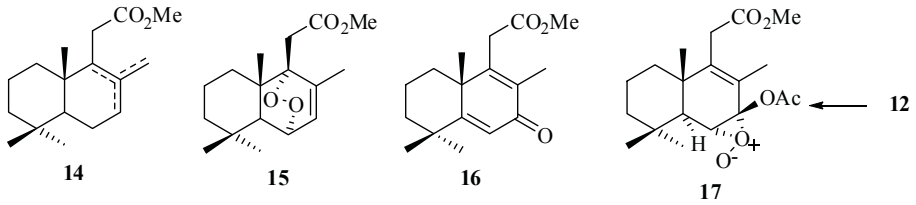

Figure 2

Taking into account the above mentioned data, it was of interest to carry out the synthesis of compound **18** with conjugated double bonds in cycle B and then investigate its behavior in photochemical process. Ketoester **13** served as the starting compound for the preparation of dienic ester **18** (scheme 1).

Compound **13** was reduced with sodium borohydride in the presence of cerium trichloride giving the methyl ester of 11-homodrim-8-ene-7β-ol-12-oic acid **19** in the 98% yield. The structure of compound **19** was elucidated on the base of its spectral data. In particular, the width the of proton's signal at C-7 on its half-height ($W_{1/2}$=7.62 Hz) and its multiplicity (triplet, *J*=8.6 Hz) indicate that hydroxyl group at C-7 is equatorially oriented.

On dehydration of hydroxyester **19** under mild conditions with concentrated H_2SO_4 solution in THF the methyl ester of 11-homodrim-6,8(9)-diene-12-oic acid **18** was obtained in 89% yield. Its IR-spectrum exhibited bands for the ester group at 1155 and 1746 and the dienic system at 2860 and 750 cm^{-1}. In its ^{1}H-NMR spectrum there are present the signals of five methyl groups: three of them bonded to quaternary carbon atoms C-4 and C-10 at 0.91, 0.93 and 0.78 ppm (H-14, H-15 and H-16, respectively), methyl group attached to C-8 (1.71 ppm) and methyl ester group at 3.65 ppm, doublet signals of protons at the double bond C-6-C-7 appear as doublet of doublet at 5.85 ppm (H-6) and 5.76 ppm (H-7) and the doublet signal of H-5 proton at 2.03 ppm. The ^{13}C-NMR spectrum also confirms the structure of ester **18**. It contains the signals of five methyl groups at 51.7, 32.3, 22.6, 18.1 and 14.9 ppm, of quaternaty carbon atoms C-8 (127.8 ppm), C-7 (128.1 ppm), 129.1 ppm (C-6), 136.0 ppm (C-9) and 172.8 ppm (the carbonyl group C-12).

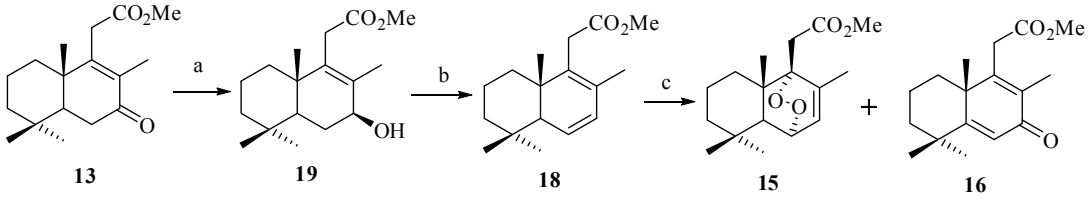

Scheme 1. *Reagents*: (a) $NaBH_4$, $CeCl_4$*$7H_2O$, MeOH, r.t., 0.5h, 98%; (b) H_2SO_4, THF, r.t., 24h, 89%; (c) hν, O_2, TPP, DCM, 5 ºC, 5h, 21% (15) and 54% (16)

The photooxygenation of dienic ester **18** was carried out in dichloromethane solution of in the presence of tetraphenylporphyrin. According to TLC data the reaction product represented a complex mixture of compounds with two major components which were separated by column chromatography on silica gel. The first compound eluted from column was the endoperoxide **15**, obtained in 21% yield (scheme 1). In the IR-spectrum of compound **15** there are bands characteristics for ester group (1730 and 1167cm^{-1}) and endoperoxyde group at 1107 cm^{-1}. Its ^{1}H-NMR spectrum displays signals of five methyl groups, two of them at 1.04 and 0.79 ppm bonded to C-4, 0.92 ppm bonded to C-10, 1.99 ppm bonded to C-8 and signal of methyl ester group at 3.66 ppm. At 6.33 ppm was present the doublet of doublet of H-7 atom and at 4.49 ppm of H-6 atom. The doublet signal of H-5 appears at 1.72 ppm. In ^{13}C-NMR spectrum of compound **15** there are signals of carbon atoms C-8 at 141.8 ppm, C-7 at 125.7 ppm, C-9 at 86.3 ppm, C-6 at 72.3 ppm and of the ester group carbonyl at 169.9 ppm. The ^{13}C-NMR spectra contain also the signals of five methyl groups at 51.7 (CO_2*Me*), 31.8 (C-15), 24.3 (C-14), 21.3 (C-13) and 20.1 (C-16). Unfortunately, the yield of target endoperoxide **15** was low. All attempts to increase it, changing the reaction condition, failed. The use of rose bengal and methylene blue as photosensitizer did not lead to an increase of the compound **15** yield.

The next compound eluted from chromatographic column was the known methyl ester of 11-homodrim-5,8(9)-diene-7-one-12-oic acid **16** (54% yield), which was identified by comparing with its authentic sample obtained earlier [11]. A possible way of the dienone **16** formation from dienic ester **18** is depicted in scheme 2.

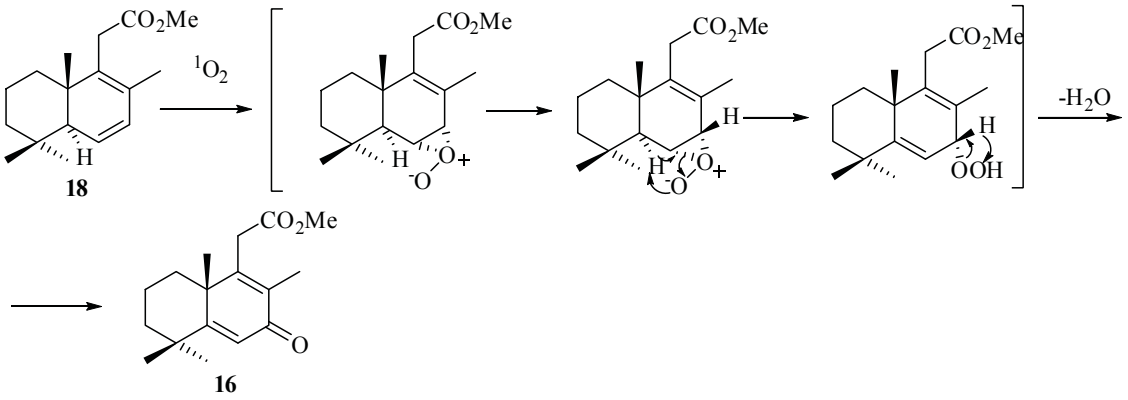

Scheme 2

The reduction of endoperoxide **15** with thioureea in MeOH leads the methyl ester of 11-homodrim-7-ene-6α,9α-diol-12-oic acid **20** in 96% yield (scheme 3). This step was carried out with the aim to obtain a more stable 6,9-disubstituted homodrimanic compound. Its IR spectrum contains characteristic bands for ester (1160 and 1710 cm^{-1}) and hydroxyl (3420 and 1205 cm^{-1}) groups. In ^{1}H-NMR spectrum of compound **20** there are present the doublet signal of the H-7 proton (5.48 ppm), doublet of doublet of the H-6 proton (4.04 ppm) and the signals of five methyl groups at 3.69 ppm (CO_2Me), 1.68 ppm (H-13), 1.14 ppm (H-15), 1.04 ppm (H-16) and 0.88 ppm (H-14). In ^{13}C-NMR spectrum of compounds **20** there are also present the signals of completely substituted carbon atoms at C-4 (32.9 ppm) and C-10 (43.6), signal of tertiary C-5 atom (49.2 ppm) and signals of methylenic atoms C-1 (33.1), C-2 (18.7 ppm), C-3 (42.9 ppm) and C-11 (38.9 ppm).

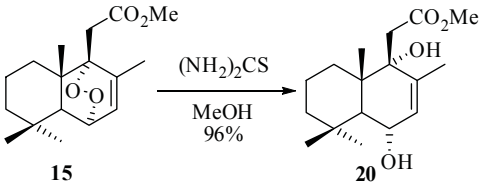

Scheme 3

3. Conclusion

Starting with the methyl 11-homodrim-8-ene-7-one-12-oate a two steps synthesis of the methyl 11-homodrim-6,8(9)-diene-12-oate was accomplished in 87% overall yield. The photooxygenation of this compound in the presence of tetraphenylporphyrin led to the mixture of methyl 11-homodrim-7-ene-6α,9α-peroxy-12-oate and methyl 11-homodrim-5,8-diene-7-one-12-oate in 21% and 54% yields, respectively. These esters are valuable intermediate in the synthesis of physiologically active drimanic and norlabdanic derivatives.

4. Experimental

Melting points (mp) were determined on a Boetius hot stage. Optical rotations were measured on a Perkin-Elmer 241 polarimeter with a 1 dm microcell, in $CHCl_3$. IR spectra were recorded on Bio-Rad-Win-IR and Perkin-Elmer Models spectrometer. ^{1}H and ^{13}C NMR spectra were recorded in $CDCl_3$ on Bruker AC-E 200 (200 and 50 MHz) and Bruker Avance DRX 400 (400 and 100 MHz) spectrometers. Chemical shifts are given in parts per million values in δ scale with $CHCl_3$ as internal standard (δ at 7.26 ppm for proton and δ 77.00 ppm for carbon) and coupling constants in Hertz. H,H-COSY, H,C-HSQC and H,C-HMBC experiments were recorded using standard pulse sequences, in the version with *z*-gradients, as delivered by Bruker. Carbon substitution degrees were established by DEPT pulse sequence. Mass spectra (MS) were run on an AEI MS 902 spectrometer (EI, 70 eV). For analytical TLC, Sorbfil silica-gel plates were used. The chromatograms were sprayed with conc. H_2SO_4 and heated at 80°C for 5 min to detect the spots. Column chromatography was carried out on Across silica gel (60–200 mesh) using petroleum ether (PE) (bp 40–60 °C) and the gradient mixture of petroleum ether and EtOAc. All solvents were purified and dried by standard techniques before use. Crude products in organic solvents were dried over anhydrous Na_2SO_4, filtered, and evaporated under reduced pressure.

Methyl ester of 11-homodrim-8-ene-7β-ol-12-oic acid 19. To a stirred solution of $CeCl_3 \cdot 7H_2O$ (671 mg, 1.80 mmol) in MeOH (5 mL) at 18°C the solution of keto ester **13** (500 mg, 1.80 mmol) in MeOH (10 ml) was added. After 3 min $NaBH_4$ (68 mg, 1.80 mmol) was added and the mixture was stirred at the same temperature for 0.5 h (TLC control). The reaction mixture was treated with cold 5% HCl solution (5 mL), and after dissolution of the precipitate it was extracted with diethyl ether (3 x 25 mL). The extract was washed with water (2 x 15 mL) and dried. After removal

of the solvent in vacuum the crude product (510 mg) was purified by column chromatography on silica gel (25 g, eluent: PE/EtOAc 85:15), to give the *methyl ester of 11-homodrim-8-ene-7β-ol-12-oic acid* **19** (492 mg, yield 98%) as a white crystals, mp 106°-107°C (from PE), $[\alpha]_D^{20}$ +50.8° ($CHCl_3$, c 0.03). IR (ν, cm^{-1}): 3493, 1146(OH), 1733 (CO_2Me). ^1H NMR (400 MHz, δ_H, ppm) 4.15 (1H, t, *J* 8.6 Hz, $W_{1/2}$ 7.62 Hz, *H*-7), 3.68 (3H, s, CO_2Me), 3.09 (1H, d, *J* 17.0 Hz), 2.99 (1H, d, *J* 17.0 Hz) (AB-system C(11)H_2), 2.12 (1H, ddd, *J* 14.0, 7.4, 6.2 Hz, *H*-6), 1.67 (3H, s, *H*-13), 1.25 (1H, m, *H*-5), 1.00 (3H, s, *H*-16), 0.89 (3H, s, *H*-15), 0.85 (3H, s, *H*-14). ^{13}C NMR (100.61 MHz, δ_C, ppm): 172.8 (C-12), 137.8 (C-9), 132.7 (C-8), 72.9 (C-7), 51.8 (CO_2Me), 49.5 (C-5), 41.2 (C-6), 39.4 (C-10), 35.9 (C-11), 33.0 (C-1), 32.9 (C-15), 32.8 (C-4), 29.7 (C-3), 21.5 (C-14), 19.7 (C-13), 18.7 (C-2), 15.5 (C-16); HRMS *m/z* (EI): found 280.20344. $C_{17}H_{28}O_3$ requires 280.20384. 280 (M^+, 14), 221 (5), 207 (25), 191 (8), 173 (9), 157 (25), 135 (11), 124 (100), 109 (65), 96 (29), 81 (14), 69 (24), 55 (31), 41 (40).

Methyl ester of 11-homodrim-6,8(9)-diene-12-oic acid 18. To a solution of hydroxyester **19** (250 mg, 0.89 mmol) in THF (4 mL) the solution of concentrated H_2SO_4 (0.16 mL) in THF (0.84 mL) was added and the obtained mixture was stirred for 24 h at room temperature, diluted with water (10 mL) and extracted with ether (3 x 15 mL). The organic layer was washed with water (2 x 20 mL) and dried. The removal of the solvent afforded an yellow oil (247 mg), which was purified by column chromatography on silica gel (5 g, eluent: PE/EtOAc 95:5), to give the *methyl ester of 11-homodrim-6,8(9)-diene-12-oic acid* **18** as white crystals (208 mg, 89.0%), mp 55-56 ºC (from PE), $[\alpha]_D^{22}$ +67.8° ($CHCl_3$, c 1.17). IR (ν, cm^{-1}): 2860 (C=C), 1746, 1155 (CO_2Me), 750 (=C-H). ^1H NMR (400 MHz, δ_H, ppm) 5.85 (1H, dd, *J* 2.95, 9.30 Hz, *H*-6), 5.76 (1H, dd, *J* 3.16, 9.30 Hz, *H*-7), 3.65 (3H, s, CO_2Me), 3.13 (1H, d, *J* 16.0 Hz), 3.02 (1H, d, *J* 16.0 Hz) (AB-system, C(11)H_2), 2.03 (1H, d, *J* 2.9 Hz, *H*-5), 1.71 (3H, s, *H*-13), 0.93 (3H, s, *H*-15), 0.91 (3H, s, *H*-14), 0.78 (3H, s, *H*-16). ^{13}C NMR (100.61 MHz, δ_C, ppm): 172.8 (C-12), 136.0 (C-9), 129.1 (C-6), 128.1 (C-7), 127.8 (C-8), 52.4 (C-5), 51.7 (CO_2Me), 40.8 (C-3), 38.7 (C-10), 35.1 (C-1), 33.1 (C-4), 32.5 (C-11), 32.3 (C-15), 22.6 (C-14), 18.8 (C-2), 18.1 (C-13), 14.9 (C-16). HRMS *m/z* (EI): found 262.19356. $C_{17}H_{26}O_2$ requires 262.19328. m/z 262 (M^+, 27), 203 (7), 191 (13), 173 (63), 159 (10), 145 (19), 133 (36), 119 (100), 105 (16), 91 (20), 83 (13), 69 (10), 55 (26), 41 (35).

Methyl esters of 11-homodrim-7-ene-6α,9α-peroxy-12-oic 15 and 11-homodrim-5,8-diene-7-one-12-oic 16 acids. To a stirred solution of diene **18** (240 mg, 0.92 mmol) in 25 mL of CH_2Cl_2 was added 2 mg of tetraphenylporphyrin (TPP). The resulting mixture was irradiated with two bulb lumps (100 W each) while oxygen was passed through stirred solution at 5 °C for 5 h. Evaporation of the solvent at the reduced pressure and chromatography of the residue (311 mg) on SiO_2 (16g, eluent: PE/EtOAc 9:1) gave the *methyl ester of 11-homodrim-7-ene-6α,9α-peroxy-12-oic acid* **15** (57 mg, 21 %), white crystals, mp 116-117 °C (from PE), $[\alpha]_D^{23}$ +11.95° ($CHCl_3$, *c* 0.21). IR (ν, cm^{-1}): 1733, 1167 (CO_2Me), 1198 (peroxy group). ^1H NMR (400 MHz, δ_H, ppm): 6.33 (1H, dd, *J* 6.0, 1.6 Hz, *H*-7), 4.49 (1H, dd, *J* 10.5, 6.0 Hz, *H*-6), 3.66 (3H, s, CO_2Me), 2.82 (1H, d, *J* 15.8 Hz), 2.59 (1H, d, *J* 15.8 Hz) (AB-system, C(11)H_2), 1.99 (3H, s, *H*-13), 1.72 (1H, d, *J* 12.08 *H*-5), 1.04 (3H, s, *H*-15), 0.92 (3H, s, *H*-16), 0.79 (3H, s, *H*-14). ^{13}C NMR (100.61 MHz, δ_C, ppm): 169.9 (C-12), 141.8 (C-8), 125.7 (C-7), 86.3 (C-9), 72.3 (C-6), 51.9 (C-5), 51.7 (CO_2Me), 45.3 (C-10), 38.8 (C-3), 32.2 (C-4), 32.0 (C-11), 31.8 (C-15), 30.5 (C-1), 24.3 (C-14), 21.3 (C-13), 20.1 (C-16), 18.6 (C-2). HRMS *m/z* (EI): found 294.18231. $C_{17}H_{26}O_4$ requires 294.18311.262 [(M^+-32, 10), 205 (3), 193 (18), 187 (19), 173 (29), 151 (10), 133 (20), 119 (44), 109 (95), 95 (57), 81 (54), 69 (78), 55 (54), 41 (100).

The next compound eluted from column with the same solvent system was the known *methyl ester of 11-homodrim-5,8(9)-diene-7-one-12-oic acid* **16** (137 mg, 54 %), white crystals, mp 111-112°C (from hexane), $[\alpha]_D^{20}$ +50.80° ($CHCl_3$, *c* 6.31). IR (ν, cm^{-1}): 1715, 1167 (CO_2Me), 1637, 1614 (dienone group), 826 (>C=C<$_H$). ^1H NMR (400 MHz, δ_H) 6.31 (1H, s, *H*-6), 3.68 (3H, s, CO_2Me), 3.43 (1H, d, *J* 16.9 Hz), 3.31 (1H, d, *J* 16.9 Hz) (AB-system, C(11)H_2), 1.84 (3H, s, *H*-13), 1.28 (3H, s, *H*-16), 1.27 (3H, s, *H*-15), 1.20 (3H, s, *H*-14). ^{13}C NMR (100.61 MHz, δ_C): 186.5 (C-7), 171.9 (C-5), 170.3 (C-12), 154.8 (C-9), 133.3 (C-8), 123.7 (C-6), 52.1 (CO_2Me), 43.6 (C-10), 40.1 (C-3), 37.2 (C-1), 34.9 (C-4), 34.3 (C-11), 32.3 (C-15), 28.5 (C-14), 25.2 (C-16), 18.1 (C-2), 11.6 (C-13). HRMS *m/z* (EI): found 276.17209. $C_{17}H_{24}O_3$ requires 276.17254.276. (M^+, 100), 261 (22), 244 (17), 233 (53), 220 (26), 203 (89), 189 (30), 174 (61), 159 (69), 147 (33), 133 (20), 119 (44), 105 (33), 91 (42), 81 (18), 69 (48), 55 (46), 41 (78).

Methyl ester of 11-homodrim-7-ene-6α,9α-diol-12-oic acid 20. To a solution of the endoperoxyde **15** (55 mg, 0.19 mmol) in MeOH (1.5 mL) was added during 10 minutes at the room temperature solution of thioureea (29 mg, 0.37 mmol) in MeOH (1 mL). Reaction mixture was stirred 3h at room temperature, then diluted with water (25mL) and extracted with diethyl ether (3 x 25 ml). After drying of solution and solvent removing the crud product (58 mg) was subjected to column chromatography on silica gel (5 g, eluent: PE/EtOAc 8:2) to give *methyl ester of 11-homodrim-7-ene*-6α,9α-*diol-12-oic acid* **20** (55 mg, 96%) as an oil; $[\alpha]_D^{20}$=-5.74° (*c* 2.3); IR (ν, cm^{-1}) ν_{max} (film): 3420, 1205 (OH), 1710, 1160 (CO_2Me), ^1H NMR (400 MHz, δ_H): 5.48 (1H, dd, *J* 5.2, 2.0 Hz , *H*-7), 4.04 (1H, dd, *J* 10.0, 2.0 Hz, *H*-6), 3.69 (3H, s, CO_2Me), 2.54 (1H, d, *J* 16.0 Hz), 2.46 (1H, d, *J* 16.0 Hz) (AB-system C(11)H_2), 1.81 (1H, d, *J* 10.0 Hz, *H*-5), 1.68 (3H, s, *H*-13), 1.14 (3H, s, *H*-15), 1.04 (3H, s, *H*-16), 0.88 (3H, s, *H*-14). ^{13}C NMR (100.61 MHz, δ_C): 175.4 (C-12), 136.0 (C-8), 131.1 (C-7), 76.2 (C-9), 68.7 (C-6), 51.9 (CO_2Me), 49.2 (C-5), 43.6 (C-10), 42.9 (C-3), 38.9 (C-11), 36.1 (C-15), 33.1 (C-1), 32.9 (C-4), 22.6 (C-14), 19.0 (C-13), 18.7 (C-2), 17.7 (C-16). HRMS *m/z* (EI): found 296.19777. $C_{17}H_{28}O_4$ requires 296.19876. 296 (M^+, 3), 278 (25), 263 (15), 207 (19), 193 (7), 172 (32), 154 (100), 135 (23), 121 (16), 109 (32), 98 (53), 81 (20), 69 (55), 55 (49), 41 (84).

5. Acknowledgements

The author thanks to Academician P.F. Vlad and Doctors A. Ciocârlan and A. Barbă for their help in the realization of this work.

6. References

[1]. Jansen, B.J.M.; de Groot, A. *Nat. Prod. Rep*. **1991**, *8*(3), 309-318.
[2]. Jansen, B.J.M.; de Groot, A. *Nat. Prod. Rep.* **2004**, *21*(4), 449-477.
[3]. Kida, T.; Shiba, H.; Seto, H. *J. Antibiotics*, **1986**, *39*(4), 613-615.
[4]. Brooks, C.J.W.; Draffan, G.H. *Tetrahedron*, **1969**, *25*(14), 2887-2898.
[5]. Canonica, L.; Corbella, A.; Gariboldi, P.; Jommi, G.; Knepinsky, J.; Casagrande, G. *Tetrahedron*, **1969**, *25*(17), 3895-3902.
[6]. Kubo, I.; Makumoto, T.; Kakooko, A.B.; Mubiru, N.K. *Chem Lett.*, **1983**, *7*, 979-980.
[7]. Ayer, W.A.; Pena-Rodrigues, L.M. *J. Nat. Prod.*, **1987**, *50*(3), 408-417.
[8]. Urones, J.G.; Diez, D.; Gomez, P.M.; Mercos, J.S.; Basabe, P.; Moro, R.F. *Nat. Prod. Lett.*, **1998**, *11*(22), 145-152.
[9]. Urones, J.G.; Diez, D.; Gomez, P.M.; Mercos, J.S.; Basabe, P.; Moro, R.F. *J. Chem. Soc., Pekin I*, **1997**, *12*, 1815-1818.
[10]. Lopez, J.; Sierra, J.; Cortes, M. *Chem Lett.*, **1986**, *12*, 2073-2074.
[11]. Vlad, P.F.; Coltsa, M.N.; Aricu, A.N.; Ciocarlan, A.G.; Gorincioi, E.C.; Edu, C.E.; Deleanu, C. *Russ. Chem. Bull., Int. Ed.*, **2006**, *55*, 703-707.
[12]. Vlad, P.F.; Vorobieva, E.A. *Chem. Nat.Compd.* **1983**, 148.
[13]. Koltsa, M.N.; Mironov, G.N.; Malinovskii, S.; Vlad, P.F. *Russ. Chem. Bull.*, **1996**, *45*, 208.
[14]. Clennan, E.L. *Tetrahedron*, **1991**, *47*, 1343-1382.
[15]. Prein, M.; Adam, W. *Angew. Chem., Int. Ed. Engl.*, **1996**, *35*, 477-494.
[16]. Stratakis, M.; Orfanopoulos, M. *Tetrahedron*, **2000**, *56*, 1595-1615.

AB INITIO STUDY OF CHEMICAL ACTIVATION AND HYDROGENATION OF WHITE PHOSPHORUS IN REACTION WITH RHODIUM TRIHYDRIDE COMPLEX

Iolanta I. Balan*, Natalia N. Gorinchoy

Institute of Chemistry, Academy of Sciences of Moldova, Academy str.,3, MD-2028, Chisinau, Republic of Moldova
*E-mail: ibalan02@yahoo.com

Abstract: The four-stage mechanism of reaction of the rhodium trihydride complex [(triphos)RhH_3] (triphos=1,1,1-tris(diphenylphosphanylmethyl)ethane) with the white phosphorus molecule resulting in the phosphane and the *cyclo*-P_3 complex [(triphos)M(η^3-P_3] is analyzed on the basis of *ab initio* calculations of reactants, products, and intermediate complexes of reaction. It is shown that generation of the transient complex [(triphos)RhH(η^1:η^1-P_4)] followed by intramolecular hydrogen atom migration from the metal to one of the phosphorus atoms is the energetically favourable process. Calculations also show that P_4 molecule is activated by coordination to the above complex: the metal-bonded P-P edge is broken, and the tetrahedron P_4 is opened to form the *butterfly* geometry. This activation is realized mainly due to the one-orbital back donation of 4*d*-electron density from the atom of Rh to the unoccupied antibonding triple degenerate t_1*-MO of P_4.

Keywords: white phosphorus, triphos, rhodium trihydride complex, ab initio calculations.

1. Introduction

From the experimental data it is known that the transition metal complexes are efficient in the white phosphorus functionalization processes (see, e.g., reviews on coordination of white phosphorus [1-3] and references therein). These compounds activate the P_4 molecule by its oxidation or reduction that leads to the breaking of some bonds in the phosphorus molecule preparing it for further chemical transformations.

As an example of the functionalization of the P_4 molecule and of its fragmentation mediated by transition metal complexes can serve the reaction of the trihydride complex [(triphos)MH_3] (where M= Rh, Ir and triphos=1,1,1-tris(diphenylphosphanylmethyl)ethane, $MeC(CH_2PPh_2)_3$) with the white phosphorus resulting in the phosphane and [(triphos)MP_3] complex. On the base of the experimental data it was supposed [4-7] that this process is performed through the next steps (See Scheme 1):

A - the thermal reductive elimination of H_2 from [(triphos)RhH_3] (**I**) and the generation of the transient complex [(triphos)MH] (**II**);
B - the oxidative addition of P_4 with formation of the hydrido –η^1:η^1-P_1 complexes [(triphos)MH(η^1:η^1-P_4)] (**III**);
C - the intramolecular migration of hydrogen atom from the metal to the phosphorus to yield [(triphos)M(η^1:η^2-HP_4)] (**IV**);
D - the final addition of hydrogen molecule to the complex **IV** with the P-P bond cleavage and phosphane separation.

To confirm the possibility of realization of this mechanism it is desirable to study experimentally or (and) theoretically the energy profile of the respective reaction pathway. Some stages of the process indirectly confirmed by experiment. Thus, the conclusion about the formation of the intermediate complex **III** was based on the reaction of P_4 with iridium complex [(triphos)$IrH_2(C_2H_5)$], which reductively eliminates ethane rather than H_2. In this case microcrystals of the complex [(triphos)IrH(η^1:η^1-P_4)] were obtained [7]. The presence of the hydrogen tetraphosphide moiety HP_4 in the complex **IV** with M=Rh was clearly supported by the NMR spectroscopy [7]. However, to our knowledge, the theoretical study of the entire reaction has not been done so far.

In this work all the stages of the hydrogenation of white phosphorus by the Rh trihydride complex are analyzed on the basis of quantum chemical calculations of all the initial ([(triphos)RhH_3] **I**, P_4), the intermediate ([(triphos)RhH] **II**, [(triphos)RhH(η^1:η^1-P_4)] **III**, [(triphos)Rh(η^1:η^2-HP_4)] **IVa**, **IVb**, and **IVc**,) and the final ([(triphos)RhP_3] **V**, PH_3) compounds of the reaction from Scheme 1. Special attention is given to clarifying the nature of the Rh-P_4 binding, and the reasons for the distortion (activation) of coordinated P_4 molecule.

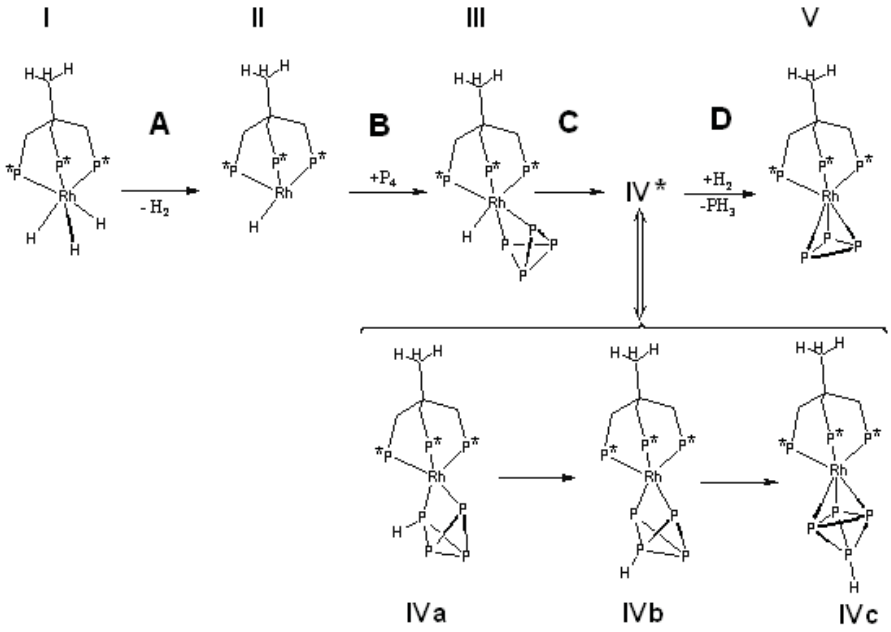

Scheme 1. Reaction of white phosphorus with [(triphos)RhH_3].
P* denotes the phosphorus atoms of the triphos ligand connected with two phenyl rings

2. Computational details

All calculations were carried out using the PC GAMESS version [8] of the GAMESS (US) QC package [9]. For each compound considered, a full geometry optimization was performed at *ab initio* restricted Hartree-Fock (RHF) and density functional (DFT/B3LYP [10, 11]) levels of theory. *Ab initio* calculations were carried out with the split-valence basis sets for atoms of Rh (3-21G [12]) and P (6-31G(d) [13]) which are directly involved in the reaction, and STO-6G [14] basis set for all other atoms. DFT calculations were performed using the LANL2DZ basis set with non-relativistic effective core potential for Rh, the 6-31G(d) for the phosphorus atoms and 6-31G basis set for all other atoms in the systems. The geometry of the complexes was optimized at their highest possible symmetry: C_{3v} for the systems **I**, **II**, **IVc**, **V** and PH_3, and C_s for the **III**, **IVa** and **IVb**. To analyze the possibility of intramolecular hydrogen atom migration, complexes **IVa** and **IVb** were also calculated without any symmetry constraints.

In the experimental studies cited above [4-7], the spin states of the complexes are not discussed. To be sure that the total spin of the system does not change during the reaction, all the complexes were calculated for two values of the total spin (S=0, 1), followed by CI calculations at optimized geometries. Looking ahead, we say that the ground state of all the systems from Scheme 1 is the spin singlet, the triplet states are much higher in energy (more than fifty kcal/mol). Therefore, further discussion refers only to the results of calculations of singlet states of the complexes.

3. Results and discussion

3.1. The [(triphos)RhH_3] (I) and [(triphos)RhP_3] (V) complexes

The geometry optimization of the complexes **I** and **V** was carried out in the assumption that the spatial nuclear configuration of them corresponds to the C_{3v} point group of symmetry. These compounds contain three groups of three equivalent atoms: the three phosphorus atoms of the tripodal ligand, the three phosphorus atoms of a triangular P_3 unit (**V**) or three hydrogen atoms linked to the metal in (**I**), and the three hydrogen atoms of the methyl group. For both compounds, we fully optimize the geometries of the four possible spatial structures, corresponding to the different mutual orientation of these three groups of equivalent atoms. Results of calculation are presented in table 1. One can see that the conformations labeled as “a” are the global minima for both systems. They correspond to the staggered mutual orientation of the two group of atoms linked to the metal. The energies of configuration with their eclipsed orientation (c) are higher in the energy by the values of 10.8 kcal/mol for the **I** and 14.9 kcal/mol for the **V**. The energy barrier to rotation of the methyl group is low (compare the structures “b” and “a”).

Table 1

Total energies (*E*, hartree) and the relative energies (Δ*E*, kcal/mol) of four possible structures of C_{3v} symmetry of the I and V complexes [a), b), c)]

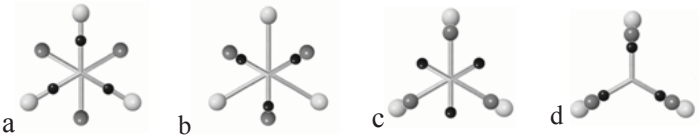

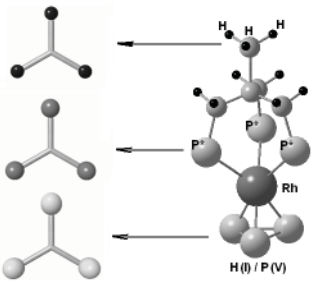

		a	b	c	d
I	*E*	**-7264.6494**	-7264.6430	-7264.6322	-7264.6237
	Δ*E*	**0.**	4.0	10.8	16.1
V	*E*	**-8285.2223**	-8285.2154	-8285.1986	-8285.1896
	Δ*E*	**0.**	4.3	14.9	20.5

[a)] Results of RHF calculations

[b)] The symmetry axis C_3 in figs. a-d is perpendicular to the plane of the figures.

[c)] White circles represent the hydrogen atoms in (**I**) or the triangular P_3 unit in (**V**), gray circles – phosphorus atoms P* of the tripodal ligand, and black circles - the hydrogen atoms of the methyl group

The most relevant calculated geometry parameters for considered complexes in the lowest energy configurations ("a" from Table 1) are summarized in Table 2. The available experimental data for the [(triphos)RhP_3] system are also presented. As can be seen, the method used in the present work provides structural parameters which are in close agreement with the experimental values.

Table 2

Selected geometry parameters for compounds I and V (bond lengths in Å and bond angles in degrees)

Parameters	**I**		**V**			**Atomic designation**
	HFR	DFT	HFR	DFT	exp.[15]	
Rh-P* [a)]	2.53	2.38	2.52	2.39	2.29	
Rh -H_1	1.56	1.59	---	---	---	
Rh -P_1	---	---	2.47	2.48	2.42	
H_1-H_1	2.05	2.03	---	---	---	
P_1-P_1	---	---	2.24	2.19	2.15	
∠ P*-Rh-P*	88.53	91.30	89.25	91.90	91.25	
∠H_1-Rh-H_1	81.39	79.39	---	---	---	
∠P_1-Rh-P_1	---	---	54.17	52.28	52.86	

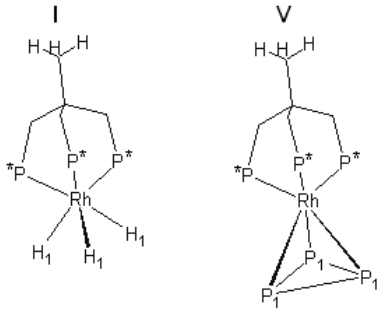

[a)] A-B denotes the interatomic distance

3.2. The intermediate [(triphos)RhH(η^1:η^1-P_4)] complex. P_4 activation

As mentioned in the Introduction, the iridium analogue of transition complex **III,** [(triphos)IrH(η^1:η^1-P_4)], was isolated experimentally [7]. It is obtained by removal of the hydrogen molecule from the complex **I** with formation of the transient complex **II** and simultaneous addition of P_4 molecule.

We have considered two possibilities for P_4 addition to the complex **II**: in the first case the geometry of this complex was optimized, and in the second one its structure was derived from the complex **I** by simple removing of two hydrogen atoms. For every case, three modes of approaching the P_4 molecule to the complex were considered: coordination by the vertex of the tetrahedron, by its edge, and by its plane.

Optimized structure of **II** has C_{3v} symmetry in which the remaining hydrogen atom is located on the threefold symmetry axis, i.e. corresponds to the case when the system has time to relax. Calculations showed that in this case none of the three ways of approaching of P_4 molecule to the complex **II** leads to the complex **III**.

In the second case the remaining hydrogen atom is in the same position as in the complex **I**. When P_4 approaches to the complex **II** by the vertex of the tetrahedron, its geometry is not changed, and M-P_4 bond is not formed (compare the initial structure **IIIa** with the optimized one **IIId** in Fig. 1). Geometry optimization of the other two structures (approaching of P_4 by the edge of the tetrahedron (**IIIb**) and by its plane (**IIIc**)) results in the same stable complex **IIIe** (Fig. 1).

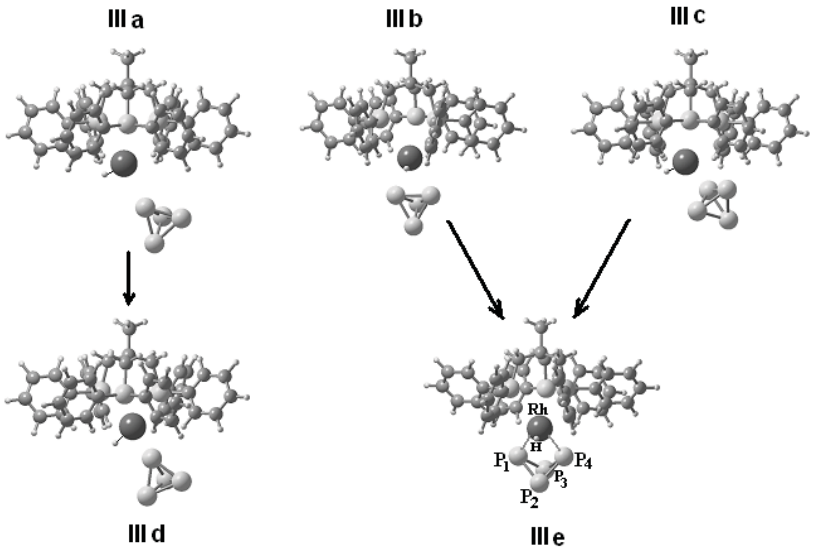

Fig. 1. Different modes of approaching the P_4 molecule to the complex [(triphos)RhH]: coordination by the vertex of the tetrahedron (III a), by its edge (III b), and by its plane (III c)

It is seen (Fig. 1, **IIIe**) that the geometrical structure of P_4 is significantly changed by its coordination to the complex: one of the P-P bonds is broken, and the tetrahedron P_4 is opened to form the *butterfly* geometry. Calculated geometrical parameters for the free tetrahedron P_4 molecule, for its reduced form P_4^- and for the coordinated (in **IIIe**) P_4 are presented in Table 3. The data from the Table 3 show that geometrical parameters of coordinated P_4 molecule have almost the same values as in the reduced form P_4^-.

Table 3

Calculated geometrical parameters for the free P_4, for its reduced form P_4^-, and for the coordinated P_4 molecule (bond lengths in Å and bond angles in degrees)

	P_4 free [a]	P_4^-	P_4^{coord} **(III e)**
$R(P_1\text{-}P_4)$	2.19	2.82	2.95
$R(P_2\text{-}P_3)$	2.19	2.19	2.22
$R(P_1/P_4\text{-}P_2/P_3)$	2.19	2.23	2.28
dih $\angle P_1P_2P_3\text{-}P_4P_2P_3$	70.53	94.66	95.25
$n(P_1\text{-}P_4)$ [b]	0.97	0.45	0.13
$n(P_2\text{-}P_3)$	0.97	0.96	0.89
$n(P_1/P_4\text{-}P_2/P_3)$	0.97	0.94	0.81

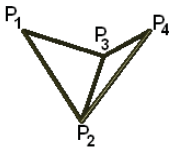

[a] Experimental value of R(P-P) is 2.21 Å [16]
[b] n(A-B) is the bond order of the A-B bonding

In our recent work [17] it was shown that the butterfly geometry of the coordinated P_4 molecule is due to the Jahn-Teller effect induced by the charge transfer to its triple degenerate excited state. In analysing the electronic redistribution details in the [(triphos)RhH(η^1:η^1-P_4)] complex **IIIe** it seems appropriate to use the definition of the ligand binding suggested by Bersuker in the monograph [18]. In the MO terminology "the multiplicity of the orbital bonding (mono-, di-, and multiorbital) equals the number of complex-ligand bonding MOs uncompensated by the antibonding orbitals" [18]. It follows from this definition that the electron charge transfer to and from the ligand is due to formation of such uncompensated bonding molecular orbitals of the entire complex.

A molecular orbital energy-level scheme of the active valence zone of the whole [(triphos)RhH(η^1:η^1-P_4)] complex and that of its fragments, [(triphos)RhH] and P_4, is given in Fig. 2. Consider first of all the changes of the molecular orbitals of P_4 due to its coordination. As shown above, the tetrahedron P_4 is distorted significantly by coordination to the complex. The symmetry of molecule decreases, which causes the splitting of its degenerated MOs. In particular, in the complex **IIIe** with the point group C_s the empty antibonding triple degenerate t_1*-MO splits into the two MOs of *a"* symmetry and one *a'*-MO. When forming the complex, these MOs of P_4 molecule interact with appropriate orbitals of the Rh atom, giving rise to the Rh-P_4 bonding.

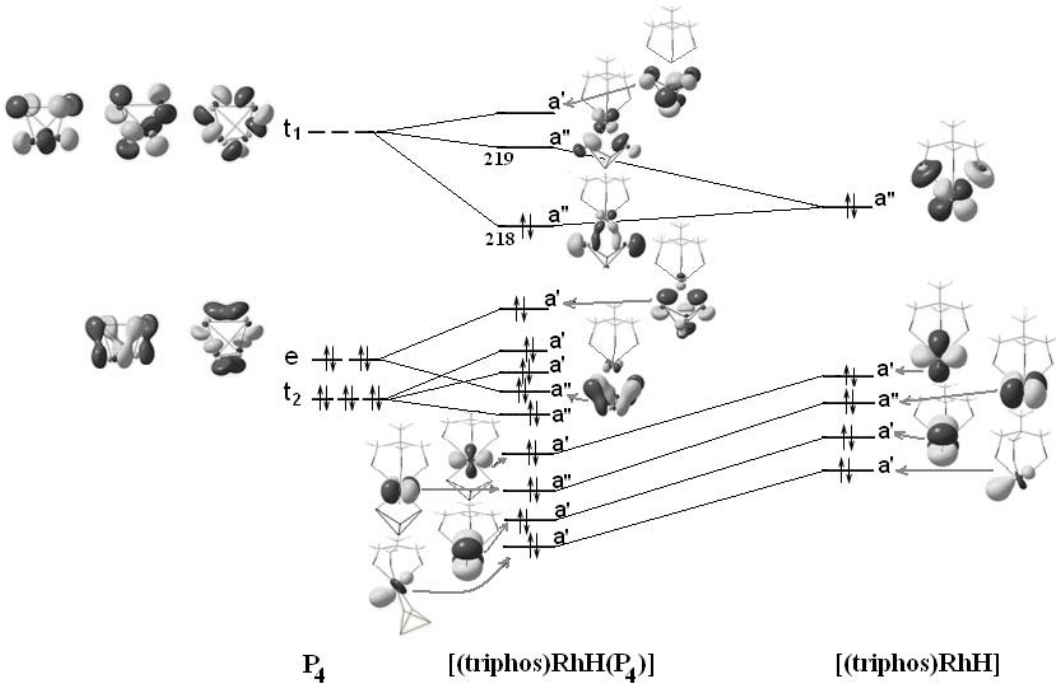

Fig. 2. MO energy-level scheme for bonding between P_4 and [(triphos)RhH]

One can see from fig. 2 that only one bonding MO (218 ***a″***) provides the Rh-P_4 binding, being uncompensated by antibonding orbital (i.e. corresponding antibonding MO 219 ***a″*** is not occupied). Therefore the Rh-P_4 bonding in the studied complex can be classified as mainly mono-orbital one. This π-type MO is composed from the filled ***a″*** MO of the complex **II** which is mainly $4d_{xz}$ AO of the atom of Rh (see on the right side in Fig. 2) and the appropriate component of empty t_1 orbital of P_4. Due to forming of this (218 ***a***'') MO the electron density is transferred from the $4d_{xz}$ AO of the Rh to the unoccupied t_1 orbital of P_4 (the π-type back donation) triggering the JTE t_2 type distortion [18] that result in the *butterfly* geometry of P_4. The orbital charge transfer is quite significant, Dq = 0.68 ē.

3.3. Intramolecular hydrogen atom migration

To analyze the possibility of intramolecular hydrogen atom migration from the metal to the phosphorus, the geometry optimization of all the complexes **IVa, IVb** and **IVc** from Scheme 1 corresponding to different types of the P-H bonding was carried out. Calculated geometry parameters and the values of the total energies are summarized in Table 4.

Table 4

Total energies (E, hartree), interatomic distances A-B (Å) and bond orders (in parentheses) for intermediate compounds III and IV

	III		**IVa**		**IVb**		**IVc**	
	HFR [a)]	DFT [b)]	HFR [a)]	DFT [b)]	HFR [a)]	DFT [b)]	HFR [a)]	DFT [b)]
E	-0.4570	-0.7679	-0.4617	-0.7702	-0.4654	-0.7720	-0.3618	-0.7030
Rh-P_1	2.46 (0.54)	2.42	3.32 (0.00)	3.16	2.57 (0.45)	2.47	2.65 (0.67)	2.47
Rh-P_4	2.46 (0.54)	2.42	2.57 (0.30)	2.37	2.57 (0.45)	2.47	4.51 (0.05)	2.87
P_1-P_4	3.09 (0.13)	2.87	3.37 (0.08)	3.20	3.19 (0.00)	3.05	2.59 (0.74)	2.13
P_1-P_2	2.37 (0.81)	2.26	2.38 (0.82)	2.27	2.37 (0.86)	2.27	2.31 (0.57)	3.09
P_1-P_3	2.39 (0.81)	2.27	2.38 (0.83)	2.27	2.25 (0.81)	2.20	2.31 (0.57)	3.09
P_2-P_3	2.32 (0.88)	2.18	2.34 (0.88)	2.19	3.17 (0.05)	3.07	2.31 (0.57)	3.09
P_4-P_2	2.37 (0.81)	2.26	2.37 (0.77)	2.27	2.37 (0.86)	2.27	2.59 (0.74)	2.13
P_4-P_3	2.39 (0.81)	2.27	2.38 (0.79)	2.26	2.25 (0.81)	2.20	2.59 (0.74)	2.13
P^{coord}-H	---	---	1.44 (0.78)	1.46	1.44 (0.85)	1.43	1.43 (0.89)	1.43

[a)] Values of energy are given relative to -8626.0 a.u.
[b)] Values of energy are given relative to -4081.0 a.u.

It is seen from the Table 4 that the lowest in energy structure corresponds to the complex **IVb** in which the hydrogen atom is bonded not with the nearest (to Rh) atom of phosphorus (P_1 or P_4 from Fig. 1), but with one of the distant atoms P_2 or P_3. Figure 3 depicts the optimized structures of all the intermediate compounds and the most probable path of the hydrogen atom migration from rhodium to phosphorus. Unfortunately, due to the complexity of the system, we were unable to localize transition states corresponding to the hydrogen atom transfer from the Rh to the nearest phosphorus atoms (**III→IVa**), and then to the distant atoms P_2 or P_3 (**IVa→IVb**). The structure denoted as TS in Fig.3 is obtained by point-by-point calculations of the complex at different positions of the hydrogen between the atoms P_1 and P_2, without its further optimization. So, the barrier height between the structures **IVa** and **IVb** can be regarded only as an estimate. We also calculated the structure **IVc** as being the "most prepared" for adding to the complex of two hydrogen atoms with subsequent separation of PH_3. However, its energy is too high to ensure that this complex could be formed during the reaction.

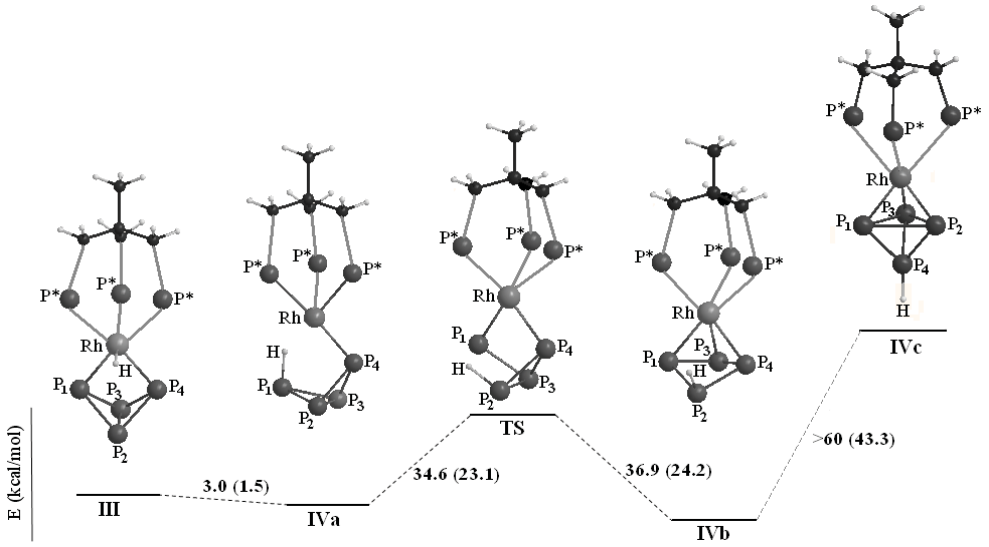

Fig. 3. Energy diagram for the hydrogen atom migration calculated at the RHF and B3LYP (in parentheses) levels of theory

Further addition of two hydrogen atoms to the complexes **IVa** and **IVb** and their subsequent optimization leads to the complex [(triphos)RhP_3] **V** and the phosphane molecule PH_3. The energy profile for the entire reaction predicted by both the RHF and DFT levels of theory is presented in Fig. 4. It is seen that generation of the transient complex [(triphos)RhH(η^1:η^1-P_4)] **III** followed by intramolecular hydrogen atom migration from the metal to the phosphorus to yield **IV** is the energetically favorable process. Every step of the reaction is accompanied by an energy gain, so that the above four-stage reaction mechanism seems to be reasonable.

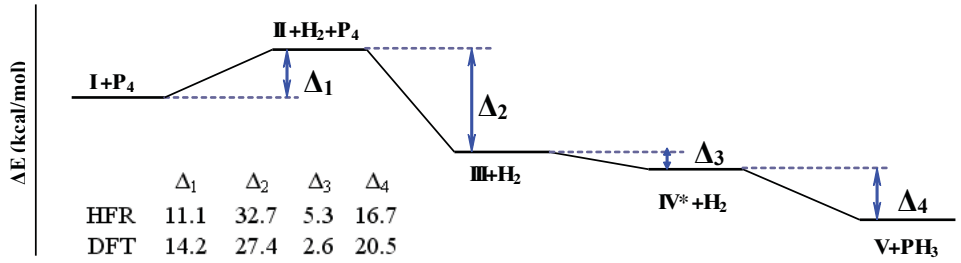

Fig. 4. Calculated energy profile of reaction from Scheme 1 (all values are in kcal/mol)

Note that both RHF and DFT calculations give qualitatively the same picture (Figs. 3, 4), differing only in the values of relative energies of the complexes.

4. Conclusion

Our calculations confirm the possibility of activation and direct hydrogenation of white phosphorus to PH_3 when promoted by rhodium trihydride complex [(triphos)RhH_3]. The proposed four-stage mechanism of reaction of P_4 with the [(triphos)RhH_3] resulting in the phosphane and the *cyclo*-P_3 complex [(triphos)M(η^3-P_3] seems to be plausible. The generation of the transient complex [(triphos)RhH(η^1:η^1-P_4)] followed by intramolecular hydrogen atom migration from the metal to the phosphorus is the energetically favorable process. P_4 molecule is activated by its coordination to the above intermediate: one of the P-P bonds (P_1-P_4) is broken, and the tetrahedron P_4 is opened to form the *butterfly* geometry. The activation is realized due to the one-orbital back donation of electron density from one of the occupied molecular orbitals of the precursor complex [(triphos)RhH] to the unoccupied antibonding triple degenerate t_1*-MO of P_4.

This work was initiated under the guidance of Professor I.Ya. Ogurtsov and was completed by the authors in his memory.

Acknowledgments

The authors are grateful to Dr. Gabriel Munteanu and Dr. Viorel Chihaia for the opportunity to carry out calculations on the hpc-icf computer cluster (http://www.hpc-icf.ro/) at the Institute of Physical Chemistry "I.Murgescu", Bucharest, Romania.

References

[1] Peruzzini, M.; de los Rios, I.; Romerosa, A.; Vizza, F. Eur. J. Inorg. Chem., 2001, N3, 593-608.
[2] Peruzzini, M.; Gonsalvi, L.; Romerosa, A.; Chem. Soc. Rev., 2005, 34, 1038.
[3] Schoeller, W.W. Inorg. Chem., 2011, 50, 22.
[4] Barbaro, P.; Ienco, A.; Mealli, C.; Peruzzini, M.; Scherer, O.J.; Schmitt, G.; Vizza,F.; Wolmershäuser, G.; Chemistry – A European Journal, 2003, 9, 5195–5210.
[5] Barbaro, P.; Caporali,M.; Ienco,A.; Mealli, C.; Peruzzini, M.; Vizza, F.; Eur. J. Inorg. Chem., 2008, 1392.
[6] Barbaro, P.; Peruzzini, M.; Ramirez, J.A.; Vizza, F. Organometallics, 1999, 18, 4237-4240.
[7] Peruzzini, M.; Ramirez, J.A.; Vizza, F.; Angew. Chem. Int. Ed., 1998, 37, 2255-2257.
[8] Granovsky, Alex A. www http://classic.chem.msu.su/gran/gamess/index.html
[9] Schmidt, M.W., et.al.; J.Comput.Chem., 1993, 14, 1347-1363.
[10] Becke, A.D. J. Phys. Chem., 1993, 98, 5648.
[11] Lee, C.; et al.; Phys. Rev. B, 1988, 37, 785.
[12] Huzinaga, S., Andzelm, J., eds. 1984 Gaussian Basis Sets for Molecular Calculations, Elsevier, Amsterdam.
[13] Dill, J. D.; Pople, J. A.; J. Chem. Phys., 1975, 62, 2921-2923.
[14] Hehre, W.J.; Stewart, R.F.; Pople, J.A.; J. Chem. Phys., 1969, 51, 2657.
[15] Bianchini, C.; Mealli, C.; Meli, A.; Sacconi, L.; Inorg. Chim. Acta, 1979, 37, L543.
[16] Osman, R.; Coffey, P., Van Wazer, J.R.; Inorg. Chem., 1976, 15, 287.
[17] Gorinchoy, N.N.; Balan, I.I.; Bersuker, I.B.; Comput. & Theor. Chem., 2011, DOI: 10.1016/j. comptc.2011.08.013.
[18] Bersuker, Isaac B. Electronic Structure and Properties of Transition Metal Compounds. Introduction to the Theory, Second Ed.; John Wiley: New York, 2010, Ch. 6.3, p.257.

PHARMACEUTICAL AMORPHOUS ORGANIC MATERIALS CHARACTERIZATION BY USING THE DIFFERENTIAL SCANNING CALORIMETRY AND DYNAMIC MECHANICAL ANALYSIS

Ion Dranca,* Igor Povar and Tudor Lupascu

Institute of Chemistry, Academy of Sciencesof Moldova
3 Academiei Str., Chisinau MD 2028, Republic of Moldova. e-mail: drancai@yahoo.com

Abstract: This research has been carried out in order to demonstrate the use of differential scanning calorimetry (DSC) in detecting and measuring α- and β-relaxation processes in amorphous pharmaceutical systems. DSC has been employed to study amorphous samples of poly (vinylpyrrolidone) (PVP), indomethacin (InM), and ursodeoxycholic acid (UDA) that are annealed at temperature (T_a) around 0.8 of their glass transition temperature (T_g). Dynamic mechanical analysis (*DMA*) is used to measure β- relaxation in PVP. Yet, the DSC has been used to study the glassy indomethacin aged at 0 and -10 °C for periods of time up to 109 and 210 days respectively. The results demonstrate the emergence of a small melting peak of the α-polymorph after aging for 69 days at 0°C and for 147 days at -10°C (i.e., ~55°C below the glass transition temperature) that provides evidence of nucleation occurring in the temperature region of the β-relaxation. The evolution of an endothermic recovery peak temperature features a plateau at longer annealing times, suggesting that the glass has made a significant progress toward reaching the supercooled liquid state. It has been found that the melting peaks become detectable after the recovery peak reaches the plateau. The results highlight the importance of studying physical aging in the temperature region of the β – relaxation as a means of evaluating the physical stability of amorphous pharmaceutical materials.

Keywords: DSC – differential scanning calorimetry; DMA – dynamic mechanical analysis; drugs; excipients; glass transition; α- and β – relaxations; crystallization; kinetics.

Introduction

Since amorphous compounds are inherently less stable, both physically and chemically, than their crystalline counterparts, numerous investigations over the last decade expectedly focused on the stabilization of amorphous pharmaceuticals [1]. DSC has been used to probe the β-relaxation for a large variety of polymers [2]. Although dielectric spectroscopy has been applied to the relaxation of indomethacin, the studies have been focused on the temperature region of the α-relaxation, and the β-process has not been reported.

General application of DTA and DSC

The results obtained using DTA and DSC are qualitatively so similar that their application usually is not treated separately. It should be noted that DTA can be used to higher temperatures than DSC (max 725 °C) but that more reliable quantitative information obtained from DSC [3]. Differential scanning calorimetry (DSC) is the most frequently used thermal analysis technique alongside TGA, TMA and DMA. DSC is used to measure enthalpy changes (figure 1) due to changes in the physical and chemical properties of a material as a function of temperature or time. The method allows identifying and characterizing materials including pharmaceuticals. DSC is the method of choice to determine thermal quantities, study thermal processes, and characterize or just simply compare materials. The *Dynamic Mechanical Analysis (DMA) basic* principles [3] can be simply described *as applying an oscillating force to a sample and analyzing the material's response to that force* (figure 2). From DMA, one calculates properties like tendency to flow (called viscosity) from the phase lag and the stiffness (*modulus*) from the sample recovery.

These properties are often described as the ability to lose energy as heat (damping) and the ability to recover from deformation (elasticity). The applied force is called *stress* and is denoted by the Greek letter, σ. When subjected to stress, a material will exhibit a deformation or strain, γ. The sample is subjected to a periodically varying stress (usually sinusoidal of angular frequency, ω). The response of the sample to this treatment can provide information on the stiffness of the material (quantified by its elastic module) and its ability to dissipate energy (measured by its damping). For a viscoelastic material, the strain resulting from the periodic stress is also periodic, but it is out of phase with the applied stress owing to energy dispersion as heat, or damping in the sample [3]. A brief history of the DMA technique is given in the book by Menard [5].

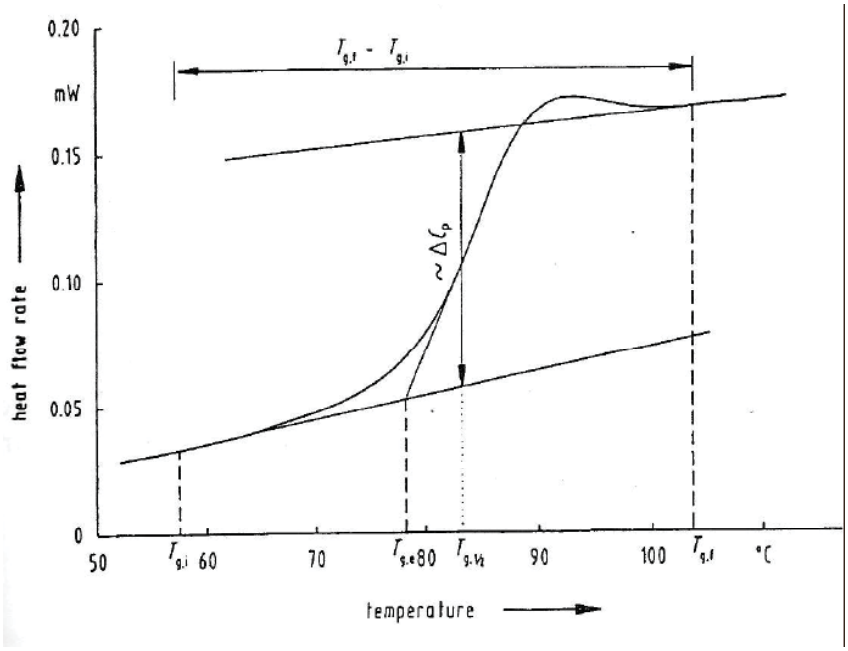

Figure 1. Definition of characteristic features of the glass transition. $T_{g.e}$ = the extrapolated onset temperature; $T_{g,½}$ = the half-step temperature at which the heat capacity is midway between the extrapolated heat capacities of the liquid and glassy states; $T_{g.i}$ and $T_{g.f}$ are the initial and final temperatures of the glass transition and $T_{g.f} - T_{g.i}$ is the temperature interval of the glass transition [4]

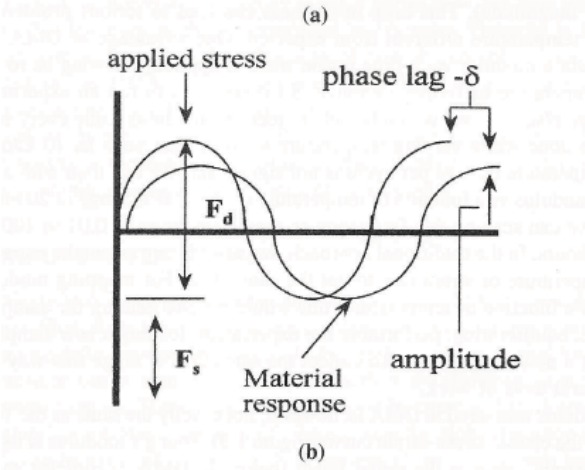

Figure 2. How DMA works. The DMA supplies an oscillatory force causing a sinusoidal stress to be applied to the sample, which generates a sinusoidal strain. By measuring both the amplitude of deformation at the peak of the sine wave and lag between the stress and strain waves, quantities like the modulus, the viscosity, and the dumping can be calculated

General Mechanism of the β-transition in Polymers and Pharmaceutics

V. A. Bershtein and V. M. Egorov have been pointed [6], in 1985 that the result of DSC investigations shows that in polymers relaxation processes the *β* –transition is a general phenomenon common to no crystallizing solids. A relationship has been found between thermo activation parameters of the transition and molecular characteristics i. e. the average length of a molecule, the length of the statistical Kuhn segment, the cohesive energy and the potential barrier of internal rotation. It is concluded that the act of *β*- transition is comparable to acts of relaxation in liquids, and take place in sites of less dense packing. For linear nonrigid polymers the act consist in the rotation of a chain fragment similar in length to the Kuhn segment involving the surmounting of preferentially intermolecular barriers with the participation of S-G transition; the kinetic unit corresponding to the *β*-transition is related to the segment of intermolecular mobility in polymers in pharmaceutics.

The use of the amorphous form of drugs and excipients to improve solubility, accelerate dissolution and promote

therapeutic activity has been advocated by many workers [7]. The rationale behind such a strategy is that a highly disordered amorphous material has a lower energetic barrier to overcome in order to enter solution than a regularly structured crystalline solid. In order to produce a usable amorphous system it is necessary to create a highly disordered molecular state (usually by a high energy process such as milling or lyophilisation) and then to stabilize that disordered state (usually by rapid drying or cooling or addition of stabilizing agents) so that all molecular motions which might induce instability are retarded over a meaningful pharmaceutical time-scale. It is the apparent chemical and physical instability of most amorphous pharmaceutical solids which is the major precluding their more widespread use in solid dosage forms [8].

Amorphous pharmaceuticals draw a great deal of interest because of their potential to enhance bioavailability. But downside of amorphous materials is their thermodynamic instability that unavoidable drives them toward the stable crystalline state.

Excipients are secondary ingredients added to a formulation to aid the delivery, processing and stability of the active drug/ drugs. Formulation stability largely depends on interaction of excipients or lack of interaction of excipients with the active drug and other excipients. Excipients are the additives used to convert pharmacologically active compounds into pharmaceutical dosage form suitable for administration to patients. Careful selection of excipients is critical for maintaining the physical structure of the dosage form, prevention of degradation of the active drug and achieving the desired bioavailability [9]. DSC has been a widely used method to analyze drug- excipient compatibility. Compared to the traditional compatibility methods DSC offers significant advantages by saving time and utilizing smaller amounts of sample. Significant changes in the DSC profile of a mixture compared to those of the individual components indicate probable interactions. Changes in the melting point of the components, peak area, shape, broadening or elongation of the endothermic or exothermic peaks, appearance of new peaks are the indicators of interactions [10,11].

Experimental section

PVP (MW ~8,000), indomethacin and ursodeoxycholic acid were used from Fisher. All the substances were used without further purification. For the annealing (β –relaxation) measurements, about 20 mg of crystalline InM or UDA was placed in 40 μL Al pans and heated to ~15°C above their respective melting points, 160 and 205°C. In the case of PVP, the samples were about 12 mg and heating was conducted up to ~70°C above its glass transition temperature of 140°C. Immediately after heating, the samples were quenched into liquid nitrogen and quickly placed into the DSC (Mettler-Toledo DSC 822^e) that was maintained at 20°C for PVP and UDA and at -40°C for InM runs. After a short period of stabilization at the initial temperature, the samples were heated to an annealing temperature, T_a, and maintained for 30 min. The annealing temperatures were -20, -10, and 0°C for InM; 50, 60, 70 80, and 90°C for PVP; and for 30, 40, 50, and 60°C for UDA. After completion of the annealing segment, the samples were cooled down either to -10°C (PVP and UDA) or to -40°C (InM), and immediately heated above T_g. The heating rates were 10, 15, 20, 25, and 30°C min^{-1}.

Results and discussion

In this paper we demonstrate, that β-relaxation in pharmaceutical glasses can be probed via DSC and DMA

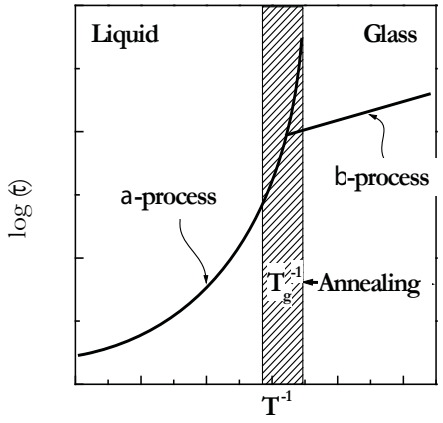

Fig. 3. Temperature dependence of relaxation time for the α- and β-processes. Hatched area represents the region around T_g, where the α- and β-processes are strongly coupled

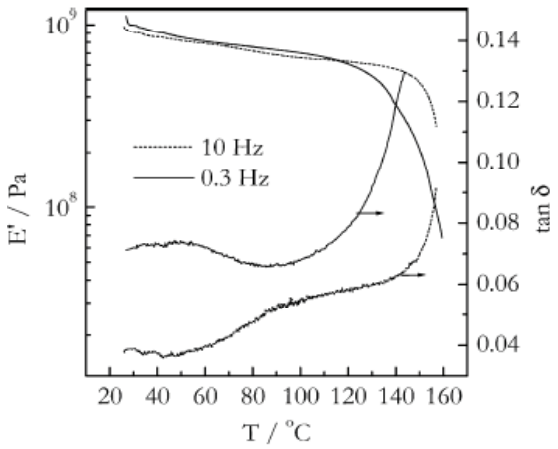

Fig. 4. DMA data (storage modulus, *E'*, and loss tangent, tan δ) for PVP sample at the two extreme frequencies

measurements of the aforementioned annealing effects. We have applied this method to several pharmaceutically relevant glasses that include poly(vinylpirrolidone) (PVP), indomethacin (InM), and ursodeoxycholic acid (UDA) and demonstrate the *E* values obtained as:

$$E = -R\frac{d\ln q}{dT_p^{-1}} \quad (1)$$

and that the activation energy, *E,* evaluated from the shift of the peak temperature, T_p, with the heating rate, q, as (1). The consistency is confirmed by comparing the obtained *E* values with independent measurements, literature values, and the empirical correlation, $E_\beta = (24\pm3)RT_g$, discovered by Kudlik *et al.*[12]. Yet, the importance of low temperature mobility of amorphous pharmaceuticals is well recognized [8].

Figure 5 displays variation of the effective activation energy with the average peak temperature for DSC and DMA.

Nucleation of amorphous indomethacin

Indomethacin (indometacin) (1-(p-chlorobenzoyl)-5-methoxy-2-metylindole-3-acetic acid) from MP Biomedicals, LLC was used without further purification. After quick melting samples were quenched into liquid nitrogen. The quenched samples had the value of T_g = 46°C that was determined by DSC as a midpoint of the glass transition step observed on heating at 10°C min^{-1}.

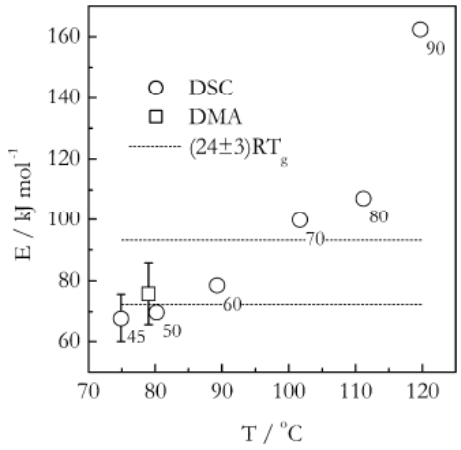

Fig. 5. Variation of the effective activation energy with the average peak temperature for DSC and DMA data on PVP. Numbers by the points represent annealing temperatures. Error bars are confidence intervals. Dash lines set lower and upper limits for (24±3) RT_g

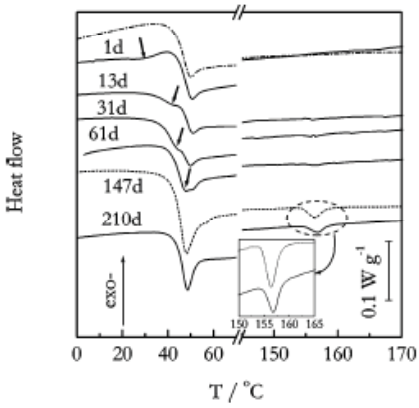

Fig. 6. DSC curves obtained on heating at 10°C min^{-1} of indomethacin after long-term annealing at T_a = -10°C. The numbers by the curves represent annealing time in days (d). Dash-dot line represents non-aged glass. Arrows show the location of the annealing peak. The melting region is circled. Inset shows a blow-up of the melting region

The quenched samples were placed in freezers kept at 0 and -10°C and annealed there for an extended period of time. In samples at T_a = -10°C , no melting peaks are detected at annealing times, t_a, less than 147 days (figure 6). We believe that our data on detecting the melting peaks after prolonged aging make a convincing case that nucleation does occur during aging. Although an alternative interpretation could be that that nucleation occurs not during aging but on heating of extensively aged glasses from T_a to T_m we consider it very unlikely.

Excipients

The local and global mobility, in two popular amorphous pharmaceutical excipients, sucrose and trehalose, have been compared. Trehalose, having a lower free volume in the glassy state due to a more tightly packed structure, experiences a greater effect of temperature on the reduction in the activation energy barrier for the glass to start flowing. This could be important in causing collapse of a lyophilized cake in that a small increase in temperature around the glass transition temperature of a formulation containing trehalose could cause pronounced viscous flow. In spite of a large difference in T_g, sucrose and trehalose are shown to have similar size of cooperatively rearranging regions (CRR) and also approximately the same number of molecules constituting the CRR, thus implying similar dynamic heterogeneity.

Conclusions

1. DSC can be used for detecting β-relaxation processes and estimating its low temperature limit, i.e., the temperature below which amorphous drugs would remain stable.
2. It can also provide comparative estimates of low temperature stability of amorphous drugs in terms of the activation energies of the β-relaxation.
3. Physical aging of indomethacin has been studied at temperatures down to T_g – 56°C or $0.83T_g$ that corresponds to the temperature region of the β-relaxation. The study demonstrates that indomethacin undergoes nucleation in this temperature region. To our knowledge, this represents the lowest temperatures, for which evidence of nucleation has been reported. Although the process is quite slow, detecting it is very important because pre-nucleated amorphous pharmaceuticals would crystallize faster when the storage temperature is increased. Clearly, studies of the kinetics of the sub-T_g relaxations should play a key role in estimating the physical stability of amorphous pharmaceuticals. Another finding of this work is that nucleation becomes detectable after glassy indomethacin has reached a significant extent of relaxation defined as a plateau in the plot of the aging peak temperature against aging time. The significance of this correlation is that it could be used for estimating the life-times of amorphous pharmaceuticals as the time of reaching the aforementioned plateau, because this period appears to determine the time to nucleation. However, whether this correlation is a common feature of crystallizable glasses remains to be seen in our ongoing investigation.
4. DSC has been employed for probing β-relaxations in pharmaceutical glasses annealed at temperatures around $0.8T_g$. The resulting annealing peaks have been used for estimating the low temperature limit of β-relaxation, i.e., the temperature below which amorphous drugs would remain practically stable. A shift in the peak temperature with the heating rate allows one to obtain a trustworthy estimate for the activation energy of β-relaxation. The trustworthiness of the estimates has been tested by comparing them against independent estimates obtained by DMA, TSDC as well as by relationship $E_\beta = (24\pm3)\ RT_g$. More than satisfactory agreement has been observed for all studied systems.
5. The local and global mobility, in two popular amorphous pharmaceutical excipients, sucrose and trehalose, have been compared.

Acknowledgment

Thanks are due to Prof. S. Vyazovkin (University of Alabama) for help with DSC and DMA measurements.

References

[1]. Pouton, C. W. *Eur. J. Polym.Sci.,* 2006, 29, 278-287.
[2]. Berstein, V.A.; Egorov, V.M. *Differential ScanningCalorimetry of Polymers,* Ellis Horwood, New York, 1994.
[3]. Brown, M.E. *Introduction to Thermal Analysis, Techniques and Applications,* Second Edition, 2001, Published by Kluwer Academic Publishers, 264 p.
[4]. Hohne, G.; Heminger, W.; Flammersheim, H.J. *Differential Scanning Calorimetry "Springer-Velag, Berlin, 1999.*
[5]. Menard, K.P.*Dynamic Mechanical Analysis – A Practical Introduction,* CRC Press, Boca Raton, USA, 1999.
[6]. Berstein, V. A.; Egorov, V.M. *Polym. Sci. USSR,* 27, 1985, 2743-2757.
[7]. Martin, A.; Swarbrick, J.; Cammarata, A. *Physical Pharmacy,* Lea and Febiger, Philadelphia, 1983
[8]. Hancock, C.; Shamblin, S.L. Zografi, G. *Pharm.Res.,* 1995, vol. 12, No. 6, 799-806.
[9]. J. Swarbrick and J. Boylan, *Encyclpedia of pharmaceutical technology,* 2nd Edition, 2002, Vol. 2, 1132.
[10]. Jackson, K.; Young, D. Pant, S. *Pharmaceutical Science and Technology today,* 2000, 3, 10, 336-345.
[11]. Wels, J. *Pharmaceutical Preformulation, the physicochemical properties of drug substances,* 1988.
[12]. Kudlik, A. *et al. J. Mol. Struct.,* (1999) 479: 201-218.